



Cite this: DOI: 10.1039/d6gc00543h

## Rethinking hydrothermal carbonization: development of lignin-focused biorefinery for generation of high-value hydrochar and lignin spheres

Valeria Pierpaoli, <sup>a</sup> Giorgio Tofani, <sup>\*b</sup> Edita Jasiukaitytė-Grojzdek, <sup>b</sup> Blaž Likozar, <sup>b</sup> Miha Grilc, <sup>\*b,c</sup> Marco Barbanera <sup>d</sup> and Manuela Romagnoli<sup>\*a</sup>

This tutorial review aims to provide a comprehensive overview of hydrothermal carbonization (HTC) as a unified platform for biomass valorisation including the most recent developments and future challenges. After the introduction, section 2 distils HTC fundamentals – operating regimes, acid-catalysed pathways (hydrolysis, dehydration, aromatization), and the distribution of solids, liquids and gases under subcritical water conditions. Section 3 examines hydrochar, highlighting how variations in feedstock, temperature, and residence time govern surface functionality, porosity and thermal stability, and enable applications in soil amendment, CO<sub>2</sub> capture, heavy-metal adsorption, and solid-acid catalysis. Section 4 surveys HTC-derived carbon spheres, demonstrating that control over dopants, activation protocols, and reaction parameters yields particles with tailored meso-/microporosity, surface chemistry, and electrochemical performance for supercapacitors and water purification. Section 5 introduces lignin-focused strategies that recover structurally preserved lignin directly from hydrochar and convert it into micro-/nanospheres with high carbon content, intact β-O-4 linkages, and tuneable functionality for catalytic and materials applications. Lastly, section 6 is dedicated to the environmental assessment of solvents and chemical reagents used in post-HTC functionalization and activation. Collectively, these developments establish HTC as a versatile, zero-waste biorefinery approach – producing hydrochar, engineered carbon nanostructures, and high-value lignin under green chemistry principles and scalable process conditions.

Received 26th January 2026,  
Accepted 24th March 2026

DOI: 10.1039/d6gc00543h

rsc.li/greenchem

### Green foundation

1. This review highlights hydrothermal carbonization (HTC) as a sustainable platform for biomass valorisation, integrating lignin-first strategies. Key advancements include the state of the art about the generation of tailored hydrochar, carbon and lignin spheres for energy storage, environmental remediation, catalysis, and biomedical applications, aligning with zero-waste principles and offering scalable alternatives to fossil-derived materials.
2. The valorisation of biomass addresses multiple global challenges: waste management, carbon neutrality and circularity. The lignin-first approach by HTC provides access to renewable aromatics, enabling high-value application in biomedicine, energy and environmental remediation.
3. The future of this field lies in the integration of HTC strategies that will contribute to obtaining new biochemicals and biomaterials for different applications. Also, environmental and economic assessments will be required, attracting scientists in this area of research to evaluate the feasibility of the scaling up of HTC processes.

## 1. Introduction

Starting in the 1940s, most commodity plastics and materials have been produced from petroleum-based chemicals, showcasing a significant dependence on non-renewable energy sources. However, as awareness of environmental pollution and the resource crisis deepens, the renewability and degradability properties of biomass materials are being increasingly recognized and valued.<sup>1,2</sup> Biomass has emerged as a critical renewable resource for creating a variety of products<sup>3</sup> and is the only renewable energy source that releases carbon dioxide

<sup>a</sup>Department of Innovation of Biology, Agrifood and Forestry system – University of Tuscia, Via San Camillo de Lellis, snc, 01100 Viterbo, Italy. E-mail: mroma@unitus.it

<sup>b</sup>Department of Catalysis and Chemical Reaction Engineering, National Institute of Chemistry, Hajdrihova 19, SI-1001 Ljubljana, Slovenia. E-mail: giorgio.tofani@ki.si, miha.grilc@ki.si

<sup>c</sup>Center of Excellence for Low Carbon Technology, Hajdrihova 19, SI-1001 Ljubljana, Slovenia

<sup>d</sup>Department of Economics Engineering Society and Business Organization (DEIM), University of Tuscia, Largo Dell'Università S.n.c., Loc. Riello, 01100 Viterbo, Italy



during use.<sup>4,5</sup> However, this release is offset by the fact that growing biomass absorbs carbon dioxide from the atmosphere through photosynthesis to store energy. Therefore, biomass resources are used sustainably, and there are no net carbon emissions over the full cycle of biomass production.<sup>4,5</sup> Globally, vast amounts of agricultural waste biomass present an opportunity for energy and material conversion:<sup>6</sup> its transformation into biofuels and biobased chemicals is gaining interest as a sustainable alternative to fossil fuels, helping to cut emission and expand renewable energy access, particularly in electricity-scarce regions.<sup>7</sup>

Lignocellulosic biomass can be considered as a collection of fibrous cellulose backbones with a hemicellulose coating that are “glued” by lignin.<sup>8</sup> Cellulose, a glucose polymer, stands for 30–50% of the biomass depending on the plant species.<sup>9</sup> It is a natural polymer composed of repeating D-glucose units, namely pyranoses.<sup>10</sup> Each pyranose ring contains three hydroxyl groups that can form intra- and intermolecular hydrogen bonds: these give cellulose its crystalline structure, mechanical strength and chemical stability.<sup>10</sup> Hemicellulose, a heteropolymer predominantly containing xylose, mannose and glucose, makes up 20–35%.<sup>9</sup> Unlike cellulose, which has a hydrolysis-resistant crystalline structure, hemicellulose is amorphous and lacks physical strength:<sup>10</sup> it is readily hydrolysed by diluted acids or bases, as well as by hemicellulose enzymes. Its polymerization degree is lower compared to that of cellulose. Among these materials, lignin stands out as the third most abundant natural polymer after cellulose, garnering extensive attention in recent years as it is the most rich and renewable resource of aromatic compounds on Earth.<sup>11</sup> Lignin has a complex phenolic chemical structure containing phenylpropane-type motifs, formed by three phenylpropane monomers: *para*-coumaryl alcohol (H units), sinapyl alcohol (S units) and coniferyl alcohol (G units).<sup>12</sup> Lignin, an aromatic-based heteropolymer accounting for 15–30% of the biomass, is crucial for water transport and structural integrity in plants.<sup>13</sup>

The ratio of these monomers differs based on plant species,<sup>14</sup> with hardwoods containing a higher methoxy content than softwoods.<sup>15</sup> Lignin plays a crucial role in maintaining cellular structural integrity and overall plant rigidity by interacting with cellulose and hemicellulose, thus protecting other components from enzymatic degradation.<sup>16</sup> Despite its importance, lignin is often underutilized in high-value applications, primarily because of its insolubility in aqueous media and its recalcitrant nature due to complex molecular linkages such as the  $\beta$ -O-4 ether bond, which makes it resistant to degradation.<sup>11,17</sup>

Traditionally, pretreatments have been focused on the valorisation of the carbohydrate fraction of lignocellulose,<sup>18</sup> and lignin, so far, has been viewed as an unwanted waste material or low value-by product that is best burnt to generate electricity or heat,<sup>15</sup> but since it possesses a higher carbon concentration and lower oxygen content compared to cellulose it can be considered as an appealing feedstock for the synthesis of chemicals.<sup>17</sup> Within the framework of the circular economy and

lignin valorisation, biorefineries serve as the ideal industrial platform for advancing essential chemical transformations. As defined by the International Energy Agency, biorefineries involve the sustainable processing of biomass into a spectrum of biobased products (food, feed, materials, chemicals) and bioenergy (fuels, power, heat).<sup>19</sup> Within this idea, papers discuss “lignin-focused” processes, new biomass fractionation methods designed to extract pure lignin in high yields and prevent the recondensation of lignin fragments.<sup>18</sup> The development of bio-based products derived from lignin is a crucial aspect of comprehensive biorefinery concepts due to its biocompatibility and biodegradability: lignin is a unique precursor for various high-value applications, including biofuels, adhesives, carbon fibres, and activated carbons, and as a source of phenolic monomer and fine chemicals.<sup>3,14</sup> However, despite its potential, only 5% of lignin is currently utilized for high-value applications:<sup>20</sup> this underutilization highlights the need to develop efficient lignin isolation processes and to engineer lignin-based products with higher commercial value, indicating significant challenges and opportunities for further research and development.<sup>2</sup>

A process currently undervalued for the development of “lignin-focused” biorefineries is hydrothermal treatment (HTT). This process presents several green aspects because it uses only water – no organic solvents or harsh chemicals – as the reaction medium, thus avoiding toxic effluents and corrosion. Operating under moderate temperatures and self-generated pressures also reduces external energy demands compared to pyrolysis.<sup>21–37</sup> Moreover, the process can run in a closed system, enabling efficient heat recovery and minimal waste generation. However, the “lignin-focused” approach is currently limited<sup>38</sup> and more focus is directed to the application of HTT directly on isolated lignin for energy purposes.<sup>39</sup> The hydrolysate from HTT is more studied, but it contains more degraded lignin fractions.<sup>40,41</sup> Therefore, high interest should go to the valorisation of lignin for the obtainment of high-value products. This review therefore places special emphasis on the preparation of lignin micro- and nanospheres – also referred to as lignin nanoparticles – which have already shown promise as antioxidant carriers and UV protectants,<sup>31,42</sup> drug-delivery vehicles,<sup>22,24,43</sup> and active components in advanced composites,<sup>11,44,45</sup> and in bioimaging,<sup>28</sup> bone tissue engineering,<sup>27</sup> and pesticide encapsulation.<sup>26,46</sup> Equally important is the residual solid fraction (*i.e.* hydrochar), which is too often discarded in favour of the liquid hydrolysate<sup>47–51</sup> since the hydrolysate contains readily extractable, high-value chemicals that can be more easily isolated and integrated into established biorefinery frameworks. While much of the early literature has emphasized the recovery of soluble, high-value compounds from the liquid phase, there is a growing recognition that the solid hydrochar fraction is equally valuable – not only as a precursor for activated carbons or soil amendments, but also as a source for structurally preserved lignin. Recent “lignin-focused” approaches seek to isolate and exploit this aromatic polymer directly from the hydrochar, opening the way to micro- and nanostructured lignin spheres with



advanced functionalities for catalysis, materials science, and biomedicine. This shift in perspective – from by-product to platform – marks an important step towards integrated, zero-waste biorefineries.

## 2. Hydrothermal carbonization

### 2.1. General description

HTT refers to a broad family of thermochemical processes where water simultaneously acts as solvent, reactant and catalyst. Under these subcritical or supercritical conditions, hot compressed water accelerates natural transformation pathways, enabling the rapid conversion of organic matter into valuable materials.<sup>52</sup> HTT is widely recognized as an umbrella term encompassing hydrothermal carbonization (HTC), aqueous phase reforming (APR), hydrothermal liquefaction (HTL) and hydrothermal gasification (HTG).<sup>7</sup> Each method operates under different temperatures and pressure, yielding distinct products in solid, liquid or gaseous form.<sup>7,52</sup> HTC produces carbon-rich solid materials with a high energy content, suitable for various applications. HTL mainly generates a viscous bio-oil that can be used as a fuel or a chemical feedstock. HTG leads to the production of hydrogen and carbon monoxide-rich syngas. Although these processes share the same aqueous reaction medium, their operational windows and target products differ substantially, justifying their classification as separate sub-processes within HTT. Among these, our study will focus on hydrothermal carbonization. HTC is described as a low-temperature process, typically operating at 150–300 °C, where water remains in the liquid phase and promotes ionic reactions leading to hydrochar formation.<sup>53,54</sup> This definition is the most adopted in studies focusing on hydrochar production; however, some authors employ a broader classification into (i) low-temperature HTC (250 °C) and (ii) high-temperature HTC (300–800 °C) based on the heating temperature and final products.<sup>52,55</sup> Low-temperature HTC is a single-step method applicable to various biomass types. It mimics the natural coalification process – usually taking millions of years – but completes it in just few hours, while only using water as the reaction medium.<sup>55</sup> In this extended framework, HTC encompasses a wider temperature range, with high-temperature HTC approaching conditions that partially overlap with slow pyrolysis while still being conducted in the presence of water. This broader definition is particularly relevant for studies operating above 300 °C and is therefore adopted in the present review to maintain terminological consistency across the literature discussed.

### 2.2 Chemical process

HTC is an eco-friendly method using only water as the reaction medium, requiring no metal catalyst, thus avoiding corrosion issues and delivering high energy efficiency.<sup>56–59</sup> This green technology primarily aims to solubilize hemicelluloses, enhance enzyme accessibility to cellulose and prevent the formation of inhibitors,<sup>57</sup> and increase the stability, carbon

content and energy content of the biomass feedstock.<sup>60</sup> Studies have investigated this process using bagasse,<sup>61</sup> wheat straw,<sup>59,62</sup> plant biomass wastes, loblolly pine and soft rush.<sup>56</sup> Typically performed at temperatures of 130–240 °C (ref. 56 and 57) and pressures of 1–3.5 MPa,<sup>57</sup> the process lasts from a few minutes to several hours.<sup>56,57</sup> Under these conditions, hot compressed water promotes the hydrolysis of lignocellulosic polymers by weakening ester, ether and  $\beta$ -1–4 glycosidic bonds, which facilitates the breakdown of hemicellulose, cellulose and extractives.<sup>7,17,56,63,64</sup>

During the treatment, hydronium ions generated from water autoionization act as acid catalysts<sup>57,65</sup> and acids are liberated from the side chains of hemicellulose, creating an acidic environment that promotes the hydrolysis of the biomass components and the polymerization of biomass into oligomers and monomers.<sup>63</sup> Maintaining a pH of 4 to 7 is essential to minimize the production of degradation products, achieved through continuous pH monitoring and adding bases like potassium hydroxide.<sup>65</sup> For some types of biomass, the addition of mineral acids such as sulphur dioxide or sulphuric acid is required to achieve effective pretreatment. However, the underlying mechanism remains consistent, driven by acid-catalysed hydrolysis.<sup>63</sup> When adding sulphur dioxide, the pretreatment results in higher glucose yields post-hydrolysis; when adding sulfuric acid, the hemicellulose sugar recovery is enhanced, and so is the inhibitor generation.<sup>63,66</sup> Cellulose and acid-insoluble lignin remain mostly intact in the treated biomass.<sup>57</sup>

Hemicellulose, the most thermochemically labile fraction of lignocellulosic biomass, hydrolysed readily below 200 °C into xylose, arabinose and xylo-oligosaccharides.<sup>55</sup> hot water infiltrates the cells of the biomass, causing water to condense within the cell structure and helping to disrupt the cell wall matrix.<sup>58,63</sup> This breakdown facilitates the formation of furfural and HMF at high concentrations and also results in the formation of other species such as acetic, furoic, formic, lactic, propionic and butyric acids that contribute to lowering the pH.<sup>56,60</sup> Following hemicellulose degradation, cellulose becomes more exposed and enzymatically accessible, while lignin undergoes partial solubilization and depolymerization.<sup>63,67</sup> Cellulose, in fact, undergoes hydrolysis at a slower rate compared to hemicellulose and the random hydrolysis of glycosidic bonds reduces its degree of polymerization.<sup>63,67</sup> Lignin is depolymerized primarily through acid hydrolysis of  $\beta$ -O-4 ether bonds, increasing its free phenolic content, but it can also rapidly repolymerize through acid-catalysed condensation reactions between carbonium ions and nucleophiles.<sup>63,68</sup> Evidence of lignin depolymerization includes a decrease in the molecular weight with extended pretreatment times,<sup>68</sup> while signs of repolymerization include an increase in molecular weight observed during shorter pretreatment.<sup>68</sup> Also, upon increasing the temperature to 220 °C (ref. 65) condensation and polymerization of cellulose and lignin lead to carbon microspheres:<sup>55</sup> prolonged reaction times enhance lignin solubility and promote structural reorganization, forming a porous carbon network. Evidence suggests that the solubility



behaviour of lignin is influenced by the presence of carbohydrates through the formation of hydrophobic aggregates or covalent bonds between lignin and hemicellulose.<sup>68</sup> Higher temperatures promote pore formation in the resulting materials by enhancing the release of volatile compounds from the biomass, thereby increasing the surface area.<sup>65</sup>

The overall effectiveness of hydrothermal carbonization strongly depends on process severity and on the nature of the original feedstock.

Pandey *et al.* reported<sup>57</sup> that the behaviour of biomass compounds was investigated during hydrothermal carbonization at temperatures ranging from 190 °C to 210 °C. The results showed that xylose was the most abundant sugar in the hydrolysate, while glucose release from cellulose was relatively low. Xylose concentration increased with reaction time at 190 °C but it degraded to furfural at higher temperatures (200–210 °C). Xylose is a key indicator of overall sugar recovery.<sup>63</sup> Both furfural and HMF concentrations increased with time and temperature, in parallel with acid formation (acetic, levulinic and formic acid), which caused a significant drop in the initial pH. Xylo-oligosaccharides were the major products at 190–200 °C for 10 minutes, but they were not detected at 210 °C and longer reaction times. The treated biomass showed an increase in glucan content and a decrease in xylan and lignin content, with glucan content peaking before starting to degrade under severe conditions. These findings confirm the central role of hemicellulose degradation in enhancing the enzymatic digestibility of cellulose.

It should be noted that HTC performance is relatively robust with respect to variations in time and temperature: products' yields often remain consistent across a range of pretreatment severities.<sup>63</sup>

### 2.3 Products generated by HTC

Under hydrothermal carbonization, cellulose and hemicellulose release furfural and HMF into the hydrolysate;<sup>56</sup> lignin can yield valuable compounds such as vanillin and syringaldehyde<sup>56</sup> – used in cosmetics and flavouring. At elevated temperatures and prolonged reaction times, lignin also produces alkyl phenols,<sup>17</sup> as shown in Table 1.

Overall, hydrothermal carbonization results in a mixture of aqueous chemicals including acetic acid, pentoses (from

hemicellulose), hexoses (from cellulose), furfural, HMF and phenolic compounds like vanillin and syringaldehyde.<sup>56,60,69</sup> Hydrothermal carbonization also generates a solid carbonaceous residue called hydrochar, which has notable features such as porosity and functional groups like hydroxyls and carbonyls.<sup>56</sup> Hydrochars are valuable by-products with higher heating values compared to their biomass precursors and have been proposed for various applications, including soil amendment and CO<sub>2</sub> capture, and as precursors for carbon materials.<sup>70–74</sup>

After hydrothermal carbonization, biomass typically retains 8–95% of its original energy content and 55–90% of its original mass: this indicates effective preservation of biomass energy and structural integrity post-treatment.<sup>60</sup> The pretreatment significantly affects biomass components: cellulose is partially degraded and loses crystallinity, enhancing its enzymatic digestibility,<sup>63</sup> whereas hemicellulose undergoes near-complete decomposition,<sup>60</sup> and its dissociation from lignin and cellulose increases overall accessibility.<sup>63</sup>

When investigated separately,<sup>56</sup> cellulose and lignin yielded the most hydrochar, respectively 88% and 81%: lignin's yield in char is slightly lower than cellulose's due to lignin's partial solubility in water but it remains more thermally stable and maintains higher yields under more severe conditions. The decomposition of hemicellulose predominantly forms liquid products with minimal gas production<sup>56</sup> and shows minimal sensitivity to severity, while the hydrochar yield decreases with increasing severity<sup>56,75</sup> – a trend also observed for cellulose and lignin. As for lignin, there is a linear decrease in liquid yield with increasing severity, indicating that volatile compounds are produced from lignin degradation right from the beginning and their production increases with higher severity.<sup>56</sup>

Compounds derived from hemicelluloses during hydrothermal carbonization have broad potential for bio-based chemicals and fuel production:<sup>57</sup> xylo-oligosaccharides,<sup>57,76–79</sup> ethanol,<sup>57,66,67,75,80,81</sup> butanol,<sup>57</sup> lactic acid,<sup>57,82,83</sup> xylitol,<sup>47,57,84–86</sup> PHA such as PHB,<sup>50,57,87,88</sup> 1,3 propanediol,<sup>49,57,89–91</sup> and 2,3 butanediol.<sup>48,51,57,92–94</sup>

Additionally, HTC pretreated biomass, enriched in cellulose and lignin, can undergo further treatments such as enzymatic hydrolysis and chemical processes to separate these components for various downstream applications. This process

**Table 1** Main reactions which biopolymers undergo during hydrothermal treatment and products generated

Biopolymers	Main reactions	Products generated
Hemicellulose	• Acid-catalysed hydrolysis	• <b>Polysaccharides:</b> xylose, arabinose, xylan • <b>Furans:</b> furfural, 5-HMF • <b>Acids:</b> acetic, furoic, propionic, butyric, formic, lactic, levulinic • <b>Xylo-oligosaccharides</b>
Cellulose	• Acid hydrolysis of glycosidic bonds (depolymerization) • Polymerization	• <b>Polysaccharides:</b> glucose, glucan • <b>Furans:</b> 5-HMF • <b>Acids:</b> formic, levulinic • <b>Carbon microspheres/hydrochar</b>
Lignin	• Acid hydrolysis of β-O-4 bonds (depolymerization) • Acid-catalysed condensation (repolymerization)	• <b>Phenolics:</b> vanillin, syringaldehyde, <i>p</i> -coumaryl alcohol • <b>Alkyl-phenols</b> • <b>Carbon microspheres/hydrochar</b>



optimization is crucial for maximizing the efficiency of biomass conversion into valuable products.<sup>57</sup>

While HTC-based biorefineries have made significant advances in carbohydrate valorisation, lignin remains underutilized. Integrating its conversion into process optimization strategies could improve both sustainability and profitability. Several studies have explored post-HTC fractionation techniques to improve the selective recovery of biomass components.

Zhang and co-authors<sup>62</sup> designed a hydrothermal carbonization followed by ultrasonic ethanol extraction to improve the efficiency of separation and utilization of cellulose, lignin and hemicellulose. The liquid products were mainly formed of ethyl formate, which comes from the breakdown of hemicellulose and cellulose into five-carbon and six-carbon sugars that dehydrate to furfural, which further reacts with ethanol and hydrolyse to ethyl formate.<sup>62</sup>

Sun and co-authors<sup>58</sup> combined hydrothermal carbonization and alkali fractionation in a two-step consecutive pretreatment, showing that sodium hydroxide or ethanol effectively breaks down the rigid structure of lignocellulosic biomass and solubilizes lignin, thereby removing hemicellulose and lignin from eucalyptus fibres for further utilization and enhancing the availability of cellulose for enzymatic action and fermentation yields.

Chen and co-authors<sup>59</sup> combined the hydrothermal carbonization and the alkaline ethanol extraction to extract lignin fractions that can be used to produce high value-added chemicals or materials and separate cellulose for the subsequent production of bioethanol. They observed that by increasing the treatment temperature, the carbohydrate concentrations in lignin-rich fractions decreased, due to hemicellulose degradation under severe conditions.

However, compared to polysaccharide-derived materials, hydrochar and lignin fractions remain less thoroughly investigated. The next sections will highlight recent advances in their valorisation.

### 3. Hydrochar

Hydrochar can be obtained from biomass, cellulose, hemicellulose and lignin *via* HTC.<sup>65</sup>

- **Cellulose:** through hydrolysis, dehydration and cracking, polymerization and condensation, aromatization, nucleation and chain propagation. It was found that reaction time and temperature had the greatest effects on the hydrochar.

- **Hemicellulose:** xylose from hydrolysis can be transformed into carbon microspheres with controllable morphologies, and the same applies to xylan-derived xylose.

- **Lignin:** dissolved lignin, also from waste, can be polymerized into microspherical carbonaceous materials *via* the hydrothermal route, increasing its yield in the presence of sulfuric acid.

At elevated temperatures, hydrochar develops rough surfaces and highly ordered crystalline structures, but has few

vesicles and a low surface area: above 350 °C, most functional groups are eliminated, with hydroxyl groups being an exception and available for further functionalization.<sup>17</sup>

Activated carbon is traditionally produced through the thermal degradation of coal or biomass, followed by activation. However, challenges such as the depletion of fossil fuels and the high cost of biomass-derived activated carbon limit its broader application. Biochar, a byproduct of biomass pyrolysis, has emerged as a low-cost alternative due to its unique surface properties: while conventional pyrolysis yields low biochar quantities, hydrothermal carbonization offers a promising solution by producing hydrochar with higher yields and abundant oxygen functional groups at milder temperatures.<sup>95</sup> One advantage of hydrochars over fossil coal and coke is their chemical purity: they virtually lack sulphur and heavy metals and have low nitrogen and ash content.<sup>74</sup> Biomass-based carbon materials have emerged to offer excellent catalytic activities, contributing to green chemistry and ecological protection as promising substitutes for acid-catalysed reactions, to provide a stable framework for catalytic active components;<sup>65,96–99</sup> they have gained prominence in energy storage applications, particularly in capacitors and supercapacitors, as a response to global energy challenges and the demand for cleaner, renewable energy sources;<sup>100–103</sup> they also have arisen as effective adsorbents for environmental remediation, particularly in the removal of heavy metals and organic pollutants due to their porous structure and high specific surface areas.<sup>95,104–110</sup> Carbonaceous materials also find applications in various fields such as agriculture – to improve soil productivity,<sup>71,111,112</sup> biomedicine<sup>113–115</sup> and magnetic applications.<sup>105</sup>

The following subsections discuss representative studies focusing on the production and structural analysis of hydrochar obtained *via* HTC of biomass (summarized in Tables 2–8) and lignin (summarized in Table 9). By comparing different approaches and feedstocks, the sections aim to delineate the key factors influencing the material's morphology and chemical composition.

#### 3.1 HTC on biomass

HTC has been widely applied to diverse biomass feedstocks, yielding hydrochar with varied physicochemical properties depending on the material's composition and processing conditions. To provide a clearer synthesis, this section organizes

**Table 2** HTC on agricultural residues – treatment parameters

Authors	Feedstock	HTC temperature and residence time
Arellano <i>et al.</i> <sup>116</sup>	Corn cob	180–350 °C, 4 hours
Guo <i>et al.</i> <sup>117</sup>	Corn stalk	180–290 °C, 8 hours
Reza <i>et al.</i> <sup>118</sup>	Corn stover, <i>Miscanthus</i> , rice hull and switch grass	200–260 °C, 5 minutes
Kambo <i>et al.</i> <sup>119</sup>	<i>Miscanthus</i>	190–260 °C, 5–30 minutes



**Table 3** HTC on woody biomass and forest-derived feedstocks – treatment parameters

Authors	Feedstock	HTC temperature and residence time
Ahmed Khan <i>et al.</i> <sup>55</sup>	Wood fibres	180–260 °C, 3–9 hours
Gao <i>et al.</i> <sup>64</sup>	Eucalyptus bark	220–300 °C, 2–10 hours
Cardarelli <i>et al.</i> <sup>120</sup>	Exhausted chestnut biomass	220 and 270 °C, 1 hour
Hoekman <i>et al.</i> <sup>121</sup>	Mixed woody biomass	215–295 °C, 5–60 minutes
Liu <i>et al.</i> <sup>122</sup>	Poplar wood and holocellulose	210–230 °C, 9 hours
Yang <i>et al.</i> <sup>123</sup>	Bamboo	180–260 °C, 10 minutes
Zhu <i>et al.</i> <sup>124</sup>	Desert shrubs	180–300 °C, 0–2 hours

**Table 4** HTC on agro-industrial by-products – treatment parameters

Authors	Feedstock	HTC temperature and residence time
Satira <i>et al.</i> <sup>125</sup>	Orange peels	150–300 °C, 30–300 minutes
Erdogan <i>et al.</i> <sup>126</sup>	Orange pomace	175–260 °C, 30–120 minutes
Petrović <i>et al.</i> <sup>127</sup>	Grape pomace	180–220 °C, 60 minutes
Fiori <i>et al.</i> <sup>128</sup>	Grape seeds and sugar	180, 220 and 250 °C, 1, 3 and 8 hours
Volpe and Fiori <i>et al.</i> <sup>129,130</sup>	Olive trimmings and olive pulp	120–250 °C, 30 minutes
Chen <i>et al.</i> <sup>131</sup>	Fresh watermelon peel waste	190–260 °C, 1, 6 or 12 hours
Liu <i>et al.</i> <sup>132</sup>	Coconut fibres, dead eucalyptus leaves	150–375 °C, 30 minutes
Parshetti <i>et al.</i> <sup>133</sup>	Palm empty fruit bunches	150–350 °C, 20 minutes

**Table 5** HTC on herbaceous biomass – treatment parameters

Authors	Feedstock	HTC temperature and residence time
Guo <i>et al.</i> <sup>134</sup>	Lawn grass	200–240 °C, 30–180 minutes

**Table 6** HTC on animal- and algae-based biomass – treatment parameters

Authors	Feedstock	HTC temperature and residence time
Lang <i>et al.</i> <sup>135</sup>	Swine manure mixed with sawdust and cornstalk	220 °C, 10 hours
Lang <i>et al.</i> <sup>136</sup>	Swine manure with CaO	180–220 °C, 10 hours
Dieguez-Alonso <i>et al.</i> <sup>137</sup>	Pine wood and corn digestate	200–240 °C, 10 to 360 minutes
Méndez <i>et al.</i> <sup>138</sup>	Macroalgae waste	200 or 230 °C, 2 or 6 hours

the literature into thematic families, highlighting trends in hydrochar yield, morphology and energy potential.

**3.1.1 HTC on agricultural residues.** Agricultural residues such as corncob, corn stalk, corn stover, rice hulls and

**Table 7** HTC on model compounds and paper sludge – treatment parameters

Authors	Feedstock	HTC temperature and residence time
Simsir <i>et al.</i> <sup>139</sup>	Cellulose, chitin, chitosan and beech wood chips	200 °C, 6–48 hours
Falco <i>et al.</i> <sup>140</sup>	Glucose, cellulose and raw rye straw	120–280 °C, 24 hours
Lin <i>et al.</i> <sup>141</sup>	Paper sludge	180–300 °C, 30 minutes

**Table 8** HTC on mixed feedstocks – treatment parameters

Authors	Feedstock	HTC temperature and residence time
Luthfi <i>et al.</i> <sup>72</sup>	<i>Sorghum</i> bagasse and microalgae	175, 250 and 225 °C, 1.25 and 2.75 hours
Reza <i>et al.</i> <sup>118</sup>	Corn stover, <i>Miscanthus</i> , rice hull and switch grass	200–260 °C, 5 minutes
Román <i>et al.</i> <sup>142</sup>	Sunflower stems, walnut shells and olive stones	220 °C, 20 hours
Xiao <i>et al.</i> <sup>143</sup>	Corn stalk and <i>Tamarix ramosissima</i>	250 °C, 4 hours
Nakason <i>et al.</i> <sup>144</sup>	Coconut husk and rice husk	140–200 °C, 1 to 4 hours
Cao <i>et al.</i> <sup>145</sup>	Bark mulch and sugar beet pulp	200–250 °C, 3–20 hours
Titirici <i>et al.</i> <sup>146</sup>	Pine needles, orange peels, pine cones and oak leaves	200 °C, 16 hours

**Table 9** HTC on lignin – treatment parameters. As it is possible to observe, the application of HTC on lignin is partially studied. Therefore, it can be an interesting field of future research. HTC on lignin instead of lignocellulose allows the valorisation of a material mainly generated as a side product in the pulp industry. Moreover, HTC applied to more “homogeneous aromatic materials” without the presence of polysaccharides can bring more valuable products

Authors	Feedstock	HTC temperature and residence time
Latham <i>et al.</i> <sup>147</sup>	Kraft lignin from birch, conifer and spruce	260 °C, 4 hours
Kang <i>et al.</i> <sup>148</sup>	Lignin, cellulose, D-xylose and pine woodmeal	225–265 °C, 20 hours

*Miscanthus* are among the most widely studied feedstock for HTC due to their abundance and potential for energy recovery. Across studies, a consistent trend emerges: increasing HTC temperature and residence time typically reduces solid yields due to enhanced decomposition of hemicellulose and cellulose, while improving carbon content, thermal stability and higher heating value (HHV). These feedstocks typically produce hydrochar with dense microsphere morphology and moderate porosity, making them suitable for solid fuel applications. However, ash content can vary depending on the severity of the process and the specific crop residue. Arellano and co-authors<sup>116</sup> treated corncob at temperatures up to 350 °C, observing globular particle formation and reduced



adsorption capacity at higher temperatures. Guo *et al.*<sup>117</sup> demonstrated that severe HTC conditions on corn stalk led to significant decomposition and removal of low-energy components (fragrances and oils), with XRD and FTIR confirming a breakdown of crystalline structure and aromatic recombination. Reza and co-authors<sup>118</sup> included corn stover, *Miscanthus*, rice hull and switch grass in a comparative study, showing complete hemicellulose degradation and lignin enrichment in hydrochar, along with effective leaching of inorganic elements, such as Ca, S, P, Mg and K, while retaining Si and reducing trace heavy metals, addressing environmental concerns in biomass valorisation.

Kambo and co-authors<sup>119</sup> also investigated *Miscanthus* under varying HTC conditions, reporting reduced hydrochar yield with rising temperature, driven by hemicellulose degradation, and increased HHV due to carbon enrichment and ash reduction *via* leaching of alkali/alkaline metals into the aqueous phase. The hydrochar also showed enhanced hydrophobicity, improving its storage stability.

**3.1.2 HTC on woody biomass and forest-derived feedstocks.** Woody biomass and forest-derived feedstocks represent a structurally robust class of materials for HTC. Their high lignin content, low moisture levels – which increases the effective solids concentration during HTC – and dense cellular architecture influence the product characteristics. This section reviews recent HTC studies highlighting how temperature, residence time, and feedstock composition affect carbon yield, morphology and fuel properties.

Rubber wood fibres, studied by Ahmed Khan and co-authors,<sup>55</sup> were subjected to HTC with temperatures up to 260 °C, observing increased carbon content, disrupted crystallinity and microsphere formation, with a low BET surface area due to particle densification. Cardarelli and co-authors<sup>120</sup> conducted HTC at 220 °C and 270 °C with four cycles of water recirculation on exhausted chestnut biomass, observing a reduced yield, but enhanced carbon content and energy density at higher temperatures. Recirculation increased hydrochar yield without significantly affecting the elemental composition or heating value, while ash stabilized. Elevated temperatures improved thermal stability and reduced combustion intensity, indicating better flame control. Hoekman and co-authors<sup>121</sup> and Gao and co-authors<sup>64</sup> both investigated the HTC of woody biomass (mixed woody biomass for Hoekman and eucalyptus bark for Gao) in the temperature range of 215–300 °C, observing a consistent decline in hydrochar yield with increasing severity, alongside enhanced carbon content and energy densification. In both cases, oxygen depletion and increased HHV were attributed to dehydration and decarboxylation, while SEM analysis revealed structural fragmentation and improved hydrophobicity. Liu and co-authors<sup>122</sup> studied poplar wood and holocellulose, highlighting the role of lignin in HTC efficiency. Holocellulose, lacking it, carbonized more readily, forming abundant microspheres and achieving greater oxygen and hydrogen reduction. Yang and co-authors<sup>123</sup> examined bamboo for HTC (180 to 260 °C, 10 minutes), observing an inverse correlation between hydrochar yield and tempera-

ture, while carbon content increased and oxygen decreased, enhancing the fuel properties. Hydrochar produced at 260 °C exhibited energy characteristics comparable to commercial solid fuels, although energy yield declined at higher temperatures, but still echoing the other authors' densification trends, despite differences in feedstock type and reaction duration. Zhu and co-authors<sup>124</sup> explored the HTC of desert shrubs (180 to 300 °C, 0–2 hours), followed by chemical activation with zinc chloride or potassium carbonate, demonstrating that HTC severity directly affects activation efficiency and pore development, with optimal porosity emerging from hydrochar at lower peak temperatures and shorter retention times, as prolonged carbonization increased aromaticity and reduced polar groups, impairing activation efficiency. Although focused on post-treatment, their findings on aromaticity and polarity complement the other authors' structural observations.

**3.1.3 HTC on agro-industrial by-products.** Agro-industrial by-products such as fruit peels and pomace are rich in sugars, pectins, and aromatic compounds, which influence HTC behaviour. Compared to lignocellulosic biomass, these residues often produce hydrochar with moderate to low yield but enhanced surface functionality and porosity, especially when processed at higher temperatures or with chemical additives. A common observation is the formation of amorphous or micro-spherical carbon structures, with increased aromaticity and decarboxylation at elevated temperatures. While their energy content may be lower than their lignocellulosic counterparts, their nutrient content and surface properties make them promising candidates for solid fuel, soil amendment and energy storage.

Citrus residues, including orange peels and pomace, were investigated by Satira and co-authors<sup>125</sup> and Erdogan and co-authors.<sup>126</sup> Both studies reported a decline in hydrochar yield with increasing temperature, while higher temperatures promoted decarboxylation, aromatization and microsphere formation. Erdogan's hydrochars showed lignite-like H/C and O/C ratios and elevated macronutrients (K, P, Ca), suggesting suitability for soil amendment. Satira highlighted the role of acid additives, with sulfuric acid enhancing hydrolysis and acetic acid accelerating degradation, while BET analysis confirmed increased surface area and porosity. Grape-derived residues, studied by Petrović and co-authors<sup>127</sup> and Fiori and co-authors,<sup>128</sup> showed similar temperature-dependent trends: reduced yield but improved carbon content, porosity and HHV. Grape seeds transformed from peat-like to coal-like hydrochar, and sugar-derived chars exhibited higher carbon enrichment but lower yield. Both studies emphasized the trade-off between fuel quality and production efficiency, and Petrović also highlighted the potential for phosphate sorption in soil applications, after appropriate surface modification. Olive pulp and trimmings, investigated by Volpe and Fiori,<sup>129,130</sup> responded to HTC with increased carbonization and HHV, reaching lignite-like properties. A high solid load favoured secondary char formation, enhancing energy density. Ash reduction in the hydrochar was noted as beneficial for combustion, reducing fouling risks in co-firing scenarios. Fruit peels and fibrous residues,



including watermelon peels (Chen and co-authors<sup>131</sup>) and coconut fibre/eucalyptus leaves (Liu and co-authors<sup>132</sup>) showed improved fuel properties with rising temperature, despite lower aromaticity in watermelon-derived char, making them better for fuel application over soil amendment. Liu's study highlighted coconut fibre's superior combustion profile due to lower nitrogen and sulphur, and demonstrated HTC's capacity to homogenize diverse feedstocks into lignite-like fuels. Lignocellulosic agro-industrial residues, such as palm empty fruit bunches (Parshetti and co-authors<sup>133</sup>), exhibited strong carbonization and microsphere formation at elevated temperatures. However, post-HTC activation was necessary to enhance porosity and surface area for energy storage applications, addressing the inherent structural limitations of raw hydrochars.

**3.1.4 HTC on herbaceous biomass.** Herbaceous biomass such as lawn grass tends to have high moisture content and lower lignin levels, leading to faster degradation and lower hydrochar yields. Guo and co-authors<sup>134</sup> conducted HTC of lawn grass. While extended residence time promoted hydrochar formation, it resulted in lower yield. Higher temperatures and longer reaction times increased carbon content due to reduced hydrogen and oxygen loss. After treatment, an absorption peak associated with aromatic ring stretching vibrations emerged, indicating the degradation of the amorphous fraction and concurrent polymerization of chemical components in lawn grass.

**3.1.5 HTC on animal- and algae-based biomass.** Non-plant feedstocks such as swine manure, digestate, and algae present unique challenges due to their high moisture, nitrogen, and inorganic content. Despite lower solid yields, HTC of these materials often results in hydrochar with improved nutrient retention, reduced heavy metal mobility, and enhanced energy density—especially when co-processed with lignocellulosic biomass or additives like CaO. Studies highlight the potential of these hydrochars for soil amendment and waste valorisation, with promising results in terms of phosphorus immobilization, ash stabilization, and combustion safety. However, process conditions must be carefully tuned to balance environmental benefits. Lang and co-authors<sup>135,136</sup> focused on swine manure is either mixed with lignocellulosic biomass (sawdust and cornstalk) or alkaline additives (CaO), highlighting the benefits of co-processing. In the first case, increasing sawdust and cornstalk proportions enhanced dehydration reactions, reduced the H/C ratio and raised the O/C ratio to values resembling lignite. A 3 : 1 swine manure-to-biomass ratio produced hydrochar suitable for soil amendment while meeting legal requirements for heavy metal safety. Mixing biomass with swine manure effectively reduced heavy metal levels and improved hydrochar fuel properties, demonstrating a promising method for sustainable waste management and hydrochar production. In the second study, the addition of CaO increased the hydrochar yield, ash content and pH – favourable for acidic soils – but reduced volatile matter and fixed carbon, likely due to enhanced transfer of organics to liquid and gas phases. Importantly, CaO-assisted HTC immobilized phosphorus and improved nutrient retention, and water-holding

capacity, suggesting benefits for soil amendment and environmental safety. Alonso and co-authors<sup>137</sup> extended this perspective by comparing pine wood and corn digestate, focusing on the role of post-treatment, since washing reduced solid yields by up to 10%, suggesting that condensed volatiles and water-soluble inorganics contribute significantly to initial mass. Interestingly, unwashed hydrochars exhibited earlier secondary oxidation peaks, attributed to surface inorganic species removed during washing. Their findings also align with Lang's observations on pH and ash content. Méndez and co-authors<sup>138</sup> investigated the HTC of industrial macroalgae waste under similar temperature conditions to Lang, observing comparable trends: increased carbon content, reduced O/C and H/C ratios, and enhanced HHV with rising severity. Although hydrochar yield decreased with temperature and time, the resulting materials exhibited improved phosphorus availability and meso- and microporous structures, beneficial for water retention and thermal stability. These properties make algae-derived hydrochars promising for use in arid soils and horticultural growth media, especially when produced at higher temperatures and longer durations.

**3.1.6 HTC on model compounds and paper sludge.** Studies on model compounds and cellulose-rich residues have provided valuable insights into the fundamental mechanisms of HTC, particularly regarding the influence of molecular structure on carbonization behaviour and product morphology. Glucose and cellulose, for instance, consistently form carbon microspheres at elevated temperatures, as shown by both Simsir and co-authors<sup>139</sup> and Falco and co-authors.<sup>140</sup> While glucose requires extended residence times to initiate solid formation due to its high solubility, it eventually yields uniform spheres. Cellulose, by contrast, undergoes earlier fragmentation into nano- and micro-spheres, reflecting its semi-crystalline structure and lower thermal stability compared to chitin-based substrates, while exhibiting a higher degree of aromatization. Chitin and chitosan, investigated by Simsir, exhibit markedly different behaviour. Chitin remains highly recalcitrant due to its stable amide groups and does not form hydrochar, whereas chitosan underwent progressive carbonization with increasing aromatic content. These findings underscore the role of nitrogen content and functional group chemistry in modulating HTC kinetics and hydrochar structure. Falco further bridged the gap between model compounds and real biomass by comparing glucose and cellulose with rye straw, which retained its fibrous morphology at lower temperatures and transitioned to spherical structures, mirroring the behaviour of cellulose. Although not a pure compound, paper sludge shares a high cellulose content and behaves similarly. Lin and co-authors<sup>141</sup> found that increasing temperature reduced volatile matter *via* dehydration and decarboxylation, while fixed carbon content rose. The H/C and O/C atomic ratios of hydrochars approached those of lignite, indicating improved coal rank with higher carbon content, lower oxygen and increased heating value compared to raw sludge. HTC also effectively removed chlorine through high-temperature leaching and enhanced leaching of light metals such as K and Na, mitigat-



ing ash-related issues. These results demonstrated potential for producing cleaner, high-value solid fuels from paper sludge.

**3.1.7 HTC on mixed feedstocks: synergies and comparative insights.** Mixed feedstocks offer a realistic and versatile approach to hydrothermal carbonization, reflecting the heterogeneity of biomass waste streams. Studies investigating combinations of agricultural, forest, and organic residues reveal synergistic effects on hydrochar yield, carbon content, and functional properties. This section synthesizes comparative HTC studies that explore the behaviour of mixed or co-processed biomasses under varying conditions, emphasizing how tailored combinations and treatment conditions shape product quality and potential use. Luthfi and co-authors<sup>72</sup> compared lignocellulosic, *sorghum* bagasse, and non-lignocellulosic biomass, and microalgae: they showed that *sorghum* bagasse retained more energy-rich components, although both decreased with severity, while microalgae had a higher heating value. This yields a hydrochar suitable for steam coal replacement from bagasse and suitable for steam coal and cooking coal at most severe conditions. Sunflower stems, walnut shells and olive stones were used by Román and co-authors<sup>142</sup> to produce microporous activated carbons, demonstrating HTC's versatility in converting lignocellulosic waste into high-surface-area adsorbents for environmental applications. Xiao and co-authors<sup>143</sup> examined agricultural waste (corn stalk) and forest waste (*Tamarix ramosissima*), revealing near-complete hydrolysis of hemicellulose and cellulose and resulting in hydrochars that were predominantly lignin-based. SEM imaging revealed a more uneven and rough surface compared to the original biomass, with numerous microspheres of varying shapes and sizes. Additionally, the higher heating value of the hydrochar increased post-treatment, consistent with enhanced energy density. Coconut husk and rice husk were investigated by Nakason and co-authors<sup>144</sup> who demonstrated that coconut husk exhibits lower yields compared to rice husk across all tested conditions. Cao and co-authors<sup>145</sup> performed HTC on bark mulch and sugar beet pulp in steam or water media, showing that steam promoted more condensed structures and lower H/C and O/C ratios. Feedstock composition influenced outcomes: sugar beet (carbohydrate-rich) and bark (lignocellulosic) both showed carbohydrate depletion and aromatic/alkyl carbon enrichment, with sugar beet retaining more oxygenated groups and bark favouring aromatic enrichment. Titirici and co-authors<sup>146</sup> processed soft (pine needles and orange peels) and hard biomass (pine cones and oak leaves) with citric acid, yielding hydrochars spectroscopically akin to peat. Soft biomass liquefied into hydrophilic carbon nanoparticles (20–200 nm), while hard biomass retained structural integrity, forming mesoporous carbons (10–100 nm pores) comparable to commercial sorbents. All hydrochars exhibited disordered carbon structures without graphene ordering, rich in oxygen-containing functional groups. The nanospheres' hydrophilicity and dispersibility contrast with hard biomass's pore architecture, highlighting feedstock-dependent outcomes for tailored applications in catalysis or adsorption.

Overall, the results summarized across this section indicate a consistent trend in HTC behaviour, regardless of feedstock origin. Increasing temperature and residence time typically enhance the carbonization degree and structural stability of hydrochar but reduce solid yield. The choice of feedstock mainly influences ash and nutrient content, while activation methods can further tune surface area and porosity, demonstrating HTC's versatility in transforming heterogeneous materials into carbon-rich solids. Across studies, hydrochars exhibit promising characteristics for multiple applications: as solid fuel, soil amendments, adsorbents and precursors for advanced materials. Nonetheless, most of these studies remain at lab-scale, with few addressing industrial feasibility or life cycle impacts.

### 3.2 HTC on lignin

Lignin occupies a unique position: it is neither a model compound nor a conventional biomass feedstock, but a complex biopolymer. Unlike cellulose or glucose, lignin is highly heterogeneous and aromatic: for this reason, it is treated separately, as its dynamics diverge significantly from those feedstocks already reviewed.

Latham and co-authors<sup>147</sup> investigated three types of kraft lignin from different biomass sources (birch, conifer and spruce) – revealing that initial morphological differences were largely erased by HTC. Post-treatment, all samples formed amorphous, fused particles with similar surface textures, suggesting that HTC homogenizes lignin's structural variability. However, yield remained dependent on lignin type. The core lignin structure was retained except for the loss of  $\beta$ -O-4 and  $\alpha$ -O-4 linkages and some methoxy groups. Kang and co-authors<sup>148</sup> extended this analysis, comparing lignin with cellulose, D-xylose and pine woodmeal. Hydrochar yields followed lignin > wood meal > cellulose > D-xylose, with lignin's phenolic stability favouring condensation reactions. Higher temperatures increased C content, C/O ratio and energy recovery, yielding hydrochars with higher heating values comparable to medium/high-rank coals. XRD confirmed the crystalline structure breakdown into amorphous components, while excessive temperatures reduced adsorption suitability. D-Xylose hydrochars form microspheres *via* furfural polymerization, while lignin produced a crack-free polyaromatic, cellulose-retained fibrous structure but developed microspheres at higher temperatures, and woodmeal exhibited fewer microspheres and pyrolysis-induced cracks.

Together, these studies underscore lignin's distinctive HTC behaviour: high carbon retention, aromatic condensation, and structural homogenization, making it a promising precursor for energy-dense hydrochar and advanced carbon materials.

### 3.3 HTC-based hydrochar applications

Hydrochar has evolved from being viewed as a low-value byproduct to a multifunctional platform with diverse environmental and catalytic applications. This section compiles recent advances demonstrating how hydrochars – whether used directly or after chemical/thermal activation – can be tailored



for pollutant adsorption, soil amendment, energy storage or catalysis. The studies highlighted reveal how both the choice of feedstock and post-treatment strategy influence surface chemistry, porosity and functional performance, supporting hydrochar's growing role in sustainable material design.

To enhance clarity and facilitate comparative analysis, the section is divided according to the feedstock used in the

hydrothermal treatment – specifically, biomass and lignin, respectively summarized in Tables 10–15 and 16.

**3.3.1 HTC on agricultural residues.** A range of agricultural residues have been hydrothermally carbonized and subsequently modified to enhance their performance in water remediation. Recent advances in HTC applications increasingly focus on post-treatment strategies – such as chemical

**Table 10** HTC on agricultural residues – parameters and applications

Authors	Feedstock	Process parameters	Applications
Khan <i>et al.</i> <sup>105</sup>	Sugarcane bagasse waste	HTC: 200 °C, 2 hours Nitrogen doping with urea	Removal of heavy metals – Pb(II) and Cd(II) from aqueous solutions
Li <i>et al.</i> <sup>110</sup>	Rice straw	HTC: microwave-assisted at 160–200 °C, 40–70 minutes	Removal of organic pollutants (Congo red, berberine hydrochloride and 2-naphthol) and heavy metal (Zn(II) and Cu(II)) from aqueous solutions
Kopp <i>et al.</i> <sup>149</sup>	Brewer's spent grain	HTC: 220 °C, 4 hours with and without FeSO <sub>4</sub> ·7H <sub>2</sub> O Pyrolytic activation at 400 °C for 2 hours	Removal of chlorophenol from aqueous solutions
Abimbola Adebisi <i>et al.</i> <sup>150</sup>	Banana empty fruit bunch	HTC: 220 °C, 12 hours Chemical activation: H <sub>3</sub> PO <sub>4</sub> (90–100 °C, 4 hours)	Removal of Pb(II) and Zn(II) from aqueous solutions
Xue <i>et al.</i> <sup>151</sup>	Peanut hull	HTC: 300 °C, 5 hours Modification with H <sub>2</sub> O <sub>2</sub> (2 hours, room temperature)	Removal of Pb(II), Ni(II), Cd(II), Cu(II) from aqueous solutions
Ramesh <i>et al.</i> <sup>153</sup>	Areca nut husk biomass	HTC: 180–220 °C, 9 hours	Bio-coal, adsorbent for Pb(II), Zn(II), Ni(II), Cr(VI) removal from aqueous solutions

**Table 11** HTC on biomass – parameters and applications

Authors	Feedstock	Process parameters	Applications
Zhang <i>et al.</i> <sup>95</sup>	Eucalyptus sawdust	HTC: 160–250 °C, 1 hour Activation: KOH or HCl, 30 °C, 1 hour	Cr(IV) removal from aqueous solutions
Lei <i>et al.</i> <sup>152</sup>	Corn stalk	HTC: 200 °C, 3–44 hours	Removal of Cr(VI) from aqueous solutions
Liu <i>et al.</i> <sup>154–156</sup>	Pinewood, sawdust and rice husk	HTC: 300 °C, 20 minutes Activation: (i) Na <sub>2</sub> CO <sub>3</sub> , NaHCO <sub>3</sub> and NaOH or (ii) 800 °C, 60 minutes	Removal of Pb(II), Cu(II), phenol
Deng <i>et al.</i> <sup>157</sup>	Sawdust	HTC: 180 °C, 10 hours Activation: HNO <sub>3</sub> and nicotinamide at 25 °C for 12 hours	Removal of Cr(VI) and Sb(V) from aqueous solutions

**Table 12** HTC on agro-industrial by-products – parameters and applications

Authors	Feedstock	Process parameters	Applications
Bibaj <i>et al.</i> <sup>158</sup>	Banana peel waste	HTC: 200 °C, 4 hours Activation: mixed and stirred overnight with H <sub>3</sub> PO <sub>4</sub> + heated under N <sub>2</sub> flow at 400–600 °C for 24 hours	Removal of Ni(II) from aqueous solutions
Zhou <i>et al.</i> <sup>159</sup>	Dehydrated banana peels	HTC: 230 °C, 2 hours with H <sub>3</sub> PO <sub>4</sub>	Removal of Pb(II) from aqueous solutions
Fernandez <i>et al.</i> <sup>160</sup>	Orange peels	HTC: 200 °C, 20 hours Thermal activation: CO <sub>2</sub> flow at 750 °C or air at 300 °C Chemical activation: H <sub>3</sub> PO <sub>4</sub> + N <sub>2</sub> flow at 600 °C	Removal of diclofenac sodium, salicylic acid and flurbiprofen
Islam <i>et al.</i> <sup>161,162</sup>	Palm date seeds and factory-rejected tea	HTC: 200 °C, 5 hours Activation: overnight NaOH + furnace at 800 °C	Removal of methylene blue from aqueous solutions
Liesaini Daefisal <i>et al.</i> <sup>163</sup>	Coconut pulp	HTC: 200 °C, 5 hours	Removal of methylene blue from aqueous solutions
Jain <i>et al.</i> <sup>164,165</sup>	Coconut shells	HTC: 200 °C, 20 minutes ZnCl <sub>2</sub> hydrothermal treatment (200–275 °C, 20 minutes) Physico-chemical activation with N <sub>2</sub> and CO <sub>2</sub>	Removal of rhodamine B, phenol and phenol red from aqueous solutions



**Table 13** HTC on herbaceous and algae-based biomass – parameters and applications

Authors	Feedstock	Process parameters	Applications
Tang <i>et al.</i> <sup>166</sup>	<i>Lentinus edodes</i> waste	HTC: 200 °C, 12 or 24 or 48 hours Activation with Na <sub>2</sub> CO <sub>3</sub> -K <sub>2</sub> CO <sub>3</sub> (600 °C, 2 hours)	Supercapacitor electrodes
Ren <i>et al.</i> <sup>100</sup>	<i>Enteromorpha prolifera</i> macroalgae	HTC: 180 °C, 24 hours Carbonization: 450 °C, 2 hours Activation: KOH at 600–800 °C, 1 hour	Carbon electrodes for energy storage

**Table 14** HTC on model compounds – parameters and applications

Authors	Feedstock	Process parameters	Applications
Luo <i>et al.</i> <sup>167</sup>	Chitosan and urea	HTC: 140 to 200 °C, 10 hours with KOH and acetic acid	Removal of Cr(IV) from aqueous solutions
Wataniyakul <i>et al.</i> <sup>96,168</sup>	(i) Glucose (ii) Defatted rice bran and glucose	HTC: (i) 180–250 °C, 6–24 hours, (ii) 180–250 °C, 1–8 hours Functionalization with H <sub>2</sub> SO <sub>4</sub> (150 °C, 15 hours)	(i) Catalyst support in the conversion of biomass to 5-hydroxymethylfurfural (ii) Catalyst for cellulose hydrolysis

**Table 15** HTC on biomass – parameters and applications

Authors	Feedstock	Process parameters	Applications
Sevilla <i>et al.</i> <sup>111,112</sup>	Eucalyptus sawdust, barley straw, potato starch and cellulose	HTC: 230–250 °C, 2 hours Activation: KOH, 600–800 °C, 1 hour	Soil amendment, productivity enhancement, CO <sub>2</sub> capture
Sun <i>et al.</i> <sup>169</sup>	Hickory wood, bagasse and bamboo	HTC: 200 °C, 5 hours	Soil amendment

**Table 16** HTC on lignin – parameters and applications

Authors	Feedstock	Process parameters	Applications
Rodríguez Correa <i>et al.</i> <sup>170</sup>	Low-sulfonate lignin, alkali kraft lignin, organosolv lignin, indulin AT lignin; beech, pine and oak bark wood	HTC: 220 °C, 1 hour Activation: KOH at 600 °C for 2 hours, followed by HCl treatment under stirring for 30 minutes	Removal of methylene blue from aqueous solutions
Ma <i>et al.</i> <sup>171</sup>	Alkali lignin	HTC: 200 °C, 18 hours Calcination under N <sub>2</sub> : 550–1000 °C, 2 hours	Catalyst for phenol adsorption
Tian <i>et al.</i> <sup>172</sup>	Black liquor and purified lignin	HTC: 150–220 °C, 30 minutes Hexamethylenediamine modification	Removal of Cr(VI) from aqueous solutions
Sangchoom <i>et al.</i> <sup>173</sup>	Lignin waste	HTC: 300–390 °C Activation: KOH at 600–900 °C, 1 hour	Gas storage material for CO <sub>2</sub> adsorption

activation and surface functionalization – as key levers to enhance hydrochar performance. Rather than relying solely on feedstock composition, these approaches allow for precise tuning of adsorption capacity, selectivity and reusability. HTC-derived hydrochars are increasingly recognized as multifunctional materials for environmental remediation: their ability to remove heavy metals and organic pollutants from water systems positions them as sustainable alternatives to conventional adsorbents. Nitrogen and iron-based modification were particularly effective. Khan and co-authors<sup>105</sup> magnetized sugarcane bagasse hydrochar magnetized *via* co-precipitation using FeCl<sub>3</sub>·6H<sub>2</sub>O and FeCl<sub>2</sub>·4H<sub>2</sub>O and subsequently modified with urea (NH<sub>2</sub>CONH<sub>2</sub>) to introduce nitrogen functionalities, yielding a material capable of removing Pb<sup>2+</sup> and Cd<sup>2+</sup>, from aqueous solutions, through electrostatic attraction, while nitro-

gen functionalities formed co-ordinate bonds. Similarly, Kopp and co-authors<sup>149</sup> incorporated FeSO<sub>4</sub>·7H<sub>2</sub>O on brewer's spent grain hydrochar, followed by pyrolytic activation, producing a porous catalyst with uneven iron distribution and dual functionality: adsorption and auto-regeneration for the removal of chlorophenol. Acid and peroxide treatments also proved valuable: Abimbola Adebisi and co-authors<sup>150</sup> activated banana empty fruit bunch with H<sub>3</sub>PO<sub>4</sub>, enhancing the porosity and surface area, to evaluate its efficacy in Pb(II) and Zn(II) removal, with performance scaling with acid concentration and temperature. Xue and co-authors<sup>151</sup> treated peanut hull hydrochar with H<sub>2</sub>O<sub>2</sub>, boosting Pb(II) (Pb > Cu > Cd > Ni), even in multi-metal systems where competition reduced lead uptake, despite a low surface. Morphological evolution during HTC also influenced adsorption: Lei and co-authors<sup>152</sup> showed that corn



stalk hydrochar transitions from a rough and fibrous structure to microspherical structures over time, with interconnected porous networks forming after 26 hours. These features, combined with oxygen-containing groups, facilitated Cr(vi) adsorption *via* protonated surface complexation under acidic conditions, with the pore architecture enhancing accessibility to active sites. Ramesh and co-authors<sup>153</sup> showed that areca nut husk hydrochar, rich in fixed carbon and aromatic domains, outperformed commercial carbon in Pb<sup>2+</sup> and Zn<sup>2+</sup> adsorption, supporting its potential as both a biocoal and a low-cost adsorbent for heavy metal removal from wastewater. Finally, Li and co-authors<sup>110</sup> applied microwave-assisted HTC to rice straw, producing hydrochars with homogeneous heating, moderate carbon content and abundant oxygen groups. These materials effectively removed both organic pollutants (Congo red, berberine hydrochloride and 2-naphthol) and heavy metals (Zn<sup>2+</sup> and Cu<sup>2+</sup>) from aqueous solution, with maximum adsorption capacities shown for Congo red and copper, proving optimum for water remediation. Together, these studies underscore the adaptability of HTC-derived hydrochars from agricultural residues, and the importance of post-treatment strategies in unlocking their full potential for targeted pollutant removal.

**3.3.2 HTC on woody biomass and forest-derived feedstocks.** As with other biomass types, activation strategies – whether alkaline, acidic or nitrogen-based – play a central role in tuning the surface chemistry, porosity, and adsorption behaviour. Recent studies on eucalyptus, pinewood, sawdust, and rice husk demonstrate how HTC-derived hydrochars from these sources can be tailored to remove heavy metals and organic pollutants with high efficiency. As demonstrated by Zhang and co-authors,<sup>95</sup> eucalyptus sawdust hydrochar activated with KOH achieved a Cr(IV) removal efficiency of over 91% under acidic conditions, with the adsorption mechanism attributed to endothermic chemical sorption involving electron exchange. The study highlighted the superior performance of alkaline activation over acidic treatment (HCl), underscoring how surface chemistry can tune adsorption behaviour. Liu and co-authors<sup>154–156</sup> expanded this approach by hydrothermally carbonizing pinewood, sawdust and rice husk followed by activation with a mixture of Na<sub>2</sub>CO<sub>3</sub>, NaHCO<sub>3</sub> and NaOH. Their materials exhibited enriched oxygen-containing functional groups and narrow pore distributions, enabling the effective removal of lead, phenol and copper. Adsorption was strongly pH-dependent, peaking at pH 5.0 for lead and 6.2 for copper – while phenol removal remained stable across acidic conditions due to hydrophobic interactions. Notably, pine-wood-derived hydrochar showed the highest phenol uptake, whereas rice husk excelled in copper adsorption, with performance rivalling commercial adsorbents, showcasing the potential for heavy metal remediation. High-temperature activation at 800 °C further enhanced the surface area and introduced ketene groups, contributing to heterogenous adsorption kinetics and outperforming pyrolytic char-derived adsorbents. Deng and co-authors<sup>157</sup> focused on sawdust hydrochar functionalized with achieving increased surface area and pore volume. The material exhibited enhanced adsorption

capacities for Cr(vi) and Sb(v), which increased with the initial concentration of the ions. Although adsorption efficiency decreased in binary ion systems, the hydrochar could use NaOH, supporting its potential for wastewater treatment applications.

Whether targeting heavy metals or organic pollutants, the interplay between feedstock structure, activation chemistry and solution conditions governs the functional behaviour of these materials, positioning them as robust candidates for sustainable water purification.

**3.3.3 HTC on agro-industrial by-products.** Agro-industrial by-products – such as banana peels, orange peels, palm date seeds, coconut shells and pulp and factory-rejected tea – have proved to be versatile precursors for hydrochars with tailored adsorption properties. When combined with chemical or thermal activation, these materials exhibit high surface areas, tuneable pore structures, and functional groups that enable the efficient removal of heavy metals, dyes and emerging organic contaminants. Phosphoric acid activation was particularly effective in enhancing adsorption performance. Bibaj and co-authors<sup>158</sup> treated banana peel waste-derived hydrochar with H<sub>3</sub>PO<sub>4</sub> at temperatures up to 600 °C, achieving a high surface area (315–320 m<sup>2</sup> g<sup>-1</sup>) and maximum Ni(II) adsorption capacity of 222 mg g<sup>-1</sup> at pH 6. Similarly, Zhou and co-authors<sup>159</sup> applied a one-step HTC with phosphoric acid to fresh or dehydrated banana peels, producing hydrochars with a low BET surface area, but rich in acidic functional groups. These enabled rapid Pb(II) removal through ion exchange and complexation, reaching adsorption equilibrium within 30 minutes. Fernandez and co-authors<sup>160</sup> extended this approach to orange peels (*Citrus sinensis*), combining phosphoric acid activation with thermal treatments under CO<sub>2</sub> and N<sub>2</sub>. Chemically activated hydrochars showed a greater specific surface area and pore volume than those that were only thermally activated and promoted the formation of more spherical particles: this promoted the selective adsorption of pharmaceuticals such as salicylic acid. In contrast diclofenac sodium adsorption was limited by rapid pore saturation and restricted accessibility. Thermally air-activated and chemically activated hydrochars demonstrated superior performance, attributed to their optimized pore structures and surface areas. Beyond phosphoric acid activation, alkaline treatments have also proved effective in enhancing adsorption performance. Islam and co-authors<sup>161,162</sup> applied NaOH activation to mesoporous hydrochar from palm date seed and factory-rejected tea *via* HTC, achieving high surface areas of 1282.49 m<sup>2</sup> g<sup>-1</sup> and strong affinity for methylene blue. For palm date seeds, adsorption followed second-order kinetics, with exothermic behaviour and spontaneity confirmed by negative  $\Delta G$  values. The high surface area and mesoporosity facilitated efficient dye uptake, aligning with physicochemical activation mechanisms. Thermodynamic parameters underscored the feasibility of scaling this process for wastewater treatments. For factory-rejected tea, adsorption tests with methylene blue revealed a rapid initial uptake due to abundant active sites, followed by slowed kinetics from intra-molecular competition. The



material demonstrated exceptional potential for cation dye wastewater treatment. In contrast, Liesaini Daefisal and co-authors<sup>163</sup> showed that even without chemical activation, HTC alone can significantly enhance adsorption properties. Hydrochar produced from coconut pulp exhibited a 99.7% removal efficiency for methylene blue, outperforming the untreated material (87.8%). The improvement was attributed to the increased pore size and volume induced by HTC, suggesting that structural evolution alone can yield functional sorbents under certain conditions. Jain and co-authors<sup>164</sup> adopted a different route, combining HTC of coconut shells using sequential treatments: HTC, followed by ZnCl<sub>2</sub> hydrothermal treatment and physico-chemical activation with N<sub>2</sub> and CO<sub>2</sub> for the removal of rhodamine B. This multi-step strategy enhanced the mesoporosity and preserved oxygenated functional groups, resulting in high adsorption capacities for rhodamine B. Interestingly, the ZnCl<sub>2</sub>-mediated activation enhanced mesoporosity proportionally to oxygen content in the precursor. Adsorption capacity correlated directly with oxygen group density, confirming their role in dye binding efficiency which demonstrates tuneable pore-chemistry control for wastewater remediation applications. They also conducted adsorption tests with phenol and phenol red<sup>165</sup> which confirmed high capacities.

**3.3.4 HTC on herbaceous and algae-based biomass.** While most hydrochar research focuses on pollutant adsorption, a growing number of studies explore its potential in advanced functional applications, such as electrode materials, emphasizing the role of activation strategies and morphological control in enhancing electrochemical performance, as shown by Tang and co-authors<sup>166</sup> and Ren and co-authors.<sup>100</sup> Tang converted *Lentinus edodes* waste into supercapacitors electrodes *via* HTC and Na<sub>2</sub>CO<sub>3</sub>-K<sub>2</sub>CO<sub>3</sub> activation. Prolonged HTC durations shifted the hydrochar morphology from porous carbon to multilayer structures and non-porous microspheres, while molten salt activation enhanced mesopore formation. These mesopores improved electrolyte ion diffusion and reduced charge transfer resistance, yielding materials with high specific capacitance and cycling stability. Ren synthesized N-doped carbon electrodes from *Enteromorpha prolifera* macroalgae biomass hydrochar, followed by further carbonization and KOH activation, yielding a spherical shape, high surface areas, increasing with activation temperature, and tuneable nitrogen content. Electrochemical analysis revealed that the sample demonstrated exceptional cycling stability with 96% capacitance retention after 10 000 cycles, linking nitrogen functionalities and pore structure directly to performance. Together these studies underscore the viability of low-cost renewable biomass sources for sustainable energy storage applications, where HTC serves as a foundation step in tailoring electrode architecture and functionality.

**3.3.5 HTC on model compounds.** Some studies on model compounds address the removal of conventional pollutants such as Cr(vi) – a topic already extensively covered in previous sections. Luo and co-authors<sup>167</sup> synthesized N-doped hydrochar by the HTC of chitosan with urea, acetic acid and KOH,

yielding a gel-like material with low porosity due to the absence of activation. Surface N-species from urea provided abundant active sites, significantly enhancing Cr(vi) adsorption, with optimal removal (90.9%) achieved at 160 °C under acidic conditions. The adsorption process was primarily chemical, supplemented by physical adsorption. NaOH proved to be the most effective desorption agent, maintaining high removal efficiency over five cycles. The recycled hydrochar outperformed many directly carbonized materials in Cr(vi) removal capacity.

Beyond pollutant removal, model compounds also have been explored in functional material design, particularly for acid catalysis, as shown by Wataniyakul and co-authors,<sup>96,168</sup> who explored the synthesis of sulfonated hydrochars from glucose and defatted rice bran. In their first study<sup>96</sup> they investigated the preparation of hydrochar from glucose as a catalyst support in the conversion of biomass to 5-hydroxymethylfurfural (5-HMF) *via* HTC, followed by functionalization with sulfuric acid. The yield was found to increase with increasing temperature. The catalyst was tested for cellulose hydrolysis and fructose dehydration, proving to be good and recyclable after 5 cycles, with acid leaching being the major concern. In the second one,<sup>168</sup> they synthesized an acid sulfonated catalyst of defatted rice bran and glucose, observing a yield decrease with rising temperature, with optimal carbon content at 250 °C and 3 hours-residence time, revealing that temperature played a dominant role in structural evolution. The sulfonated catalyst demonstrated superior cellulose hydrolysis activity compared to commercial alternatives, underscoring HTC's potential for tailored acid catalyst design. Together, these studies demonstrate how HTC applications can extend beyond conventional environmental remediation.

**3.3.6 HTC on mixed feedstocks.** While most HTC studies focus on single feedstock valorisation, a subset of research explores comparative approaches to evaluate performance across different applications. These studies often target non-conventional uses, such as soil amendment and CO<sub>2</sub> capture, where hydrochar properties like water affinity and structural stability play a decisive role. Rather than optimizing porosity or surface area alone, these works emphasize functional compatibility with environmental matrices – soil, air, or aqueous systems – and assess long-term performance under realistic conditions. Sevilla and co-authors<sup>111,112</sup> conducted a comparative study on eucalyptus sawdust and barley straw, potato starch and cellulose. Despite low porosity, the resulting hydrochars exhibited high water affinity and stable adsorption-desorption behaviour over seven cycles. SEM revealed numerous sphere-like microparticles on larger particles. Eucalyptus-derived hydrochar surfaces, rich in hydroxyl groups and with lignin forming the structural core, was selected for further KOH activation due to its low cost and effective CO<sub>2</sub> adsorption capacities – comparable to starch and cellulose-based chars. Sun and co-authors<sup>169</sup> produced hydrochar from hickory wood, bagasse and bamboo *via* HTC. The resulting hydrochars exhibited carbon, hydrogen and oxygen contents favourable for the adsorption of aqueous contaminants. Due to their



acidic nature, these hydrochars were evaluated as soil amendments to optimize soil pH for plant growth. Experimental results indicated no adverse effects on plant development, suggesting their potential use to improve soil quality.

The breadth of applications explored – from water remediation to energy storage and soil enhancement – reflects hydrochar from biomass's evolution into a tuneable material platform. Across feedstocks and activation strategies, HTC enables precise control over surface chemistry and structure, allowing hydrochars to meet diverse functional demands. This convergence of versatility and specificity positions HTC not only as a waste valorisation tool, but as a cornerstone in the design of sustainable carbon-based materials from biomass.

**3.3.7 HTC on lignin.** Despite its structural complexity and aromatic nature, lignin – often regarded as a challenging feedstock – has been increasingly explored for the same functional applications as conventional biomass. Hydrochars derived from lignin have demonstrated promising performance in pollutant adsorption, catalysis and gas storage, suggesting that its chemical distinctiveness does not preclude utility, but rather offers alternative pathways for material design. Rodríguez Correa and co-authors<sup>170</sup> compared various lignins (low sulfonate, alkali kraft, organosolv lignin and indulin AT) and biomasses (beech wood, pine and oak bark), evaluating their performance after HTC and KOH activation, followed by HCl treatment under stirring for 30 minutes. Biomasses produced lower char yields and carbon content than lignins. Lignin-derived hydrochars retained elemental compositions similar to raw lignins, indicating limited decomposition. Surface area and porosity were higher in biomasses due to cellulose content. Activated hydrochar from beech wood, indulin AT and alkali kraft lignin showed the highest adsorption capacity and low ash content. All activated hydrochars were effective in methylene blue uptake. Ma and co-authors<sup>171</sup> extended lignin's role into catalysis, synthesizing iron-doped hydrochars *via* HTC and calcination from alkali lignin with iron nitrate. Phenol adsorption improved with calcination temperature up to 800 °C, and then declined at higher temperatures. Calcination temperature critically affected the activation of potassium peroxymonosulfate (PMS), enabling complete phenol degradation within 20 minutes at 800 °C. The catalyst showed good stability over three cycles, with the 800 °C sample exhibiting the highest catalytic activity. Tian and co-authors<sup>172</sup> focused on Cr(VI) adsorption using hydrochars derived from black liquor and purified lignin, modified with hexamethylenediamine. The resulting materials exhibited abundant adsorption sites and rapid Cr(VI) uptake, with capacities surpassing previously reported hydrochars. Amine modification significantly enhanced performance, especially at higher temperatures, confirming the adsorption process as spontaneous and endothermic. Despite some inhibition from coexisting ions, the materials maintained high Cr(VI) removal rates due to strong selectivity. Black liquor-derived hydrochar outperformed that from purified lignin and showed excellent chemical stability and reusability, highlighting its promise for practical applications. Sangchoom and co-authors<sup>173</sup> investigated lignin

waste's potential for gas storage lignin, turning it into microporous carbons *via* HTC and KOH activation. Thermogravimetric analysis revealed 20 wt% mineral content in raw lignin, fully removed during HTC to yield pure carbonaceous hydrochar. Unlike cellulose-derived carbons, lignin exhibited superior activation resistance, retaining high surface areas under severe conditions. The resulting narrow micropores enhanced CO<sub>2</sub> uptake while hydrogen adsorption scaled linearly with surface area. These structural stability positions hydrothermally treated lignin as a robust precursor for gas-storage materials.

Yet, if lignin-derived hydrochars are ultimately used for the same applications as those from conventional biomass, one might question the rationale for pursuing lignin at all. However, several factors justify this direction. Lignin is abundantly available as a by-product, often underused or incinerated for low-grade energy recovery. Valorising lignin through HTC supports circular economy principles and waste minimization. Moreover, its reactive sites allow for selective functionalization, *i.e.* enabling tailored catalytic behaviour and enhanced selectivity, as seen in PMS activation and Cr(VI) removal. In short, lignin is not merely another feedstock, but a chemically distinct platform that enables new functionalities and supports industrial waste valorisation.

## 4. Carbon spheres *via* HTC

From perfectly round nanospheres to porous, heteroatom-doped microspheres, carbon structures born from hydrothermal carbonization are redefining what we expect from biomass-derived materials.<sup>174–178</sup> This section explores how HTC transforms sugars, cellulose, lignin-rich residues and industrial by-products into highly tuneable carbon spheres, tailored for applications ranging from energy storage and environmental remediation to catalysis and bioimaging – as summarized in Table 17.

Recent advances demonstrate how subtle shifts in feedstock composition, reaction conditions, and post-synthesis treatment can influence morphology, surface chemistry and performance. Through a selection of emblematic studies, we uncover how researchers are harnessing HTC not just as a thermal process, but as a precise design tool for crafting next-generation carbon materials.

Feedstock composition and thermal severity also play a critical role in morphological evolution and carbon yield: Yu and co-authors<sup>179</sup> carried out HTC of cellulose, demonstrating that increased pressure and temperature enhanced the surface area of the carbon sub-micron spheres, promoting the coalescence of carbon spheres of an average diameter of 109 nm at 300 °C. Carbon content rose with thermal severity, while pronounced aromatization and dehydration occurred above 200 °C. Surface O/C ratios were lower than bulk values, indicating preferential cellulose degradation at the surface. This disparity diminished with reaction progression, achieving compositional homogeneity above 200 °C. Critically, carbon spheres



**Table 17** Carbon spheres *via* HTC – parameters, product and possible applications

Authors	Feedstock	Process parameters	Product and possible applications
Wen <i>et al.</i> <sup>97</sup>	Glucose	HTC: 190 °C, 16 hours with acrylic acid	Carbon microspheres as catalyst
Qi <i>et al.</i> <sup>99</sup>	Glucose	HTC: 180 °C, 10 hours	Carbon microspheres as solid catalyst for the dehydration of fructose into 5-HMF
Han <i>et al.</i> <sup>107</sup>	Glucose	HTC: 190 °C, 8 hours with acrylic acid	Carbon microspheres for the chemisorption of uranium from aqueous solutions
Kazak <i>et al.</i> <sup>108</sup>	Vinasse waste	HTC: 180 °C, 12 hours Activation: KOH at 800 °C, 1 hour, under N <sub>2</sub> flow	High surface activated carbon for removal of Victoria Blue B dye from aqueous solutions
Ansari <i>et al.</i> <sup>115</sup>	<i>Stevia rebaudiana</i>	HTC: 180 °C, 1 hour	Carbon dots for cellular bio-imaging
Yu <i>et al.</i> <sup>179</sup>	Cellulose	HTC: 100–300 °C, 1.2 hours	Carbon microspheres
Chowdhury <i>et al.</i> <sup>180</sup>	Raw longan fruit peel and its holocellulose	HTC: 200–300 °C, 24 hours	Carbon microspheres with high thermal stability and electrical conductivity
Rizhikovs <i>et al.</i> <sup>181</sup>	Pelletized grey alder wood	HTC: 180 °C, 1–6 hours Superheated steam activation: 850 °C, 90 minutes	Granular activated microcarbon
Zhang <i>et al.</i> <sup>182</sup>	Glucose	HTC: 190 °C, 5 hours with NH <sub>4</sub> Cl Activation: KOH at 800 °C, 2 hours, under air flow	Irregular amorphous carbon fragments with potential for energy storage applications

formed directly from cellulose matrixes rather than monomer condensation, as evidenced by the formation on the surface of rod cellulose, suggesting that carbon spheres were formed from the original cellulose directly. Instead, Chowdhury and co-authors<sup>180</sup> performed HTC on raw longan fruit peels (LFP) and its holocellulose, showing increased carbon content, but decreased oxygen and hydrogen content – driven by aromatization reactions. Higher temperatures produced smaller, more numerous carbon microspheres *via* cellulose/hemicellulose degradation, with holocellulose-derived chars exhibiting greater microsphere density but lower surface area than lignin-containing LFP chars. Enhanced thermal stability and reduced volatiles correlated with temperature, while electrical conductivity rose slightly across all the samples. Lignin's presence impeded complete carbonization compared to holocellulose, although the surface area increased for both feedstocks at elevated temperatures. Extending this understanding to gas-phase applications, Rizhikovs and co-authors<sup>181</sup> extended this approach to pelletized grey Alder wood, combining HTC with superheated steam activation. Elevated temperatures increased pyrolysis gas emissions and fixed carbon content while reducing char yield, although palletisation-derived cellulose, lignin and polymeric substances enhanced thermal stability and mitigated yield losses. The resulting adsorbents exhibited a tailored pore architecture, with micropore volume identified as a critical metric for industrial gas purification, and thus they are promising products.

Studies have focused on energy storage performance, leveraging nitrogen doping and activation protocols. Zhang and co-authors<sup>182</sup> used NH<sub>4</sub>Cl during the HTC of glucose to promote carbon microspheres (up to 5 μm) formation and nitrogen incorporation, followed by KOH activation. This strategy yielded highly porous, irregular amorphous carbon with enhanced capacitance, where smaller precursor particles correlated with higher surface areas, while nitrogen-doped microspheres exhibited superior capacitance, highlighting their

potential for energy storage applications. In the context of pollutant adsorption, Han and co-authors<sup>107</sup> synthesized carbon microspheres from glucose, using acrylic acid as a comonomer. The material achieved a uranium adsorption capacity 9-fold higher than raw-glucose-derived carbon, driven by spontaneous, endothermic chemisorption *via* carboxyl binding sites. Structural analysis confirmed carboxyl enrichment and enhanced graphitization. The adsorbent maintained excellent reusability over 5 adsorption–desorption cycles in acidic conditions and demonstrated scalability in uranium removal from simulated industrial effluents and seawater. Also Kazak and co-authors<sup>108</sup> synthesized carbonaceous spheres *via* HTC of waste vinasse, followed by KOH activation for Victoria Blue (VB) dye removal. The materials primarily comprised carbon and oxygen, with traces of sulphur, potassium, calcium and nitrogen. KOH activation induced extensive porosity, yielding high-surface-area activated carbon. Adsorption kinetics showed rapid VB uptake at both 115 and 300 mg L<sup>-1</sup> concentrations, attributed to external diffusion to abundant surface sites. The mechanism likely involved electron-sharing interactions between the VB and the carbon matrix. Regeneration using ethanol retained 98% adsorption efficiency over five cycles, demonstrating robust reusability. Beyond adsorption and energy storage, HTC-derived spheres have also been explored for catalytic applications. Qi and co-authors<sup>99</sup> developed carbonaceous microspheres *via* HTC of glucose without further chemical modification and applied them as solid catalysts for the dehydration of fructose into 5-HMF in an ionic liquid at different temperatures. The system remained effective at high fructose concentrations and showed good reusability across five cycles with limited loss of activity, proving that sulfonation was not necessary, gaining an efficient metal-free catalyst for biomass valorisation. Wen and co-authors<sup>97</sup> synthesized carbon microspheres from glucose *via* HTC and explored its catalytic performance. By tuning glucose and acrylic acid, they gained controlled morphology and surface



functionalities. SEM revealed a spherical shape whose size influenced catalytic activity, with smaller spheres outperforming larger ones in nitrobenzene reduction, since smaller sphere size is beneficial for exposing more active sites, thus leading to superior conversion.

Finally, HTC has enabled the synthesis of fluorescent carbon dots for bioimaging. Ansari and co-authors<sup>115</sup> synthesized fluorescent and non-toxic carbon dots using *Stevia rebaudiana* Bertoni *via* HTC. The carbon dots displayed a spherical morphology and FTIR confirmed the presence of surface functional groups such as carboxyl and hydroxyl, with a high carbon and oxygen content, along with K, In, Ca, Mg, P and Cl. The carbon dots showed no living cell cytotoxicity, indicating their potential as non-toxic markers for cellular bioimaging.

These studies show that HTC is not simply a method for carbonization, but a tool for morphological precision: from nanometric spheres to porous microspheres, the ability to modulate structure and chemistry through feedstock selection and reaction design has enabled carbon materials to serve diverse roles – targeting pollutants, ions, molecules or cells. HTC-derived carbon spheres demonstrate that form and function can be co-engineered, unlocking new possibilities for sustainable technologies across disciplines.

## 5. Lignin isolation and valorisation *via* HTC

Building on the paradigm shift towards complete ligno-cellulosic biomass utilization, the focus of recent research has shifted from treating lignin as a waste by-product to harnessing it as a feedstock for advanced functional materials. Hydrothermal processes now play a dual role: facilitating the deconstruction of biomass and enabling the targeted recovery of high-quality lignin directly from the solid phase. This approach, termed “lignin-focused”, underpins the productions of lignin-based micro- and nanospheres – versatile building blocks for catalysis, energy storage, biomedicine and more – summarized in Table 18.

To emphasize the transformative potential of HTT in lignin-focused biorefineries, we begin this section by highlighting particularly comprehensive and impactful studies that take a step forward by isolating lignin directly from hydrochar, a fraction traditionally overlooked in lignin valorisation pathways. Lourencon and co-authors<sup>38</sup> proposed a remarkably integrated and sustainable biorefinery approach centred on the valorisation of lignin, demonstrating an unprecedented combination of extraction and application within a single process framework. Using birch sawdust as biomass feedstock, they performed hydrothermal treatment under optimized conditions, followed by aqueous acetone extraction under ambient temperature and pressure. This mild, green procedure enabled the direct recovery of high-yield, structurally tuneable lignins with well-defined molecular weights and tuneable  $\beta$ -O-4 linkages' content, depending on the severity of the HTC process.

Beyond separation, these lignins were converted into uniform micro- and nanoparticles *via* aerosol flow drying, achieving a 58% reduction in production costs compared to conventional methods. This study stands out among hydrothermal lignin recovery works by not only extracting high-quality lignin from HTC solids (*i.e.* hydrochar), but also directly formulating functional lignin-based materials, thereby closing the loop between isolation and application. In the context of lignin isolation and valorisation *via* hydrothermal treatment, this work represents a unique benchmark for its holistic and scalable design.

Once isolated or pretreated, lignin can be transformed into nanospheres with diverse applications. Several studies have focused on the design of morphologically controlled lignin nanoparticles with surface properties tailored for coatings, biomedical uses and environmental protection. While differing in application targets, these works share a common strategy: leveraging HTC to stabilize lignin's structure and enable downstream functionalization. Ren and co-authors<sup>183</sup> synthesized hydrothermally treated lignin nanospheres (HLNPs) from enzymatically hydrolysed lignin nanoparticles (EHLNPs), incorporating HDTMS, MTMS, PDMS and cellulose nanocrystals, to create robust superhydrophobic coatings. These coatings exhibited UV resistance and abrasion durability, and retained spherical morphology after surface modification, demonstrating the synergy between HLNPs and polymeric additives. Zhang and co-authors<sup>184</sup> produced fluorescent lignin nanoparticles (LFNP) *via* one-pot HTC with citric acid and ethylenediamine. The resulting particles showed stable fluorescence and antioxidant properties, highlighting their potential for biomedical applications. While not targeting biomedical or coating applications directly, Morsali and co-authors<sup>185</sup> synthesized hydroxymethylated lignin nanoparticles (HMLNPs) from softwood kraft lignin, crosslinked *via* HTC, forming carbon-carbon bonds that stabilized particles. Surface modification with GTMA and assembly of silver nanoparticles reduced the sphericity, while redox activity enabled enzyme-mediated phenoxy radical formation, suggesting non-biomedical technical applications with biodegradability potential.

In parallel, lignin-based nanospheres have also proved effective for catalytic activity. Chen and co-authors<sup>186</sup> developed lignin-based phenolic resin (LPR) nanospheres from black liquor lignin, and then loaded Pd nanoparticles *in situ* without additional reducing agents. These Pd@LPR catalysts showed superior activity in reducing toxic Cr(VI) and organic dyes (methyl orange, rhodamine B) compared to lignin-free catalysts, attributed to enhanced reactant diffusion and abundant active sites. The nanocatalysts demonstrated excellent stability and reusability over ten cycles with minimal Pd leaching, highlighting their potential for efficient wastewater treatment and catalytic applications. Pang and co-authors<sup>187</sup> synthesized lignin microspheres (LMS) from poplar kraft lignin *via* HTC, optimizing spheroidization with surfactants. Pd nanoparticles loaded on surfactant-assisted LMS exhibited superior catalytic activity in formic acid degradation compared to their surfactant-free counterparts, which showed no activity. Both catalysts retained morphology and performance over five



**Table 18** Lignin isolation and valorisation via HTC – parameters, product and possible applications

Authors	Feedstock	Process parameters	Product and possible applications
Chen <i>et al.</i> <sup>25</sup> Lourencon <i>et al.</i> <sup>38</sup>	Aspen and eucalyptus Birch sawdust	HTC: 170 °C, 90 minutes HTC: 175–205 °C, 7–137 minutes Aqueous acetone extraction and aerosol flow drying	Spherical lignin nanoparticles Lignin micro- and nanoparticles
Ren <i>et al.</i> <sup>183</sup>	Enzymatic hydrolysis lignin	HTC: 190 °C, 12 hours Incorporation of HDTMS, MTMS, PDMS and cellulose nanocrystals	Hydrothermally treated lignin nanospheres as superhydrophobic coating with UV resistance and robustness
Zhang <i>et al.</i> <sup>184</sup>	Enzymatic hydrolysis lignin	HTC: 180 °C, 4 hours	Fluorescent lignin nanoparticles for biomedical applications
Morsali <i>et al.</i> <sup>185</sup>	Softwood kraft lignin	HTC: 150 °C, overnight	Hydroxymethylated lignin nanoparticles
Chen <i>et al.</i> <sup>186</sup>	Black liquor lignin	HTC: 120 °C, 12 hours Pd loading	Lignin-based phenolic resin nanospheres for wastewater treatment and catalytic applications
Pang <i>et al.</i> <sup>187</sup>	Poplar kraft lignin	HTC: 120–180 °C, 5–30 minutes	Lignin microspheres for catalytic applications
Cui and co-authors <sup>188</sup>	Softwood kraft lignin	HTC: 240 °C, 12 hours Carbonization with urea	Nitrogen-doped carbon spheres for photocatalytic properties
Cha <i>et al.</i> <sup>189</sup>	<i>Miscanthus sacchariflorus</i> 's black liquor	HTC: 121 °C, 1–3 hours with H <sub>2</sub> SO <sub>4</sub>	Lignin microspheres for agricultural aims, heavy metal adsorption and UV blocking
Mao <i>et al.</i> <sup>190</sup>	Enzymatic hydrolysis lignin	HTC: 220–280 °C, 3–7 hours Activation: mixed with KOH, 110 °C, 2 hours	Lignin-derived activated carbon spheres for energy storage and remediation applications
Fan and co-authors <sup>191</sup>	Lignosulphonates	HTC: 250 °C, 60 hours under acidic conditions Carbonization: 900–1550 °C	Anode material for lithium-ion batteries
Fan <i>et al.</i> <sup>192</sup>	Industrial lignin	HTC: 250 °C, 12 hours with aminophenol	Nitrogen-doped carbon microspheres for sodium ion batteries
Gao <i>et al.</i> <sup>193</sup>	Sodium lignosulfonate	HTC: 260 °C, 24 hours Carbonization: 900 °C, 90 minutes Activation: CO <sub>2</sub> at 700 °C, 1 hour	Microspheres of lignin-based porous carbon for carbon dioxide capture
Wang <i>et al.</i> <sup>194–197</sup>	Enzymatic hydrolysis lignin  (iv) Enzymatic hydrolysis lignin and kraft lignin from softwood and hardwood	HTC: (i) 70–190 °C, 12 hours  HTC: (ii) and (iii) 160 °C, 12 hours  HTC: (iv) 120 °C, 12 hours  (i) and (ii) Carbonization: 700–900 °C, 2 hours  (iii) Mixed with urea and carbonization at 600–800 °C under N <sub>2</sub> atmosphere (iv) Carbonization: 900 °C, 2 hours	(i) Lignin nanospheres and carbon nanospheres for superhydrophobic coatings (ii) All-lignin carbon nanospheres to be used in supercapacitors  (iii) Nitrogen-doped lignin nanospheres to be used as electrode (iv) Lignin-based hierarchical porous carbon nanospheres for energy storage, biomedical applications, coatings, optics and bioink
Krutov <i>et al.</i> <sup>198</sup>	Softwoods' acid hydrolysis lignin	HTC: 220 °C, 12 hours with NaOH	Technical hydrolysis lignin for valued-added polymer applications
Agarwal <i>et al.</i> <sup>199</sup>	Poplar wood	HTC: 170 °C, 45 minutes	High-lignin-containing and lignin-free cellulose nanocrystals
Chun Ho <i>et al.</i> <sup>200</sup>	Organosolv lignin	HTC: 200 °C, 5–20 hours with DMSO Carbonization: 800–1600 °C, 1 hour under N <sub>2</sub> atmosphere	Micronized spherical carbon particles
Pierpaoli <i>et al.</i> <sup>201</sup>	Chestnut wood residues	HTC: 200 °C, 2 hours	Isolation of lignin derivatives from hydrochar and characterization

reuse cycles, demonstrating stability without Pd aggregation or leaching. This highlights surfactant-enhanced LMS as robust supports for noble metal catalysts in sustainable chemical processes. Cui and co-authors<sup>188</sup> used acetylated softwood kraft lignin *via* HTC, producing stable lignin-derived carbon spheres (HCLSs). Subsequent co-carbonization with urea formed successfully coated carbon spheres. Overall, this method produces well-defined nitrogen-doped carbon spheres with enhanced photocatalytic properties.

Other studies have focused on carbon microspheres derived from lignin for energy storage and environmental remediation. Cha and co-authors<sup>189</sup> used *Miscanthus sacchariflorus* to produce black liquor to obtain lignin microspheres (LMSs) *via* HTC with sulphuric acid, yielding smooth-surfaced spheres suitable for agricultural drug delivery, heavy metal adsorption, and UV protection in sunscreens. Mao and co-authors<sup>190</sup> applied microwave-assisted HTC and KOH activation to extracted enzymatic hydrolysis lignin to produce lignin-derived



carbon spheres with high surface area and oxygen functionality, demonstrating potential for sustainable energy storage and environmental remediation applications. Fan and co-authors<sup>191</sup> used sodium lignosulphonates to obtain lignin-based carbon microspheres (LNCS) *via* HTC under acidic conditions, followed by carbonization. The resulting microspheres showed uniform morphology and smooth surfaces and an amorphous carbon structure with an increasing graphitization degree at higher temperatures. Electrochemical tests demonstrated high specific capacity and excellent capacity retention, making it a promising low-cost anode material for lithium-ion batteries. They<sup>192</sup> also used industrial lignin with 3-aminophenol as a nitrogen source to produce nitrogen-doped carbon microspheres (NLC) that showed a high capacity even after 300 cycles, making it promising for sodium-ion battery performance, while Gao and co-authors<sup>193</sup> applied HTC on sodium lignosulfonate from industrial waste at varying pH, followed by carbonization and CO<sub>2</sub> activation. Lower pH promoted the formation of agglomerated microspheres. Increased carbon content and reduced oxygen content were observed. Pore structure varied with pH and so did crystallinity and graphitization degree, showing that acid-assisted HTC enables tuneable morphology and surface chemistry in lignin-derived carbon for carbon dioxide capture.

Wang and co-authors have extensively studied lignin-derived carbon nanospheres through a series of systematic investigations, demonstrating that HTC and carbonization preserved the spherical morphology and introduced graphitic domains. Initially<sup>194</sup> they prepared lignin nanospheres *via* enzymatic hydrolysis and self-assembly, followed by HTC, producing stabilized lignin nanospheres that retained their ordered spherical shape, without cross-linking. Increasing HTC temperature reduced particle size and enhanced thermal stability, attributed to covalent cross-linking and lignin condensation. The carbon nanospheres obtained a tuneable size based on the lignin initial concentration, suitable for eco-friendly superhydrophobic coatings, offering an alternative to silica coatings. In a subsequent study,<sup>195</sup> lignin nanospheres from enzymatic hydrolysis lignin were synthesized *via* a solvent exchange method, stabilized through HTC and subsequently carbonized to produce all-lignin carbon nanospheres (LCNS), with a well-defined spherical morphology, narrow micropore distribution and moderate mesoporosity. These LCNS demonstrated outstanding electrochemical performance, with an exceptionally short relaxation time and remarkable cycling stability over 10 000 charge–discharge cycles. Further nitrogen-doping of lignin-derived carbon nanospheres was achieved by incorporating urea after HTC and before carbonization,<sup>196</sup> resulting in homogeneous N integration into the carbon matrix. Micropores were internal to nanospheres, while mesopores arose from aggregation. High nitrogen content increased structural disorder, reducing capacitance at high current densities due to ion diffusion and charge transfer limitations. Nonetheless, nitrogen enhanced electrolyte ion attraction, improving electric double-layer formation, stability and overall electrochemical performance by 40% compared to undoped samples. The spherical mor-

phology remained intact after cycling, supporting their suitability for advanced energy storage. Lastly, comparing kraft lignin (softwood/hardwood) and enzymatic hydrolysis lignin, nanospheres were prepared *via* solvent-shifting, HTC, absolute ethanol treatment and carbonization to yield lignin-based hierarchical porous carbon nanospheres (LHPCS).<sup>197</sup> Hydrothermal treatment fragmented lignin into condensates, depolymerized monomers and sidechain micromolecules, concentrating active hydroxyl and methoxy groups. Post-HTC, the nanospheres maintained their uniform spherical morphology but developed rough surfaces after ethanol detachment. Carbonization caused pore wall collapse, enlarging pore diameter and reducing particle size *via* volatile release. The hierarchical porosity minimized light scattering, enhancing photon capture for optical applications, and enabled rapid heating beneficial for biomedical and desalination uses. LHPCS also matched commercial carbon ink performance in bioink applications and showed promise for energy storage due to interconnected pores. Collectively these studies highlight lignin's versatility in producing structurally and functionally tailored carbon nanospheres with applications spanning coatings, energy storage, optics and biomedicine.

Finally, HTC has also been employed as a tool for chemical upgrading and nanocrystal formation. Krutov and co-authors<sup>198</sup> synthesized technical hydrolysis lignin (THL) from softwoods *via* acid hydrolysis at 0.25 mm (L1) and 0.05 mm (L2), followed by hydrothermal alkaline treatment to convert insoluble THL into low molecular weight, water-soluble lignin free of polysaccharides, ash and extractives, showing that micronization influences hydrothermal upgrading, producing water-soluble lignins suitable for value-added polymer applications. Agarwal and co-authors<sup>199</sup> compared poplar wood high-lignin-containing (HLCNCs) and lignin-free cellulose nanocrystals (LFCNCs) produced *via* HTC and sulfuric acid hydrolysis, finding that lignin-rich CNCs exhibited greater hydrophobicity, thermal stability and dispersibility. Chen and co-authors<sup>25</sup> studied LNPs prepared from aspen and eucalyptus, pretreated *via* HTC. Lignin was extracted and self-assembled in DMSO to form nanoparticles. Hydrothermal pretreatments generated mainly conjugated carbonyl groups and with abundant hydroxyl. Compared to aspen, eucalyptus lignin showed greater cleavage and condensation of aromatic linkages, resulting in increased phenolic hydroxyl content and smaller, more uniform LNPs. Lignin condensation enhanced aromatic hydrophobicity, providing more anchoring sites for self-assembly. Ho and co-authors<sup>200</sup> synthesized micronized spherical carbon particles *via* solvothermal treatment with DMSO and high-temperature carbonization under nitrogen. Key findings include that lignin polymerizes and condenses into crosslinked structures precipitating out of the solution.

Taken together, these studies illustrate how HTC enables the transformation of lignin into structurally precise and functionally diverse lignin spheres: whether targeting coatings, catalysis, energy storage, biomedical use or polymer integration, HTC provides a versatile platform for lignin valorisation across scales and applications.



In the quest to valorise hydrochar and lignin, recent efforts have begun to explore not only the recovery of lignin from hydrothermal systems, but also its deeper characterization as a path toward functional applications.

Pierpaoli and co-authors<sup>201</sup> used chestnut wood residues as feedstock, subjecting them to HTC (200 °C, 2 hours), followed by acetone extraction or mild acidolysis. The hydrochar-derived lignin fractions were recovered in solid form and characterized by means of FTIR, HPSEC, SEM, solubility tests, TGA and 2D HSQC NMR, tracing the structural, morphological and thermal signatures of the isolated materials, revealing the persistence of  $\beta$ -O-4 linkages. This study wants to be a step further in the isolation and valorisation, at the same time, of hydrochar and lignin derivatives.

## 6. Environmental risks and proposed mitigation measures

HTC is widely recognized as green and energy saving when compared to pyrolysis, which requires fully dried biomass and therefore incurs substantial energy penalties.<sup>202–204</sup> In contrast, hydrothermal treatments operate with water as the sole reaction medium and no additional solvents are required, avoiding the energy-intensive drying step that can account for 84.9% of the total energy input in biomass-based fuel production.<sup>205</sup> Beyond HTC specifically, several comprehensive reviews on HTL and HTG have highlighted environmental advantages that are intrinsic to hydrothermal conversion technologies as a whole. Although HTC, HTL and HTG differ in operating conditions and product distribution, they share key sustainability features: the ability to process wet feedstocks, the use of water as the only solvent and the potential for reduced secondary pollution<sup>204</sup> and greenhouse gas emissions.<sup>54</sup> Recent HTL assessments further show that coupling hydrothermal plants with waste-producing facilities can reduce substrate costs, while heat-integration strategies significantly lower the energy required to reach operating temperatures.<sup>206</sup> At the same time, these studies emphasize that downstream management of aqueous phases and co-products remains a critical factor in determining the true environmental performance of hydrothermal processes<sup>202,206,207</sup> which will later be discussed.

Within this broader context, the subsequent activation and functionalization steps used to tailor hydrochars introduce additional considerations, as their sustainability strongly depends on the nature of the reagents employed. This section critically evaluates the sustainability profile of the mentioned chemicals, distinguishing between green and environmentally concerning reagents, based on metrics such as toxicity, biodegradability and waste generation.

The classification of reagents presented in this section is grounded in internationally recognized toxicological and environmental data. Specifically, we relied on the Organisation for Economic Co-operation and Development (OECD) assessments, including the Screening Information Data Sets (SIDS)

and the agreed conclusions of the OECD Initial Assessment Meetings (SIAM).<sup>208</sup> These documents provide harmonized evaluations of chemical substances based on standardized testing, covering acute and chronic toxicity, biodegradability, bioaccumulation, and ecotoxicological impact.

This approach ensures that the classification into *green-compatible* or *environmentally concerning* reagents is based on robust, peer-reviewed data and reflects the current international consensus on chemical safety and sustainability.

These compounds are generally considered low-impact or acceptable under green chemistry principles:

- Urea presents several advantages: it is highly water-soluble, exhibits low acute ecotoxicity to aquatic organisms, and undergoes complete degradation in inherent biodegradability tests. Its endogenous nature in mammalian metabolism further supports its low toxicity profile for humans and most animals, making it a suitable candidate for sustainable material modification. However, its environmental impact is not entirely negligible: long-term and indirect effects such as eutrophication, groundwater contamination, soil acidification, and ammonia emissions must be considered.<sup>208</sup> Despite these concerns, when used in closed systems or in low concentrations, urea remains one of the most environmentally acceptable nitrogen sources available. Moreover, green urea synthesis from captured CO<sub>2</sub> and green ammonia is under development.<sup>209</sup>

- FeSO<sub>4</sub>: from a human health perspective, it exhibits low acute toxicity in mammals and no evidence of mutagenicity or carcinogenicity *in vivo*. It is non-irritating in aqueous solutions and its system toxicity is limited to high exposure levels. Environmentally, it is highly water-soluble and rapidly oxidized to Fe(III) in oxygenated media, forming insoluble precipitates. Fe(II) ions can exhibit ecotoxic effects under specific conditions, such as low pH and oxygen levels, where they may cause respiratory inflammation in aquatic species due to colloidal clogging. However, chronic toxicity thresholds for aquatic organisms are above 10 mg L<sup>-1</sup>, suggesting low environmental hazard under standard conditions, but potential risks in sensitive ecosystems. It can be considered a green reagent, provided that its application is well-managed and environmental discharge is minimized.<sup>208</sup>

- H<sub>2</sub>O<sub>2</sub>: it is widely recognized as a green oxidizing agent, due to its simple decomposition into water and oxygen. It is naturally produced by aerobic organisms, does not bioaccumulate and degrades rapidly in air, water and soil. These properties make it highly compatible with green chemistry principles, especially in closed systems. However, it is toxic to aquatic organisms at low concentrations. Chronic exposure may affect sensitive species, particularly in environments lacking biological wastewater treatment. Despite this, rapid degradation and lack of persistent residues justify its classification as green, provided that environmental discharge is controlled.<sup>208</sup>

- Na<sub>2</sub>CO<sub>3</sub> and NaHCO<sub>3</sub>: both compounds are non-toxic, biodegradable, and naturally occurring in mineral deposits and biological systems. Their low corrosivity, high water solu-



bility and minimal aquatic toxicity make them highly compatible with green chemistry principles. They also exhibit low acute toxicity, are non-sensitizing, are commonly used in food and pharmaceuticals, and pose a minimal risk to human health under standard laboratory conditions. Environmentally, they do not bioaccumulate and have negligible impact on ecosystems, if pH levels are controlled.<sup>208</sup>

- Acetic acid: it is a naturally occurring carboxylic acid, fully miscible in water, readily biodegradable and non-bioaccumulative, making it one of the most environmentally compatible acids available for biomass valorisation. From a human health perspective, it exhibits low systemic toxicity and its primary hazard is local corrosivity; however, dilute solutions are widely used in food, pharmaceuticals and cosmetic applications, underscoring its low-risk profile in controlled settings. Environmentally, it is rapidly metabolized by microorganisms in soil and water and it does not persist in sediments or bioaccumulate in aquatic organisms. Its degradation products – carbon dioxide and water – are benign, so it does not contribute to eutrophication. Its use over mineral acids offers several advantages since it provides mild acidification without introducing corrosive residues or toxic anions and it can be easily neutralized with benign bases, like  $\text{Na}_2\text{CO}_3$  and  $\text{NaHCO}_3$ .<sup>208</sup>

- Nicotinamide: it is biologically derived, non-toxic, biodegradable, non-corrosive and non-toxic to aquatic organisms. It is widely used in pharmaceuticals and cosmetics. Its use aligns well with green chemistry principles, especially when compared to synthetic amines or halogenated modifiers.<sup>208</sup>

- NaOH: although highly corrosive, it is non-volatile, non-bioaccumulative and readily neutralized in aqueous systems. It is extensively used in water treatment and industrial processes, and its environmental impact is primarily related to pH shifts, not intrinsic toxicity. From a green chemistry point of view, it is not inherently benign, but its predictable behaviour, low persistence and ease of neutralization make it acceptable when used with proper containment and pH control.<sup>208</sup>

- DMSO: low in acute and chronic toxicity, environmentally it is readily biodegradable and does not bioaccumulate, and its aquatic toxicity is extremely low. It is mobile in soil but does not adsorb to sediments or suspended solids. It is naturally produced by phytoplankton and participates in the global sulphur cycle, further supporting its environmental compatibility.<sup>208</sup>

Other chemicals, on the other hand, pose challenges due to toxicity, corrosiveness or poor biodegradability:

- KOH: similar to NaOH, but more aggressive, it is corrosive to skin and eyes and its release into the environment can cause alkaline pH shifts harmful to aquatic life. It does not bioaccumulate and is not persistent, and its acute toxicity is linked to pH shifts rather than intrinsic toxicity.<sup>208</sup>

- $\text{ZnCl}_2$ : it is a highly soluble and corrosive salt, widely used for the chemical activation of carbon materials. While zinc is an essential micronutrient,  $\text{Zn}^{2+}$  ions are acutely toxic to aquatic organisms.  $\text{ZnCl}_2$  is also corrosive to skin and mucosa, and acutely toxic by inhalation and ingestion. Its use in open systems poses risks of zinc accumulation in sediments and disruption of aquatic ecosystems.<sup>208</sup>

- $\text{H}_2\text{SO}_4$ : it is highly corrosive and hazardous from both a human health and environmental perspective. From a toxicological standpoint, is strongly corrosive to skin, eyes and mucous membranes. Inhalation of aerosolized acid mist can cause severe respiratory irritation and squamous metaplasia and has been associated with laryngeal cancer, leading IARC to classify it as a Group 1 carcinogen. Its primary hazard is local tissue damage, not systemic toxicity. Environmentally, sulfuric acid is fully dissociated in water, forming sulfate ions and hydrated protons. Its ecotoxicity is therefore linked to acidification, not the sulfate itself. Even low concentrations can disrupt fish reproduction, plankton community structure and invertebrate populations. Although sulfate is naturally present in ecosystems, the acidifying potential of  $\text{H}_2\text{SO}_4$  makes it incompatible with green chemistry principles. Its use generates hazardous effluents that require careful neutralization and pH monitoring.<sup>208</sup>

- HCl: is a strong inorganic acid, and while effective, its hazard profile raises significant concerns in the context of green chemistry. From a human health perspective, it is highly corrosive to the skin, eyes and respiratory tract. Inhalation of vapors or aerosols can cause several mucosal irritation. Although systemic toxicity is limited, its local effects are severe, and occupational exposure requires strict containment and personal protective equipment. Environmentally, it is fully dissociated in water, forming chloride ions and hydrated protons. Its ecotoxicity is primarily linked to acidification, not to chloride itself. Even low concentrations can disrupt aquatic ecosystems by lowering pH, affecting enzyme activity, and the reproduction and survival of sensitive species. It does not bioaccumulate, but its reactivity and corrosiveness make it incompatible with uncontrolled or large-scale applications.<sup>208</sup>

- $\text{HNO}_3$ : it is a strong oxidizer with high environmental risk. From a toxicological perspective, it is highly corrosive to the skin, eyes and respiratory tissues. Its inhalation can cause severe respiratory distress. Although systemic toxicity is limited, the local corrosive effects are severe and require strict controls. Environmentally, nitric acid is fully dissociated in water: its acute aquatic toxicity is primarily due to acidification. Chronic exposure to nitrate ions can contribute to eutrophication, oxygen depletion, and disruption of aquatic ecosystems. Nitric acid is not bioaccumulative, but its oxidizing nature, volatility, and contribution to acid rain and nitrate loading make it problematic. Its use generated acidic and nitrate-rich effluents, which require neutralization and careful management to avoid downstream ecological damage.<sup>208</sup>

- Hexamethylenediamine: from a human health perspective, it exhibits moderate acute toxicity *via* the oral and dermal routes, causing severe skin burns, eye damage, and respiratory tract irritation upon exposure. Environmentally, it is readily biodegradable and water-soluble and has low bioaccumulation potential. However, its high solubility and amine reactivity can pose risks to aquatic organisms, especially in poorly managed effluent systems.<sup>208</sup>

- Acrylic acid: it is a highly reactive unsaturated carboxylic acid. From a human health standpoint, it is corrosive to the



skin, eyes and respiratory tract. Inhalation exposure causes degenerative lesions in the mucosa and it shows clastogenic potential *in vitro*, with repeated exposure leading to gastric and renal damage in animal models. Environmentally, it is fully miscible in water, readily biodegradable and not bioaccumulative. However, it exhibits high acute and chronic toxicity to aquatic organisms and ecosystems.<sup>208</sup>

•  $\text{H}_3\text{PO}_4$ : though corrosive, it is less hazardous than mineral acids like  $\text{H}_2\text{SO}_4$  or  $\text{HCl}$ . It is fully miscible in water, does not bioaccumulate and is non-genotoxic. Acute toxicity is moderate and is considered low priority for further toxicological investigation. Environmentally it poses limited direct toxicity; however, its dissociation into phosphate ions contributes to eutrophication and, for this reason, it is best classified here. It should always be used in controlled systems with minimal phosphate release.<sup>208</sup>

To align HTC-derived material development with green chemistry principles, future research should: (i) prioritize benign dopants and activators (such as urea,  $\text{H}_2\text{O}_2$ ,  $\text{FeSO}_4$ ), (ii) explore bio-based alternatives to corrosive acids and metal salts, (iii) implement closed-loop systems for acid recovery and reagent recycling, and (iv) quantify environmental impact using green chemistry metrics such as e-factor, atom economy and life cycle analysis.<sup>210</sup>

Although HTC processes do not employ organic solvents, they inevitably generate substantial volumes of wastewater with a high organic load alongside the solid and gaseous products.<sup>211</sup> This process water cannot be directly discharged into the environment because it contains elevated concentrations of organic matter, including phenols, nitrogen-containing compounds and other potentially toxic substances.<sup>211</sup> At the European level, water protection and the obligations related to wastewater management are defined primarily by Directive 2000/60/EC (Water Framework Directive), which provides a harmonized legal framework for water policy. In the specific context of wastewater treatment and disposal, two additional directives are particularly relevant: Directive 91/271/EEC (Urban Wastewater Treatment Directive) and the Industrial Emissions Directive (IIED, 2010/75/EU). The former regulates the collection, treatment and discharge of urban wastewater and the treatment and discharge of wastewater from selected industrial sectors, while both directives require EU Member States to report regularly on their implementation status. Together, they establish the conditions under which industrial effluents may be discharged into municipal wastewater treatment plants. Annex 1 of the Urban Wastewater Treatment Directive further specifies the requirements for industrial discharges into sewers and municipal WWTPs.<sup>212</sup>

The management of HTC process waters remains one of the major bottlenecks for the commercial deployment of the technology. Several studies have explored the integration of hydrothermal treatments with anaerobic digestion, but the highly variable and unpredictable composition of HTT liquors – rich in short-chain organic acids, oxygenates, N-containing compounds and inorganic materials<sup>207,213,214</sup> – poses significant challenges. While some of these compounds can be effec-

tively degraded anaerobically, others may inhibit microbial activity depending on their concentration.<sup>215</sup> During HTC, macromolecules in the feedstock are hydrolysed into smaller molecules such as sugars, amino acids and fatty acid monomers which can serve as substrates for acidogenesis, acetogenesis and methanogenesis in anaerobic digestion.<sup>207</sup> Reported methane yields vary widely depending on the original feedstock, whereas COD removal efficiencies tend to be less variable.<sup>211</sup> However, the presence of organic acids, total ammonia nitrogen (TAN) and toxic organic compounds such as aldehydes, phenols, alcohols, pyridine and related derivatives<sup>216</sup> may limit energy recovery in anaerobic digestion due to inhibitory effects, and therefore require further investigation. An alternative strategy is the partial or complete recirculation of process water back into the HTC reactor. Although this does not eliminate the need for final wastewater disposal, internal reuse can significantly reduce operating costs.<sup>207,212,214</sup> Additional treatment options include co-digestion of process water with other substrates,<sup>217–219</sup> wet oxidation,<sup>220–222</sup> nutrient recovery with precipitation and crystallization or ammonium stripping,<sup>223–225</sup> and even the use of process water as a liquid fertilizer for the development and growth of plants and fungi.<sup>226–228</sup>

For toxic compounds, such as phenols, dedicated detoxification steps are required, as phenolic substances are highly recalcitrant and persist through conventional treatment processes.<sup>229</sup> Depending on the industrial source, phenol concentrations in discharged wastewaters may reach several thousands ppm. Since many conventional methods remove only up to about 60% of these recalcitrant components,<sup>229,230</sup> emerging cross-disciplinary technologies<sup>227–229</sup> as well as hybrid processes are gaining attention for their higher efficiency, operational flexibility and reduced environmental footprint. These systems typically exploit complementary advantages in reaction kinetics, efficiency, regeneration potential, anti-fouling behaviour and the overall costs.<sup>231</sup>

In summary, the complex composition of HTC process water remains a key barrier to large-scale deployment of the technology. Addressing it will require integrated, adaptable treatment strategies that balance efficiency and environmental performance, while leaving room for further technological innovation.

## 7. Conclusions and future outlook

Hydrothermal treatment is no longer just a preparatory step in biomass valorisation – it is increasingly recognised as a creative axis in the development of functional carbon-based materials. Across this review, we have seen how HTC transcends its conventional role, offering an integrated route to unlock the chemical and structural potential of lignocellulosic residues. Whether isolating structurally preserved lignin, engineering hydrochar with tuned surface functionalities or shaping precise carbon spheres, HTC demonstrates its adaptability, scalability and green credentials.



Through modulated temperature, time and biomass composition researchers have shown how it can sculpt carbon materials with sophisticated architectures: from nanospheres and mesoporous adsorbents to catalytically active solids and energy storage electrodes. In parallel, a renewed focus on lignin-focused strategies has revealed novel ways to recover, characterize and transform this underused aromatic polymer – often within the solid hydrochar fraction, a side stream historically overlooked. What emerges is a shift in mindset: from treating hydrochar as a waste to recognizing it as a versatile product and from isolating lignin as an afterthought to engineering it as a functional platform. Yet challenges remain and lignin valorisation *via* HTC is still fragmented. Bridging this gap will require deeper integration between isolation methods, material applications and life-cycle perspectives. Moreover, the environmental footprint has been overlooked. In response, we have introduced a dedicated section assessing the chemistry profile of reagents used, classifying them as green or environmentally concerning. This addition aims to support more sustainable design choices. Equally crucial is the management of HTC process waters, whose complex composition continues to limit industrial deployment: advancing robust, flexible and regulation-compliant treatment strategies will be essential to ensure that hydrothermal technologies evolve within a truly sustainable framework.

The advancement of lignin-focused biorefineries and carbon material synthesis *via* HTC will benefit from a broad scientific ecosystem. Organic chemists can drive the development of functionalized materials and shape eco-friendly reaction pathways; chemical engineers are essential for scale-up optimization; biotechnologists may contribute to biomedical applications; and agronomists and environmental scientists are critical to assess soil interactions and carbon sequestration. Together, these efforts will help to realize the full potential of hydrothermal biorefineries.

Nonetheless, critical gaps persist. The scale-up of hydrothermal lignin valorisation and hydrochar engineering is still in its infancy, hindered by feedstock variability, process complexity, and the lack of standardized protocols. HTC of herbaceous and algae-based biomass, as well as model compounds, remains underexplored despite their relevance for understanding mechanisms and expanding feedstock diversity. Moreover, comprehensive life cycle and techno-economic assessments are rare but essential to validate the true sustainability of these emerging materials. Bridging these gaps will require coordinated research efforts that span chemistry, engineering, agronomy, and environmental science – laying the groundwork for the next generation of green biorefineries.

## Author contributions

V. P.: conceptualisation, writing (original draft), G. T.: conceptualisation, writing (original draft), supervision, E. J. G.: visualisation, B. L.: writing (review & editing), M. G.: conceptualisation, writing (review & editing), funding acquisition, M. B.:

data curation, M. R.: conceptualisation, writing (original draft), supervision. The manuscript was written through the contributions of all the authors.

## Conflicts of interest

There are no conflicts to declare.

## Abbreviations

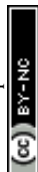
HTT	Hydrothermal treatment
HTC	Hydrothermal carbonization
HTL	Hydrothermal liquefaction
HTG	Hydrothermal gasification
APR	Aqueous phase reforming
HHV	Higher heating value
LFP	Longan fruit peels
VB	Victoria Blue
HLNPs	Hydrothermally treated lignin nanospheres
EHLNPs	Enzymatically hydrolysed lignin nanoparticles
HDTMS	Hexadecyltrimethoxysilane
MTMS	Methyltrimethoxysilane
PDMS	Polydimethylsiloxane
HMLNPs	Hydroxymethylated lignin nanoparticles
LFNP	Fluorescent lignin nanoparticles
HCLs	Lignin-derived carbon spheres
LMS	Lignin microspheres
LNCS	Lignin-based carbon microspheres
NLC	Nitrogen-doped carbon microspheres
LCNS	Lignin carbon nanospheres
LHPCS	Lignin-based hierarchical porous carbon nanospheres
LNPs	Lignin nanoparticles
HLCNCs	High-lignin-containing cellulose nanocrystals
LFCNCs	Lignin-free cellulose nanocrystals
OECD	Organisation for Economic Co-operation and Development
SIDS	Screening Information Data Sets
SIAM	Initial Assessment Meetings
WWTPs	Wastewater treatment plants
TAN	Total ammonia nitrogen

## Data availability

No primary research results, software or code have been included, and no new data were generated or analysed as part of this review.

## Acknowledgements

This research was carried out in the frame of Project ECS 0000025 RomeTechnopole – CUP B83C22002820006, PNRR Mission 4 Component 2 Investment 1.5, funded by the



European Union – NextGenerationEUR. In preparing this manuscript, artificial intelligence-based tools were occasionally employed to assist with linguistic refinement and clarity. All intellectual and scientific content reflects the authors' own work and interpretations.

## References

- B. M. Upton and A. M. Kasko, Strategies for the conversion of lignin to high-value polymeric materials: Review and perspective, *Chem. Rev.*, 2016, 2275–2306, DOI: [10.1021/acs.chemrev.5b00345](https://doi.org/10.1021/acs.chemrev.5b00345), PubMed PMID: 26654678.
- Z. Zhang, V. Terrasson and E. Guénin, Lignin nanoparticles and their nanocomposites, *Nanomaterials*, 2021, **11**, 1336, DOI: [10.3390/nano11051336](https://doi.org/10.3390/nano11051336).
- M. Siddique, H. Ahmad, K. Khan, A. Abbas and S. Khan, M. A. Lignin extraction and green-like lignocellulose biomass pyrolysis as an alternative sustainable biofuel, *MOJ Biol. Med.*, 2023, **8**(2), 87–91, DOI: [10.15406/mojbm.2023.08.00190](https://doi.org/10.15406/mojbm.2023.08.00190).
- N. Sriram and M. Shahidehpour, Renewable Biomass Energy, Report.
- A. T. Hoang, H. C. Ong, I. M. R. Fattah, C. T. Chong, C. K. Cheng, R. Sakthivel, *et al.*, Progress on the lignocellulosic biomass pyrolysis for biofuel production toward environmental sustainability, *Fuel Process. Technol.*, 2021, **223**, 106997, DOI: [10.1016/j.fuproc.2021.106997](https://doi.org/10.1016/j.fuproc.2021.106997).
- S. Tamantini, A. D. Lungo, M. Romagnoli, A. Paletto, M. Keller, J. Bersier, *et al.*, Basic steps to promote biorefinery value chains in forestry in Italy, *Sustainability*, 2021, **13**, 11731, DOI: [10.3390/su132111731](https://doi.org/10.3390/su132111731).
- M. K. Hrnčič, G. Kravanja and Ž. Knez, Hydrothermal treatment of biomass for energy and chemicals, *Energy*, 2016, **116**, 1312–1322, DOI: [10.1016/j.energy.2016.06.148](https://doi.org/10.1016/j.energy.2016.06.148).
- Z. Strassberger, S. Tanase and G. Rothenberg, The pros and cons of lignin valorisation in an integrated biorefinery, *RSC Adv.*, 2014, **4**(48), 25310–25318, DOI: [10.1039/c4ra04747h](https://doi.org/10.1039/c4ra04747h).
- Y. Meng, J. Lu, Y. Cheng, Q. Li and H. Wang, Lignin-based hydrogels: A review of preparation, properties, and application, *Int. J. Biol. Macromol.*, 2019, 1006–1019, DOI: [10.1016/j.ijbiomac.2019.05.198](https://doi.org/10.1016/j.ijbiomac.2019.05.198), PubMed PMID: 31154040.
- V. Dhyani and T. Bhaskar, A comprehensive review on the pyrolysis of lignocellulosic biomass, *Renewable Energy*, 2018, **129**, 695–716, DOI: [10.1016/j.renene.2017.04.035](https://doi.org/10.1016/j.renene.2017.04.035).
- Y. Wang, X. Ji, Q. Wang, Z. Tian, S. Liu, G. Yang, *et al.*, Recent advanced application of lignin nanoparticles in the functional composites: A mini-review, *Int. J. Biol. Macromol.*, 2022, 2498–2511, DOI: [10.1016/j.ijbiomac.2022.10.034](https://doi.org/10.1016/j.ijbiomac.2022.10.034), PubMed PMID: 36223867.
- M. Norgren and H. Edlund, Lignin: Recent advances and emerging applications, *Curr. Opin. Colloid Interface Sci.*, 2014, 409–416, DOI: [10.1016/j.cocis.2014.08.004](https://doi.org/10.1016/j.cocis.2014.08.004).
- W. Schutyser, T. Renders, S. Van Den Bosch, S. F. Koelewijn, G. T. Beckham and B. F. Sels, Chemicals from lignin: An interplay of lignocellulose fractionation, depolymerisation, and upgrading, *Chem. Soc. Rev.*, 2018, 852–908, DOI: [10.1039/c7cs00566k](https://doi.org/10.1039/c7cs00566k), PubMed PMID: 29318245.
- A. Tagami, C. Gioia, M. Lauberts, T. Budnyak, R. Moriana, M. E. Lindström, *et al.*, Solvent fractionation of softwood and hardwood kraft lignins for more efficient uses: Compositional, structural, thermal, antioxidant and adsorption properties, *Ind. Crops Prod.*, 2019, **129**, 123–134, DOI: [10.1016/j.indcrop.2018.11.067](https://doi.org/10.1016/j.indcrop.2018.11.067).
- P. Karagoz, S. Khiawjan, M. P. C. Marques, S. Santzouk, T. D. H. Bugg and G. J. Lye, Pharmaceutical applications of lignin-derived chemicals and lignin-based materials: linking lignin source and processing with clinical indication, *Biomass Convers. Biorefin.*, 2023, **14**, 26553–26574, DOI: [10.1007/s13399-023-03745-5](https://doi.org/10.1007/s13399-023-03745-5).
- M. Siddique, A. Nawaz Mengal, S. Khan, L. Ali Khan and E. Khan Kakar, Pretreatment of lignocellulosic biomass conversion into biofuel and biochemical: a comprehensive review, *Biol. Med.*, 2023, **8**(1), 39–43, DOI: [10.15406/mojbm.2023.08.00181](https://doi.org/10.15406/mojbm.2023.08.00181).
- M. Erfani Jazi, G. Narayanan, F. Aghabozorgi, B. Farajidizaji, A. Aghaei, M. A. Kamyabi, *et al.*, Structure, chemistry and physicochemistry of lignin for material functionalization, *SN Appl. Sci.*, 2019, **1**, 1094, DOI: [10.1007/s42452-019-1126-8](https://doi.org/10.1007/s42452-019-1126-8).
- F. Brienza, D. Cannella, D. Montesdeoca, I. Cybulska and D. P. Debecker, A guide to lignin valorization in biorefineries: traditional, recent, and forthcoming approaches to convert raw lignocellulose into valuable materials and chemicals, *RSC Sustain.*, 2023, 37–90, DOI: [10.1039/d3su00140g](https://doi.org/10.1039/d3su00140g).
- S. Sethupathy, G. Murillo Morales, L. Gao, H. Wang, B. Yang, J. Jiang, *et al.*, Lignin valorization: Status, challenges and opportunities, *Bioresour. Technol.*, 2022, **347**, 126696, DOI: [10.1016/j.biortech.2022.126696](https://doi.org/10.1016/j.biortech.2022.126696), PubMed PMID: 35026423.
- S. Beisl, A. Friedl and A. Miltner, Lignin from micro- To nanosize: Applications, *Int. J. Mol. Sci.*, 2017, **18**, 2367, DOI: [10.3390/ijms18112367](https://doi.org/10.3390/ijms18112367), PubMed PMID: 29117142.
- A. K. Varma, R. Shankar and P. Mondal, A review on pyrolysis of biomass and the impacts of operating conditions on product yield, quality, and upgradation, in *Recent Advancements in Biofuels and Bioenergy Utilization*, Springer Singapore, 2018, pp. 227–259. DOI: [10.1007/978-981-13-1307-3\\_10](https://doi.org/10.1007/978-981-13-1307-3_10).
- Z. Pourmoazzen, H. Sadeghifar, G. Yang and L. Lucia, Cholesterol-modified lignin: A new avenue for green nanoparticles, meltable materials, and drug delivery, *Colloids Surf., B*, 2020, **186**, 110685, DOI: [10.1016/j.colsurfb.2019.110685](https://doi.org/10.1016/j.colsurfb.2019.110685), PubMed PMID: 31812802.
- Q. Tang, Y. Qian, D. Yang, X. Qiu, Y. Qin and M. Zhou, Lignin-based nanoparticles: A review on their preparations and applications, *Polymers*, 2020, 1–22, DOI: [10.3390/polym12112471](https://doi.org/10.3390/polym12112471).
- Y. Chai, Y. Wang, B. Li, W. Qi, R. Su and Z. He, Microfluidic Synthesis of Lignin/Chitosan Nanoparticles



- for the pH-Responsive Delivery of Anticancer Drugs, *Langmuir*, 2021, **37**(23), 7219–7226, DOI: [10.1021/acs.langmuir.1c00778](https://doi.org/10.1021/acs.langmuir.1c00778), PubMed PMID: 34078082.
- 25 Y. Chen, Y. Jiang, D. Tian, J. Hu, J. He, G. Yang, *et al.*, Fabrication of spherical lignin nanoparticles using acid-catalyzed condensed lignins, *Int. J. Biol. Macromol.*, 2020, **164**, 3038–3047, DOI: [10.1016/j.ijbiomac.2020.08.167](https://doi.org/10.1016/j.ijbiomac.2020.08.167), PubMed PMID: 32853606.
- 26 Y. Yin, S. Qin, S. Deng, Z. Li, A. Tang, Q. Li, *et al.*, Thermoresponsive lignin-based polyelectrolyte complexes for the preparation of spherical nanoparticles: Application in pesticide encapsulation, *Int. J. Biol. Macromol.*, 2025, **288**, 138623, DOI: [10.1016/j.ijbiomac.2024.138623](https://doi.org/10.1016/j.ijbiomac.2024.138623).
- 27 M. K. Haider, D. Kharaghani, L. Sun, S. Ullah, M. N. Sarwar, A. Ullah, *et al.*, Synthesized bioactive lignin nanoparticles/polycaprolactone nanofibers: A novel nanobiocomposite for bone tissue engineering, *Biomater. Adv.*, 2023, **1**, 144, DOI: [10.1016/j.bioadv.2022.213203](https://doi.org/10.1016/j.bioadv.2022.213203).
- 28 D. A. Ali and M. M. Mehanna, Role of lignin-based nanoparticles in anticancer drug delivery and bioimaging: An up-to-date review, *Int. J. Biol. Macromol.*, 2022, 934–953, DOI: [10.1016/j.ijbiomac.2022.09.007](https://doi.org/10.1016/j.ijbiomac.2022.09.007), PubMed PMID: 36089088.
- 29 A. Moreno and M. H. Sipponen, Overcoming Challenges of Lignin Nanoparticles: Expanding Opportunities for Scalable and Multifunctional Nanomaterials, *Acc. Chem. Res.*, 2024, **57**(14), 1918–1930, DOI: [10.1021/acs.accounts.4c00206](https://doi.org/10.1021/acs.accounts.4c00206), PubMed PMID: 38965046.
- 30 Y. Wang, Z. Li, D. Yang, X. Qiu, Y. Xie and X. Zhang, Microwave-mediated fabrication of silver nanoparticles incorporated lignin-based composites with enhanced antibacterial activity via electrostatic capture effect, *J. Colloid Interface Sci.*, 2021, **583**, 80–88, DOI: [10.1016/j.jcis.2020.09.027](https://doi.org/10.1016/j.jcis.2020.09.027), PubMed PMID: 32977194.
- 31 S. R. Yearla and K. Padmasree, Preparation and characterization of lignin nanoparticles: evaluation of their potential as antioxidants and UV protectants, *J. Exp. Nanosci.*, 2016, **11**(4), 289–302, DOI: [10.1080/17458080.2015.1055842](https://doi.org/10.1080/17458080.2015.1055842).
- 32 M. S. Alqahtani, A. Alqahtani, A. Al-Thabit, M. Roni and R. Syed, Novel lignin nanoparticles for oral drug delivery, *J. Mater. Chem. B*, 2019, **7**(28), 4461–4473, DOI: [10.1039/c9tb00594c](https://doi.org/10.1039/c9tb00594c).
- 33 D. Tian, J. Hu, J. Bao, R. P. Chandra, J. N. Saddler and C. Lu, Lignin valorization: Lignin nanoparticles as high-value bio-additive for multifunctional nanocomposites, *Biotechnol. Biofuels*, 2017, **10**, 192, DOI: [10.1186/s13068-017-0876-z](https://doi.org/10.1186/s13068-017-0876-z).
- 34 R. Tian, Y. Liu, C. Wang, W. Jiang, S. Janaswamy, G. Yang, *et al.*, Strong, UV-blocking, and hydrophobic PVA composite films containing tunable lignin nanoparticles, *Ind. Crops Prod.*, 2024, **208**, 117842, DOI: [10.1016/j.indcrop.2023.117842](https://doi.org/10.1016/j.indcrop.2023.117842).
- 35 W. Yang, E. Fortunati, F. Bertoglio, J. S. Owczarek, G. Bruni, M. Kozanecki, *et al.*, Polyvinyl alcohol/chitosan hydrogels with enhanced antioxidant and antibacterial properties induced by lignin nanoparticles, *Carbohydr. Polym.*, 2018, **181**, 275–284, DOI: [10.1016/j.carbpol.2017.10.084](https://doi.org/10.1016/j.carbpol.2017.10.084), PubMed PMID: 29253973.
- 36 J. M. Gutiérrez-Hernández, A. Escalante, R. N. Murillo-Vázquez, E. Delgado, F. J. González and G. Toriz, Use of Agave tequilana-lignin and zinc oxide nanoparticles for skin photoprotection, *J. Photochem. Photobiol., B*, 2016, **163**, 156–161, DOI: [10.1016/j.jphotobiol.2016.08.027](https://doi.org/10.1016/j.jphotobiol.2016.08.027), PubMed PMID: 27573548.
- 37 W. D. H. Schneider, A. J. P. Dillon and M. Camassola, Lignin nanoparticles enter the scene: A promising versatile green tool for multiple applications, *Biotechnol. Adv.*, 2021, **47**, 107685, DOI: [10.1016/j.biotechadv.2020.107685](https://doi.org/10.1016/j.biotechadv.2020.107685), PubMed PMID: 33383155.
- 38 T. V. Lourencon, L. G. Greca, D. Tarasov, M. Borrega, T. Tamminen, O. J. Rojas, *et al.*, Lignin-First Integrated Hydrothermal Treatment (HTT) and Synthesis of Low-Cost Biorefinery Particles, *ACS Sustain. Chem. Eng.*, 2020, **8**(2), 1230–1239, DOI: [10.1021/acssuschemeng.9b06511](https://doi.org/10.1021/acssuschemeng.9b06511).
- 39 P. Azadi, O. R. Inderwildi, R. Farnood and D. A. King, Liquid fuels, hydrogen and chemicals from lignin: A critical review, *Renewable Sustainable Energy Rev.*, 2013, 506–523, DOI: [10.1016/j.rser.2012.12.022](https://doi.org/10.1016/j.rser.2012.12.022).
- 40 C. Wang, S. Zhang, S. Huang, Z. Cao, J. Xu and J. Lyu, Effect of hydrothermal treatment on biomass structure with evaluation of post-pyrolysis process for wood vinegar preparation, *Fuel*, 2021, **305**, 121513, DOI: [10.1016/j.fuel.2021.121513](https://doi.org/10.1016/j.fuel.2021.121513).
- 41 D. Sun, Z. W. Lv, J. Rao, R. Tian, S. N. Sun and F. Peng, Effects of hydrothermal pretreatment on the dissolution and structural evolution of hemicelluloses and lignin: A review, *Carbohydr. Polym.*, 2022, **281**, 119050, DOI: [10.1016/j.carbpol.2021.119050](https://doi.org/10.1016/j.carbpol.2021.119050), PubMed PMID: 35074121.
- 42 M. B. Marulasiddeshwara, S. S. Dakshayani, M. N. Sharath Kumar, R. Chethana, P. Raghavendra Kumar and S. Devaraja, Facile one-pot green synthesis, antibacterial, antifungal, antioxidant and antiplatelet activities of lignin capped silver nanoparticles: A promising therapeutic agent, *Mater. Sci. Eng., C*, 2017, **81**, 182–190, DOI: [10.1016/j.msec.2017.07.054](https://doi.org/10.1016/j.msec.2017.07.054), PubMed PMID: 28887963.
- 43 J. Zhao, D. Zheng, Y. Tao, Y. Li, L. Wang, J. Liu, *et al.*, Self-assembled pH-responsive polymeric nanoparticles based on lignin-histidine conjugate with small particle size for efficient delivery of anti-tumor drugs, *Biochem. Eng. J.*, 2020, **156**, 107526, DOI: [10.1016/j.bej.2020.107526](https://doi.org/10.1016/j.bej.2020.107526).
- 44 J. Domínguez-Robles, E. Larrañeta, M. L. Fong, N. K. Martin, N. J. Irwin, P. Mutjé, *et al.*, Lignin/poly(butylene succinate) composites with antioxidant and antibacterial properties for potential biomedical applications, *Int. J. Biol. Macromol.*, 2020, **145**, 92–99, DOI: [10.1016/j.ijbiomac.2019.12.146](https://doi.org/10.1016/j.ijbiomac.2019.12.146), PubMed PMID: 31870868.
- 45 G. Parvathy, A. S. Sethulekshmi, J. S. Jayan, A. Raman and A. Saritha, Lignin based nano-composites: Synthesis and applications, *Process Saf. Environ. Prot.*, 2021, **145**, 395–410, DOI: [10.1016/j.psep.2020.11.017](https://doi.org/10.1016/j.psep.2020.11.017).
- 46 C. Gazzarelli, A. Migliori, P. P. Mazzeo, M. Carcelli, S. Pietarinen, G. Leonardi, *et al.*, Making Agriculture More



- Sustainable: An Environmentally Friendly Approach to the Synthesis of Lignin@Cu Pesticides, *ACS Sustain. Chem. Eng.*, 2020, **8**(39), 14886–14895, DOI: [10.1021/acsschemeng.0c04645](https://doi.org/10.1021/acsschemeng.0c04645).
- 47 C. F. Huang, Y. F. Jiang, G. L. Guo and W. S. Hwang, Development of a yeast strain for xylitol production without hydrolysate detoxification as part of the integration of co-product generation within the lignocellulosic ethanol process, *Bioresour. Technol.*, 2011, **102**(3), 3322–3329, DOI: [10.1016/j.biortech.2010.10.111](https://doi.org/10.1016/j.biortech.2010.10.111), PubMed PMID: 21095119.
- 48 C. C. Okonkwo, V. Ujor and T. C. Ezeji, Production of 2,3-Butanediol from non-detoxified wheat straw hydrolysate: Impact of microbial inhibitors on *Paenibacillus polymyxa* DSM 365, *Ind. Crops Prod.*, 2021, **1**, 159, DOI: [10.1016/j.indcrop.2020.113047](https://doi.org/10.1016/j.indcrop.2020.113047).
- 49 L. Yang, G. Jiang, J. Chen, Z. Xu, Y. Yang, B. Zheng, *et al.*, Production of 1,3-propanediol using enzymatic hydrolysate derived from pretreated distillers' grains, *Bioresour. Technol.*, 2023, **374**, 128773, DOI: [10.1016/j.biortech.2023.128773](https://doi.org/10.1016/j.biortech.2023.128773), PubMed PMID: 36828224.
- 50 K. Dietrich, E. R. Oliveira-Filho, M. J. Dumont, J. G. C. Gomez, M. K. Taciro, L. F. da Silva, *et al.*, Increasing PHB production with an industrially scalable hardwood hydrolysate as a carbon source, *Ind. Crops Prod.*, 2020, **154**, 112703, DOI: [10.1016/j.indcrop.2020.112703](https://doi.org/10.1016/j.indcrop.2020.112703).
- 51 L. Q. Jiang, Z. Fang, F. Guo and L. B. Yang, Production of 2,3-butanediol from acid hydrolysates of *Jatropha* hulls with *Klebsiella oxytoca*, *Bioresour. Technol.*, 2012, **107**, 405–410, DOI: [10.1016/j.biortech.2011.12.083](https://doi.org/10.1016/j.biortech.2011.12.083), PubMed PMID: 22230777.
- 52 B. Zhang, B. K. Biswal, J. Zhang and R. Balasubramanian, Hydrothermal Treatment of Biomass Feedstocks for Sustainable Production of Chemicals, Fuels, and Materials: Progress and Perspectives, *Chem. Rev.*, 2023, **7193–7294**, DOI: [10.1021/acs.chemrev.2c00673](https://doi.org/10.1021/acs.chemrev.2c00673), PubMed PMID: 37159561.
- 53 J. González-Arias, M. E. Sánchez, J. Cara-Jiménez, F. M. Baena-Moreno and Z. Zhang, Hydrothermal carbonization of biomass and waste: A review, *Environ. Chem. Lett.*, 2022, 211–221, DOI: [10.1007/s10311-021-01311-x](https://doi.org/10.1007/s10311-021-01311-x).
- 54 J. O. Ighalo, F. C. Akaeme, J. Georjin, J. S. de Oliveira and D. S. P. Franco, Biomass Hydrochar: A Critical Review of Process Chemistry, Synthesis Methodology, and Applications, *Sustainability*, 2025, **17**, 1660, DOI: [10.3390/su17041660](https://doi.org/10.3390/su17041660).
- 55 T. Ahmed Khan, H. J. Kim, A. Gupta, S. S. Jamari and R. Jose, Synthesis and characterization of carbon microspheres from rubber wood by hydrothermal carbonization, *J. Chem. Technol. Biotechnol.*, 2019, **94**(5), 1374–1383, DOI: [10.1002/jctb.5867](https://doi.org/10.1002/jctb.5867).
- 56 A. M. Borrero-López, E. Masson, A. Celzard and V. Fierro, Modelling the reactions of cellulose, hemicellulose and lignin submitted to hydrothermal treatment, *Ind. Crops Prod.*, 2018, **124**, 919–930, DOI: [10.1016/j.indcrop.2018.08.045](https://doi.org/10.1016/j.indcrop.2018.08.045).
- 57 A. Pandey, S. Negi, P. Binod and C. Larroche, in *Pretreatment of biomass: processes and technologies [Internet]*, ed. A. Pandey, P. Binod, S. Negi and C. Larroche, Elsevier Ltd, 1st edn, 2014, pp. 272. Available from: <https://www.sciencedirect.com/book/9780128000809/pretreatment-of-biomass#book-description>, DOI: [10.1016/C2013-0-13432-0](https://doi.org/10.1016/C2013-0-13432-0).
- 58 S. Sun, X. Cao, S. Sun, F. Xu, X. Song, R. C. Sun, *et al.*, Improving the enzymatic hydrolysis of thermo-mechanical fiber from *Eucalyptus urophylla* by a combination of hydrothermal pretreatment and alkali fractionation, *Biotechnol. Biofuels*, 2014, **7**, 116, DOI: [10.1186/s13068-014-0116-8](https://doi.org/10.1186/s13068-014-0116-8).
- 59 X. Chen, H. Li, S. Sun, X. Cao and R. Sun, Effect of hydrothermal pretreatment on the structural changes of alkaline ethanol lignin from wheat straw, *Sci. Rep.*, 2016, **6**, 39354, DOI: [10.1038/srep39354](https://doi.org/10.1038/srep39354), PubMed PMID: 27982101.
- 60 S. Wang, G. Dai, H. Yang and Z. Luo, Lignocellulosic biomass pyrolysis mechanism: A state-of-the-art review, *Prog. Energy Combust. Sci.*, 2017, 33–86, DOI: [10.1016/j.pecs.2017.05.004](https://doi.org/10.1016/j.pecs.2017.05.004).
- 61 M. Sasaki, T. Adschiri and K. Arai, Fractionation of sugarcane bagasse by hydrothermal treatment. Report.
- 62 N. Zhang, C. Tian, P. Fu, Q. Yuan, Y. Zhang, Z. Li, *et al.*, The Fractionation of Corn Stalk Components by Hydrothermal Treatment Followed by Ultrasonic Ethanol Extraction, *Energies*, 2022, **15**, 2616, DOI: [10.3390/en15072616](https://doi.org/10.3390/en15072616).
- 63 S. Ewanick and R. Bura, Hydrothermal pretreatment of lignocellulosic biomass, in *Bioalcohol Production: Biochemical Conversion of Lignocellulosic Biomass*, Elsevier Inc., 2010, pp. 3–23. DOI: [10.1533/9781845699611.1.3](https://doi.org/10.1533/9781845699611.1.3).
- 64 P. Gao, Y. Zhou, F. Meng, Y. Zhang, Z. Liu, W. Zhang, *et al.*, Preparation and characterization of hydrochar from waste eucalyptus bark by hydrothermal carbonization, *Energy*, 2016, **97**, 238–245, DOI: [10.1016/j.energy.2015.12.123](https://doi.org/10.1016/j.energy.2015.12.123).
- 65 Y. Wang, Y. J. Hu, X. Hao, P. Peng, J. Y. Shi, F. Peng, *et al.*, Hydrothermal synthesis and applications of advanced carbonaceous materials from biomass: a review, *Adv. Compos. Hybrid Mater.*, 2020, 267–284, DOI: [10.1007/s42114-020-00158-0](https://doi.org/10.1007/s42114-020-00158-0).
- 66 I. Cybulska, T. Chaturvedi, G. P. Brudecki, Z. Kádár, A. S. Meyer, R. M. Baldwin, *et al.*, Chemical characterization and hydrothermal pretreatment of *Salicornia bigelovii* straw for enhanced enzymatic hydrolysis and bioethanol potential, *Bioresour. Technol.*, 2014, **153**, 165–172, DOI: [10.1016/j.biortech.2013.11.071](https://doi.org/10.1016/j.biortech.2013.11.071), PubMed PMID: 24362358.
- 67 A. Romani, G. Garrote, J. L. Alonso and J. C. Parajó, Bioethanol production from hydrothermally pretreated *Eucalyptus globulus* wood, *Bioresour. Technol.*, 2010, **101**(22), 8706–8712, DOI: [10.1016/j.biortech.2010.06.093](https://doi.org/10.1016/j.biortech.2010.06.093), PubMed PMID: 20634063.
- 68 H. L. Trajano, N. L. Engle, M. Foston, A. J. Ragauskas, T. J. Tschaplinski and C. E. Wyman, The fate of lignin



- during hydrothermal pretreatment, *Biotechnol. Biofuels*, 2013, **6**, 110, DOI: [10.1186/1754-6834-6-110](https://doi.org/10.1186/1754-6834-6-110).
- 69 M. G. Ma, N. Jia, J. F. Zhu, S. M. Li, F. Peng and R. C. Sun, Isolation and characterization of hemicelluloses extracted by hydrothermal pretreatment, *Bioresour. Technol.*, 2012, **114**, 677–683, DOI: [10.1016/j.biortech.2012.03.048](https://doi.org/10.1016/j.biortech.2012.03.048), PubMed PMID: 22487132.
- 70 J. Mollinedo, T. E. Schumacher and R. Chintala, Influence of feedstocks and pyrolysis on biochar's capacity to modify soil water retention characteristics, *J. Anal. Appl. Pyrolysis*, 2015, **114**, 100–108, DOI: [10.1016/j.jaap.2015.05.006](https://doi.org/10.1016/j.jaap.2015.05.006).
- 71 D. A. Laird, The charcoal vision: A win-win-win scenario for simultaneously producing bioenergy, permanently sequestering carbon, while improving soil and water quality, *Agron. J.*, 2008, **100**(1), 178–181, DOI: [10.2134/agronj2007.0161](https://doi.org/10.2134/agronj2007.0161).
- 72 N. Luthfi, T. Fukushima, X. Wang and K. Takisawa, Hydrochar as an Alternative to Coal: A Comparative Study of Lignocellulosic and Nonlignocellulosic Biomass, *Resources*, 2024, **13**, 49, DOI: [10.3390/resources13040049](https://doi.org/10.3390/resources13040049).
- 73 C. A. Mullen, A. A. Boateng, N. M. Goldberg, I. M. Lima, D. A. Laird and K. B. Hicks, Bio-oil and bio-char production from corn cobs and stover by fast pyrolysis, *Biomass Bioenergy*, 2010, **34**(1), 67–74, DOI: [10.1016/j.biombioe.2009.09.012](https://doi.org/10.1016/j.biombioe.2009.09.012).
- 74 C. Rodríguez Correa, T. Hehr, A. Voglhuber-Slavinsky, Y. Rauscher and A. Kruse, Pyrolysis vs. hydrothermal carbonization: Understanding the effect of biomass structural components and inorganic compounds on the char properties, *J. Anal. Appl. Pyrolysis*, 2019, **140**, 137–147, DOI: [10.1016/j.jaap.2019.03.007](https://doi.org/10.1016/j.jaap.2019.03.007).
- 75 M. Ø Petersen, J. Larsen and M. H. Thomsen, Optimization of hydrothermal pretreatment of wheat straw for production of bioethanol at low water consumption without addition of chemicals, *Biomass Bioenergy*, 2009, **33**(5), 834–840, DOI: [10.1016/j.biombioe.2009.01.004](https://doi.org/10.1016/j.biombioe.2009.01.004).
- 76 A. Moure, P. Gullón, H. Domínguez and J. C. Parajó, Advances in the manufacture, purification and applications of xylo-oligosaccharides as food additives and nutraceuticals, *Process Biochem.*, 2006, 1913–1923, DOI: [10.1016/j.procbio.2006.05.011](https://doi.org/10.1016/j.procbio.2006.05.011).
- 77 R. Kumar, G. Næss and M. Sørensen, Xylooligosaccharides from lignocellulosic biomass and their applications as nutraceuticals: a review on their production, purification, and characterization, *J. Sci. Food Agric.*, 2024, **104**, 7765–7775, DOI: [10.1002/jsfa.13523](https://doi.org/10.1002/jsfa.13523).
- 78 M. J. Vázquez, J. L. Alonso, H. Domínguez and J. C. Parajo, Xylooligo-saccharides: manufacture and applications Production of xylooligosaccharides from lignocellulosic materials, *Report*, 2000, **11**, 387–393, DOI: [10.1016/S0924-2244\(01\)00031-0](https://doi.org/10.1016/S0924-2244(01)00031-0).
- 79 Y. Chen, Y. Xie, K. M. Ajuwon, R. Zhong, T. Li, L. Chen, *et al.*, Xylo-Oligosaccharides, Preparation and Application to Human and Animal Health: A Review, *Front. Nutr.*, 2021, **8**, 731930, DOI: [10.3389/fnut.2021.731930](https://doi.org/10.3389/fnut.2021.731930).
- 80 Y. Sun and J. Cheng, Hydrolysis of lignocellulosic materials for ethanol production: a review q, Report.
- 81 M. Ø. Petersen, J. Larsen and M. H. Thomsen, Optimization of hydrothermal pretreatment of wheat straw for production of bioethanol at low water consumption without addition of chemicals, *Biomass Bioenergy*, 2009, **33**(5), 834–840, DOI: [10.1016/j.biombioe.2009.01.004](https://doi.org/10.1016/j.biombioe.2009.01.004).
- 82 Y. Li, S. S. Bhagwat, Y. R. Cortés-Penã, D. Ki, C. V. Rao, Y. S. Jin, *et al.*, Sustainable Lactic Acid Production from Lignocellulosic Biomass, *ACS Sustain. Chem. Eng.*, 2021, **9**(3), 1341–1351, DOI: [10.1021/acssuschemeng.0c08055](https://doi.org/10.1021/acssuschemeng.0c08055).
- 83 A. G. Daful, M. Loridon and M. R. Chandraratne. Lactic Acid Production from Lignocellulosic Biomass [Internet]. Report. Available from: <https://www.intechopen.com>.
- 84 E. Takata, T. Tsuruoka, K. Tsutsumi, Y. Tsutsumi and K. Tabata, Production of xylitol and tetrahydrofurfuryl alcohol from xylan in napier grass by a hydrothermal process with phosphorus oxoacids followed by aqueous phase hydrogenation, *Bioresour. Technol.*, 2014, **167**, 74–80, DOI: [10.1016/j.biortech.2014.05.112](https://doi.org/10.1016/j.biortech.2014.05.112), PubMed PMID: 24971947.
- 85 D. Umair, R. Kayalvizhi, V. Kumar and J. S. Xylitol, Bioproduction and Applications-A Review, *Front. Sustain.*, 2022, **3**, 826190, DOI: [10.3389/frsus.2022.826190](https://doi.org/10.3389/frsus.2022.826190).
- 86 J. L. Cerioni, M. E. Vallejos, F. E. Felissia, M. C. Area, N. N. Nichio and G. F. Santori, Obtaining Xylitol By Hydrolysis-Hydrogenation Of Liquors Derived From Sugarcane Bagasse, *Chem. Ind. Chem. Eng. Q.*, 2023, **29**(1), 43–52, DOI: [10.2298/CICEQ210721012C](https://doi.org/10.2298/CICEQ210721012C).
- 87 G. Mohan, R. L. Johnson and J. Yu, Conversion of Pine Sawdust into Polyhydroxyalkanoate Bioplastics, *ACS Sustain. Chem. Eng.*, 2021, **9**(25), 8383–8392, DOI: [10.1021/acssuschemeng.1c00009](https://doi.org/10.1021/acssuschemeng.1c00009).
- 88 A. D. Tripathi, P. K. Mishra, K. Khosarvi-Darani, A. Agarwal and V. Paul, Hydrothermal treatment of lignocellulose waste for the production of polyhydroxyalkanoates copolymer with potential application in food packaging, *Trends Food Sci. Technol.*, 2022, 233–250, DOI: [10.1016/j.tifs.2022.03.018](https://doi.org/10.1016/j.tifs.2022.03.018).
- 89 H. Russmayer, M. Egermeier, H. Marx, V. Leitner and M. Sauer, Entirely oil palm-based production of 1,3-propanediol with *Lentilactobacillus diolivorans*, *Environ. Technol. Innovation*, 2023, **29**, 103024, DOI: [10.1016/j.eti.2023.103024](https://doi.org/10.1016/j.eti.2023.103024).
- 90 W. Wang, X. Yu, Y. Wei, R. Ledesma-Amaro and X. J. Ji, Reprogramming the metabolism of *Klebsiella pneumoniae* for efficient 1,3-propanediol production, *Chem. Eng. Sci.*, 2021, **236**, 116539, DOI: [10.1016/j.ces.2021.116539](https://doi.org/10.1016/j.ces.2021.116539).
- 91 X. Wang, L. Zhang, S. Liang, Y. Yin, P. Wang, Y. Li, *et al.*, Enhancing the capability of *Klebsiella pneumoniae* to produce 1, 3-propanediol by overexpression and regulation through CRISPR-dCas9, *Microb. Biotechnol.*, 2022, **15**(7), 2112–2125, DOI: [10.1111/1751-7915.14033](https://doi.org/10.1111/1751-7915.14033), PubMed PMID: 35298861.
- 92 S. H. Hazeena, N. J. Shurpali, H. Siljanen, R. Lappalainen, P. Anoop, V. P. Adarsh, *et al.*, Bioprocess development of



- 2, 3-butanediol production using agro-industrial residues, *Bioprocess Biosyst. Eng.*, 2022, **45**(9), 1527–1537, DOI: [10.1007/s00449-022-02761-5](https://doi.org/10.1007/s00449-022-02761-5), PubMed PMID: 35960335.
- 93 Y. Bai, H. Feng, N. Liu and X. Zhao, Biomass-Derived 2,3-Butanediol and Its Application in Biofuels Production, *Energies*, 2023, **16**, 5802, DOI: [10.3390/en16155802](https://doi.org/10.3390/en16155802).
- 94 S. Xie, Z. Li, G. Zhu, W. Song and C. Yi, Cleaner production and downstream processing of bio-based 2,3-butanediol: A review, *J. Cleaner Prod.*, 2022, **343**, 131033, DOI: [10.1016/j.jclepro.2022.131033](https://doi.org/10.1016/j.jclepro.2022.131033).
- 95 X. Zhang, L. Zhang and A. Li, Eucalyptus sawdust derived biochar generated by combining the hydrothermal carbonization and low concentration KOH modification for hexavalent chromium removal, *J. Environ. Manage.*, 2018, **206**, 989–998, DOI: [10.1016/j.jenvman.2017.11.079](https://doi.org/10.1016/j.jenvman.2017.11.079), PubMed PMID: 30029349.
- 96 P. Wataniyakul, P. Boonnoun, A. T. Quitain, M. Sasaki, T. Kida, N. Laosiripojana, *et al.*, Preparation of hydrothermal carbon as catalyst support for conversion of biomass to 5-hydroxymethylfurfural, *Catal. Commun.*, 2018, **104**, 41–47, DOI: [10.1016/j.catcom.2017.10.014](https://doi.org/10.1016/j.catcom.2017.10.014).
- 97 G. Wen, B. Wang, C. Wang, J. Wang, Z. Tian, R. Schlögl, *et al.*, Hydrothermal Carbon Enriched with Oxygenated Groups from Biomass Glucose as an Efficient Carbocatalyst, *Angew. Chem., Int. Ed.*, 2017, **56**(2), 600–604, DOI: [10.1002/anie.201609047](https://doi.org/10.1002/anie.201609047), PubMed PMID: 27925400.
- 98 F. Su and Y. Guo, Advancements in solid acid catalysts for biodiesel production, *Green Chem.*, 2014, 2934–2957, DOI: [10.1039/c3gc42333f](https://doi.org/10.1039/c3gc42333f).
- 99 X. Qi, N. Liu and Y. Lian, Carbonaceous microspheres prepared by hydrothermal carbonization of glucose for direct use in catalytic dehydration of fructose, *RSC Adv.*, 2015, **5**(23), 17526–17531, DOI: [10.1039/c4ra15296d](https://doi.org/10.1039/c4ra15296d).
- 100 M. Ren, Z. Jia, Z. Tian, D. Lopez, J. Cai, M. M. Titirici, *et al.*, High Performance N-Doped Carbon Electrodes Obtained via Hydrothermal Carbonization of Macroalgae for Supercapacitor Applications, *ChemElectroChem*, 2018, **5**(18), 2686–2693, DOI: [10.1002/celec.201800603](https://doi.org/10.1002/celec.201800603).
- 101 J. Liu, H. Li, H. Zhang, Q. Liu, R. Li, B. Li, *et al.*, Three-dimensional hierarchical and interconnected honeycomb-like porous carbon derived from pomelo peel for high performance supercapacitors, *J. Solid State Chem.*, 2018, **257**, 64–71, DOI: [10.1016/j.jssc.2017.07.033](https://doi.org/10.1016/j.jssc.2017.07.033).
- 102 Y. Hu, H. Liu, Q. Ke and J. Wang, Effects of nitrogen doping on supercapacitor performance of a mesoporous carbon electrode produced by a hydrothermal soft-templating process, *J. Mater. Chem. A*, 2014, **2**(30), 11753–11758, DOI: [10.1039/c4ta01269k](https://doi.org/10.1039/c4ta01269k).
- 103 M. Sevilla and R. Mokaya, Energy storage applications of activated carbons: Supercapacitors and hydrogen storage, *Energy Environ. Sci.*, 2014, 1250–1280, DOI: [10.1039/c3ee43525c](https://doi.org/10.1039/c3ee43525c).
- 104 S. Krstić, M. Kragović, M. Pagnacco, V. Dodevski, B. Kaluderović, M. Momčilović, *et al.*, Hydrothermal synthesized and alkaline activated carbons prepared from glucose and fructose—detailed characterization and testing in heavy metals and methylene blue removal, *Minerals*, 2018, **8**, 246, DOI: [10.3390/min8060246](https://doi.org/10.3390/min8060246).
- 105 M. A. Khan, A. A. Alqadami, M. Otero, M. R. Siddiqui, Z. A. Allothman, I. Alsohaimi, *et al.*, Heteroatom-doped magnetic hydrochar to remove post-transition and transition metals from water: Synthesis, characterization, and adsorption studies, *Chemosphere*, 2019, **218**, 1089–1099, DOI: [10.1016/j.chemosphere.2018.11.210](https://doi.org/10.1016/j.chemosphere.2018.11.210), PubMed PMID: 30609488.
- 106 S. J. Lee, J. H. Park, Y. T. Ahn and J. W. Chung, Comparison of heavy metal adsorption by peat moss and peat moss-derived biochar produced under different carbonization conditions, *Water, Air, Soil Pollut.*, 2015, **226**, 1–11, DOI: [10.1007/s11270-014-2275-4](https://doi.org/10.1007/s11270-014-2275-4).
- 107 B. Han, E. Zhang, G. Cheng, L. Zhang, D. Wang and X. Wang, Hydrothermal carbon superstructures enriched with carboxyl groups for highly efficient uranium removal, *Chem. Eng. J.*, 2018, **338**, 734–744, DOI: [10.1016/j.cej.2018.01.089](https://doi.org/10.1016/j.cej.2018.01.089).
- 108 O. Kazak, Y. R. Eker, H. Bingöl and A. Tor, Preparation of chemically-activated high surface area carbon from waste vinasse and its efficiency as adsorbent material, *J. Mol. Liq.*, 2018, **272**, 189–197, DOI: [10.1016/j.molliq.2018.09.085](https://doi.org/10.1016/j.molliq.2018.09.085).
- 109 J. S. Clemente, S. Beauchemin, T. MacKinnon, J. Martin, C. T. Johnston and B. Joern, Initial biochar properties related to the removal of As, Se, Pb, Cd, Cu, Ni, and Zn from an acidic suspension, *Chemosphere*, 2017, **170**, 216–224, DOI: [10.1016/j.chemosphere.2016.11.154](https://doi.org/10.1016/j.chemosphere.2016.11.154), PubMed PMID: 28006756.
- 110 Y. Li, N. Tsend, T. K. Li, H. Liu, R. Yang, X. Gai, *et al.*, Microwave assisted hydrothermal preparation of rice straw hydrochars for adsorption of organics and heavy metals, *Bioresour. Technol.*, 2019, **273**, 136–143, DOI: [10.1016/j.biortech.2018.10.056](https://doi.org/10.1016/j.biortech.2018.10.056), PubMed PMID: 30423497.
- 111 M. Sevilla and A. B. Fuertes, Sustainable porous carbons with a superior performance for CO<sub>2</sub> capture, *Energy Environ. Sci.*, 2011, **4**(5), 1765–1771, DOI: [10.1039/c0ee00784f](https://doi.org/10.1039/c0ee00784f).
- 112 M. Sevilla, J. A. Maciá-Agulló and A. B. Fuertes, Hydrothermal carbonization of biomass as a route for the sequestration of CO<sub>2</sub>: Chemical and structural properties of the carbonized products, *Biomass Bioenergy*, 2011, **35**(7), 3152–3159, DOI: [10.1016/j.biombioe.2011.04.032](https://doi.org/10.1016/j.biombioe.2011.04.032).
- 113 S. Ahmadian-Fard-Fini, M. Salavati-Niasari and D. Ghanbari, Hydrothermal green synthesis of magnetic Fe<sub>3</sub>O<sub>4</sub>-carbon dots by lemon and grape fruit extracts and as a photoluminescence sensor for detecting of *E. coli* bacteria, *Spectrochim. Acta, Part A*, 2018, **203**, 481–493, DOI: [10.1016/j.saa.2018.06.021](https://doi.org/10.1016/j.saa.2018.06.021), PubMed PMID: 29898431.
- 114 R. Atchudan, T. N. J. I. Edison, K. R. Aseer, S. Perumal and Y. R. Lee, Hydrothermal conversion of Magnolia liliiflora into nitrogen-doped carbon dots as an effective turn-off fluorescence sensing, multi-colour cell imaging and fluorescent ink, *Colloids Surf., B*, 2018, **169**, 321–328, DOI: [10.1016/j.colsurfb.2018.05.032](https://doi.org/10.1016/j.colsurfb.2018.05.032), PubMed PMID: 29800907.



- 115 F. Ansari and D. Kahrizi, Hydrothermal synthesis of highly fluorescent and non-toxic carbon dots using Stevia rebaudiana Bertoni, *Cell. Mol. Biol.*, 2018, **64**(12), 32–36, DOI: [10.14715/cmb/2018.64.12.7](https://doi.org/10.14715/cmb/2018.64.12.7), PubMed PMID: 30301499.
- 116 O. Arellano, M. Flores, J. Guerra, A. Hidalgo, D. Rojas and A. Strubinger, Hydrothermal carbonization of corncob and characterization of the obtained hydrochar, *Chem. Eng. Trans.*, 2016, **50**, 235–240, DOI: [10.3303/CET1650040](https://doi.org/10.3303/CET1650040).
- 117 S. Guo, X. Dong, T. Wu, F. Shi and C. Zhu, Characteristic evolution of hydrochar from hydrothermal carbonization of corn stalk, *J. Anal. Appl. Pyrolysis*, 2015, **116**, 1–9, DOI: [10.1016/j.jaap.2015.10.015](https://doi.org/10.1016/j.jaap.2015.10.015).
- 118 M. T. Reza, J. G. Lynam, M. H. Uddin and C. J. Coronella, Hydrothermal carbonization: Fate of inorganics, *Biomass Bioenergy*, 2013, **49**, 86–94, DOI: [10.1016/j.biombioe.2012.12.004](https://doi.org/10.1016/j.biombioe.2012.12.004).
- 119 H. S. Kambo and A. Dutta, Comparative evaluation of torrefaction and hydrothermal carbonization of lignocellulosic biomass for the production of solid biofuel, *Energy Convers. Manag.*, 2015, **105**, 746–755, DOI: [10.1016/j.enconman.2015.08.031](https://doi.org/10.1016/j.enconman.2015.08.031).
- 120 A. Cardarelli, C. Cordelli, M. Romagnoli, F. Pizzo and M. Barbanera, Investigation of Hydrothermal Carbonization of Exhausted Chestnut from Tannin Extraction: Impact of Process Water Recirculation for Sustainable Fuel Production, *Energies*, 2024, **17**, 2732, DOI: [10.3390/en17112732](https://doi.org/10.3390/en17112732).
- 121 S. K. Hoekman, A. Broch and C. Robbins, Hydrothermal carbonization (HTC) of lignocellulosic biomass, *Energy Fuels*, 2011, **25**(4), 1802–1810, DOI: [10.1021/ef101745n](https://doi.org/10.1021/ef101745n).
- 122 F. Liu and M. Guo, Comparison of the characteristics of hydrothermal carbons derived from holocellulose and crude biomass, *J. Mater. Sci.*, 2015, **50**(4), 1624–1631, DOI: [10.1007/s10853-014-8723-0](https://doi.org/10.1007/s10853-014-8723-0).
- 123 W. Yang, H. Wang, M. Zhang, J. Zhu, J. Zhou and S. Wu, Fuel properties and combustion kinetics of hydrochar prepared by hydrothermal carbonization of bamboo, *Bioresour. Technol.*, 2016, **205**, 199–204, DOI: [10.1016/j.biortech.2016.01.068](https://doi.org/10.1016/j.biortech.2016.01.068), PubMed PMID: 26826960.
- 124 X. Zhu, Y. Liu, F. Qian, C. Zhou, S. Zhang and J. Chen, Role of Hydrochar Properties on the Porosity of Hydrochar-based Porous Carbon for Their Sustainable Application, *ACS Sustain. Chem. Eng.*, 2015, **3**(5), 833–840, DOI: [10.1021/acssuschemeng.5b00153](https://doi.org/10.1021/acssuschemeng.5b00153).
- 125 A. Satira, E. Paone, V. Bressi, D. Iannazzo, F. Marra, P. S. Calabrò, *et al.*, Hydrothermal carbonization as sustainable process for the complete upgrading of orange peel waste into value-added chemicals and bio-carbon materials, *Appl. Sci.*, 2021, **11**, 10983, DOI: [10.3390/app112210983](https://doi.org/10.3390/app112210983).
- 126 E. Erdogan, B. Atila, J. Mumme, M. T. Reza, A. Toptas, M. Elibol, *et al.*, Characterization of products from hydrothermal carbonization of orange pomace including anaerobic digestibility of process liquor, *Bioresour. Technol.*, 2015, **196**, 35–42, DOI: [10.1016/j.biortech.2015.06.115](https://doi.org/10.1016/j.biortech.2015.06.115), PubMed PMID: 26226579.
- 127 J. Petrović, N. Perišić, J. D. Maksimović, V. Maksimović, M. Kragović, M. Stojanović, *et al.*, Hydrothermal conversion of grape pomace: Detailed characterization of obtained hydrochar and liquid phase, *J. Anal. Appl. Pyrolysis*, 2016, **118**, 267–277, DOI: [10.1016/j.jaap.2016.02.010](https://doi.org/10.1016/j.jaap.2016.02.010).
- 128 L. Fiori, D. Basso, D. Castello and M. Baratieri, Hydrothermal carbonization of biomass: Design of a batch reactor and preliminary experimental results, *Chem. Eng. Trans.*, 2014, **37**, 55–60, DOI: [10.3303/CET1437010](https://doi.org/10.3303/CET1437010).
- 129 M. Volpe and L. Fiori, From olive waste to solid biofuel through hydrothermal carbonisation: The role of temperature and solid load on secondary char formation and hydrochar energy properties, *J. Anal. Appl. Pyrolysis*, 2017, **124**, 63–72, DOI: [10.1016/j.jaap.2017.02.022](https://doi.org/10.1016/j.jaap.2017.02.022).
- 130 M. Volpe, L. Fiori, R. Volpe and A. Messineo, Upgrading of olive tree trimmings residue as biofuel by hydrothermal carbonization and torrefaction: A comparative study, *Chem. Eng. Trans.*, 2016, **50**, 13–18, DOI: [10.3303/CET1650003](https://doi.org/10.3303/CET1650003).
- 131 X. Chen, Q. Lin, R. He, X. Zhao and G. Li, Hydrochar production from watermelon peel by hydrothermal carbonization, *Bioresour. Technol.*, 2017, **241**, 236–243, DOI: [10.1016/j.biortech.2017.04.012](https://doi.org/10.1016/j.biortech.2017.04.012), PubMed PMID: 28570889.
- 132 Z. Liu, A. Quek, S. Kent Hoekman and R. Balasubramanian, Production of solid biochar fuel from waste biomass by hydrothermal carbonization, *Fuel*, 2013, 943–949, DOI: [10.1016/j.fuel.2012.07.069](https://doi.org/10.1016/j.fuel.2012.07.069).
- 133 G. K. Parshetti, S. Kent Hoekman and R. Balasubramanian, Chemical, structural and combustion characteristics of carbonaceous products obtained by hydrothermal carbonization of palm empty fruit bunches, *Bioresour. Technol.*, 2013, **135**, 683–689, DOI: [10.1016/j.biortech.2012.09.042](https://doi.org/10.1016/j.biortech.2012.09.042), PubMed PMID: 23127830.
- 134 S. Guo, X. Dong, K. Liu, H. Yu and C. Zhu, Chemical, energetic, and structural characteristics of hydrothermal carbonization solid products for lawn grass, *BioResources*, 2015, **10**(3), 4613–4625, DOI: [10.15376/biores.10.3.4613-4625](https://doi.org/10.15376/biores.10.3.4613-4625).
- 135 Q. Lang, Y. Guo, Q. Zheng, Z. Liu and C. Gai, Co-hydrothermal carbonization of lignocellulosic biomass and swine manure: Hydrochar properties and heavy metal transformation behavior, *Bioresour. Technol.*, 2018, **266**, 242–248, DOI: [10.1016/j.biortech.2018.06.084](https://doi.org/10.1016/j.biortech.2018.06.084), PubMed PMID: 29982044.
- 136 Q. Lang, B. Zhang, Z. Liu, W. Jiao, Y. Xia, Z. Chen, *et al.*, Properties of hydrochars derived from swine manure by CaO assisted hydrothermal carbonization, *J. Environ. Manage.*, 2019, **233**, 440–446, DOI: [10.1016/j.jenvman.2018.12.072](https://doi.org/10.1016/j.jenvman.2018.12.072), PubMed PMID: 30593003.
- 137 A. Dieguez-Alonso, A. Funke, A. Anca-Couce, A. G. Rombolà, G. Ojeda, J. Bachmann, *et al.*, Towards biochar and hydrochar engineering-influence of process conditions on surface physical and chemical properties, thermal stability, nutrient availability, toxicity and wettability, *Energies*, 2018, **11**, 496, DOI: [10.3390/en11030496](https://doi.org/10.3390/en11030496).



- 138 A. Méndez, G. Gascó, B. Ruiz and E. Fuente, Hydrochars from industrial macroalgae “Gelidium Sesquipedale” biomass wastes, *Bioresour. Technol.*, 2019, **275**, 386–393, DOI: [10.1016/j.biortech.2018.12.074](https://doi.org/10.1016/j.biortech.2018.12.074), PubMed PMID: 30602135.
- 139 H. Simsir, N. Eltugral and S. Karagoz, Hydrothermal carbonization for the preparation of hydrochars from glucose, cellulose, chitin, chitosan and wood chips via low-temperature and their characterization, *Bioresour. Technol.*, 2017, **246**, 82–87, DOI: [10.1016/j.biortech.2017.07.018](https://doi.org/10.1016/j.biortech.2017.07.018), PubMed PMID: 28712778.
- 140 C. Falco, N. Baccile and M. M. Titirici, Morphological and structural differences between glucose, cellulose and lignocellulosic biomass derived hydrothermal carbons, *Green Chem.*, 2011, **13**(11), 3273–3281, DOI: [10.1039/c1gc15742f](https://doi.org/10.1039/c1gc15742f).
- 141 Y. Lin, X. Ma, X. Peng, S. Hu, Z. Yu and S. Fang, Effect of hydrothermal carbonization temperature on combustion behavior of hydrochar fuel from paper sludge, *Appl. Therm. Eng.*, 2015, **91**, 574–582, DOI: [10.1016/j.applthermaleng.2015.08.064](https://doi.org/10.1016/j.applthermaleng.2015.08.064).
- 142 S. Román, J. M. Valente Nabais, B. Ledesma, J. F. González, C. Laginhas and M. M. Titirici, Production of low-cost adsorbents with tunable surface chemistry by conjunction of hydrothermal carbonization and activation processes, *Microporous Mesoporous Mater.*, 2013, **165**, 127–133, DOI: [10.1016/j.micromeso.2012.08.006](https://doi.org/10.1016/j.micromeso.2012.08.006).
- 143 L. P. Xiao, Z. J. Shi, F. Xu and R. C. Sun, Hydrothermal carbonization of lignocellulosic biomass, *Bioresour. Technol.*, 2012, **118**, 619–623, DOI: [10.1016/j.biortech.2012.05.060](https://doi.org/10.1016/j.biortech.2012.05.060), PubMed PMID: 22698445.
- 144 K. Nakason, B. Panyapinyopol, V. Kanokkantarapong, N. Viriya-empikul, W. Kraithong and P. Pavasant, Hydrothermal carbonization of unwanted biomass materials: Effect of process temperature and retention time on hydrochar and liquid fraction, *J. Energy Inst.*, 2018, **91**(5), 786–796, DOI: [10.1016/j.joei.2017.05.002](https://doi.org/10.1016/j.joei.2017.05.002).
- 145 X. Cao, K. S. Ro, J. A. Libra, C. I. Kammann, I. Lima, N. Berge, *et al.*, Effects of biomass types and carbonization conditions on the chemical characteristics of hydrochars, *J. Agric. Food Chem.*, 2013, **61**(39), 9401–9411, DOI: [10.1021/jf402345k](https://doi.org/10.1021/jf402345k), PubMed PMID: 24004410.
- 146 M. M. Titirici, A. Thomas, S. H. Yu, J. O. Müller and M. Antonietti, A direct synthesis of mesoporous carbons with bicontinuous pore morphology from crude plant material by hydrothermal carbonization, *Chem. Mater.*, 2007, **19**(17), 4205–4212, DOI: [10.1021/cm0707408](https://doi.org/10.1021/cm0707408).
- 147 K. G. Latham, L. Matsakas, J. Figueira, U. Rova, P. Christakopoulos and S. Jansson, Examination of how variations in lignin properties from Kraft and organosolv extraction influence the physicochemical characteristics of hydrothermal carbon, *J. Anal. Appl. Pyrolysis*, 2021, **1**, 155, DOI: [10.1016/j.jaap.2021.105095](https://doi.org/10.1016/j.jaap.2021.105095).
- 148 S. Kang, X. Li, J. Fan and J. Chang, Characterization of hydrochars produced by hydrothermal carbonization of lignin, cellulose, d-xylose, and wood meal, in *Industrial and Engineering Chemistry Research*, 2012, pp. 9023–9031. DOI: [10.1021/ie300565d](https://doi.org/10.1021/ie300565d).
- 149 M. Kopp, P. Anabalón, S. Rocha, M. E. Gonzalez, J. M. Romero-García, E. Castro, *et al.* Synthesis of Iron Oxide/Activated Hydrochar Composite from Residual Brewery Biomass for Remediation of Water Contaminated with Chlorophenol [Internet]. 2024. Available from: <https://www.researchsquare.com/article/rs-5290572/v1> DOI: [10.21203/rs.3.rs-5290572/v1](https://doi.org/10.21203/rs.3.rs-5290572/v1).
- 150 G. Abimbola Adebisi, Z. Zaman Chowdhury, S. Bee Abd Hamid and E. Ali, Hydrothermally Treated Banana Empty Fruit Bunch Fiber Activated Carbon for Pb(II) and Zn(II) Removal, *BioResources*, 2016, **11**, 9686–9709.
- 151 Y. Xue, B. Gao, Y. Yao, M. Inyang, M. Zhang, A. R. Zimmerman, *et al.*, Hydrogen peroxide modification enhances the ability of biochar (hydrochar) produced from hydrothermal carbonization of peanut hull to remove aqueous heavy metals: Batch and column tests, *Chem. Eng. J.*, 2012, **200–202**, 673–680, DOI: [10.1016/j.cej.2012.06.116](https://doi.org/10.1016/j.cej.2012.06.116).
- 152 Y. Lei, H. Su and R. Tian, Morphology evolution, formation mechanism and adsorption properties of hydrochars prepared by hydrothermal carbonization of corn stalk, *RSC Adv.*, 2016, **6**(109), 107829–107835, DOI: [10.1039/c6ra21607b](https://doi.org/10.1039/c6ra21607b).
- 153 S. Ramesh, P. Sundararaju, K. S. P. Banu, S. Karthikeyan, U. Doraiswamy and K. Soundarapandian, Hydrothermal carbonization of arecanut husk biomass: fuel properties and sorption of metals, *Environ. Sci. Pollut. Res.*, 2019, **26**(4), 3751–3761, DOI: [10.1007/s11356-018-3888-8](https://doi.org/10.1007/s11356-018-3888-8), PubMed PMID: 30539398.
- 154 Z. Liu and F. S. Zhang, Removal of lead from water using biochars prepared from hydrothermal liquefaction of biomass, *J. Hazard. Mater.*, 2009, **167**(1–3), 933–939, DOI: [10.1016/j.jhazmat.2009.01.085](https://doi.org/10.1016/j.jhazmat.2009.01.085), PubMed PMID: 19261383.
- 155 Z. Liu, F. S. Zhang and J. Wu, Characterization and application of chars produced from pinewood pyrolysis and hydrothermal treatment, *Fuel*, 2010, **89**(2), 510–514, DOI: [10.1016/j.fuel.2009.08.042](https://doi.org/10.1016/j.fuel.2009.08.042).
- 156 Z. Liu and F. S. Zhang, Removal of copper(II) and phenol from aqueous solution using porous carbons derived from hydrothermal chars, *Desalination*, 2011, **267**(1), 101–106, DOI: [10.1016/j.desal.2010.09.013](https://doi.org/10.1016/j.desal.2010.09.013).
- 157 J. Deng, X. Li, X. Wei, Y. Liu, J. Liang, Y. Shao, *et al.*, Different adsorption behaviors and mechanisms of a novel amino-functionalized hydrothermal biochar for hexavalent chromium and pentavalent antimony, *Bioresour. Technol.*, 2020, **310**, 123438, DOI: [10.1016/j.biortech.2020.123438](https://doi.org/10.1016/j.biortech.2020.123438), PubMed PMID: 32353770.
- 158 E. Bibaj, K. Lysigaki, J. W. Nolan, M. Seyedsalehi, E. A. Deliyanni, A. C. Mitropoulos, *et al.*, Activated carbons from banana peels for the removal of nickel ions, *Int. J. Environ. Sci. Technol.*, 2019, **16**(2), 667–680, DOI: [10.1007/s13762-018-1676-0](https://doi.org/10.1007/s13762-018-1676-0).
- 159 N. Zhou, H. Chen, J. Xi, D. Yao, Z. Zhou, Y. Tian, *et al.*, Biochars with excellent Pb(II) adsorption property pro-



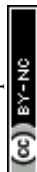
- duced from fresh and dehydrated banana peels via hydrothermal carbonization, *Bioresour. Technol.*, 2017, **232**, 204–210, DOI: [10.1016/j.biortech.2017.01.074](https://doi.org/10.1016/j.biortech.2017.01.074), PubMed PMID: 28231538.
- 160 M. E. Fernandez, B. Ledesma, S. Román, P. R. Bonelli and A. L. Cukierman, Development and characterization of activated hydrochars from orange peels as potential adsorbents for emerging organic contaminants, *Bioresour. Technol.*, 2015, **183**, 221–228, DOI: [10.1016/j.biortech.2015.02.035](https://doi.org/10.1016/j.biortech.2015.02.035), PubMed PMID: 25742754.
- 161 M. A. Islam, I. A. W. Tan, A. Benhouria, M. Asif and B. H. Hameed, Mesoporous and adsorptive properties of palm date seed activated carbon prepared via sequential hydrothermal carbonization and sodium hydroxide activation, *Chem. Eng. J.*, 2015, **270**, 187–195, DOI: [10.1016/j.cej.2015.01.058](https://doi.org/10.1016/j.cej.2015.01.058).
- 162 M. A. Islam, A. Benhouria, M. Asif and B. H. Hameed, Methylene blue adsorption on factory-rejected tea activated carbon prepared by conjunction of hydrothermal carbonization and sodium hydroxide activation processes, *J. Taiwan Inst. Chem. Eng.*, 2015, **52**, 57–64, DOI: [10.1016/j.jtice.2015.02.010](https://doi.org/10.1016/j.jtice.2015.02.010).
- 163 O. Liesaini Daefisal, D. Dama Yanti, M. Alvin Reagen, S. S. Yudha and J. Hendri, Hydrothermal Carbonization of Coconut Pulp and the Adsorption Activity toward Methylene Blue, *Adv. J. Chem., Sect. A*, 2024, **7**, 386–395, DOI: [10.48309/AJCA.2024.433543.1471](https://doi.org/10.48309/AJCA.2024.433543.1471).
- 164 A. Jain, R. Balasubramanian and M. P. Srinivasan, Production of high surface area mesoporous activated carbons from waste biomass using hydrogen peroxide-mediated hydrothermal treatment for adsorption applications, *Chem. Eng. J.*, 2015, **273**, 622–629, DOI: [10.1016/j.cej.2015.03.111](https://doi.org/10.1016/j.cej.2015.03.111).
- 165 A. Jain, R. Balasubramanian and M. P. Srinivasan, Tuning hydrochar properties for enhanced mesopore development in activated carbon by hydrothermal carbonization, *Microporous Mesoporous Mater.*, 2015, **203**(C), 178–185, DOI: [10.1016/j.micromeso.2014.10.036](https://doi.org/10.1016/j.micromeso.2014.10.036).
- 166 D. Tang, Y. Luo, W. Lei, Q. Xiang, W. Ren, W. Song, *et al.*, Hierarchical porous carbon materials derived from waste lentinus edodes by a hybrid hydrothermal and molten salt process for supercapacitor applications, *Appl. Surf. Sci.*, 2018, **462**, 862–871, DOI: [10.1016/j.apsusc.2018.08.153](https://doi.org/10.1016/j.apsusc.2018.08.153).
- 167 L. Luo, S. Cheng, L. Yue, Z. You and J. Cai, N-doped biochar from chitosan gel-like solution: Effect of hydrothermal temperature and superior aqueous Cr(VI) removal performance, *Colloids Surf. A Physicochem. Eng. Asp.*, 2022, **641**, 128426, DOI: [10.1016/j.colsurfa.2022.128426](https://doi.org/10.1016/j.colsurfa.2022.128426).
- 168 P. Wataniyakul, P. Boonnoun, A. T. Quitain, T. Kida, N. Laosiripojana and A. Shotipruk, Preparation of hydrothermal carbon acid catalyst from defatted rice bran, *Ind. Crops Prod.*, 2018, **117**, 286–294, DOI: [10.1016/j.indcrop.2018.03.002](https://doi.org/10.1016/j.indcrop.2018.03.002).
- 169 Y. Sun, B. Gao, Y. Yao, J. Fang, M. Zhang, Y. Zhou, *et al.*, Effects of feedstock type, production method, and pyrolysis temperature on biochar and hydrochar properties, *Chem. Eng. J.*, 2014, **240**, 574–578, DOI: [10.1016/j.cej.2013.10.081](https://doi.org/10.1016/j.cej.2013.10.081).
- 170 C. Rodríguez Correa, M. Stollovsky, T. Hehr, Y. Rauscher, B. Rolli and A. Kruse, Influence of the Carbonization Process on Activated Carbon Properties from Lignin and Lignin-Rich Biomasses, *ACS Sustain. Chem. Eng.*, 2017, **5**(9), 8222–8233, DOI: [10.1021/acssuschemeng.7b01895](https://doi.org/10.1021/acssuschemeng.7b01895).
- 171 Q. Ma, L. Cui, S. Zhou, Y. Li, W. Shi and S. Ai, Iron nanoparticles in situ encapsulated in lignin-derived hydrochar as an effective catalyst for phenol removal, *Environ. Sci. Pollut. Res.*, 2018, **25**(21), 20833–20840, DOI: [10.1007/s11356-018-2285-7](https://doi.org/10.1007/s11356-018-2285-7), PubMed PMID: 29761356.
- 172 Y. Tian, Y. Yin, H. Liu and H. Zhou, One-step hydrothermal carbonization of amine modified black liquor and lignin for efficient Cr(VI) adsorption, *J. Water Process Eng.*, 2022, **46**, 102583, DOI: [10.1016/j.jwpe.2022.102583](https://doi.org/10.1016/j.jwpe.2022.102583).
- 173 W. Sangchoom and R. Mokaya, Valorization of Lignin Waste: Carbons from Hydrothermal Carbonization of Renewable Lignin as Superior Sorbents for CO<sub>2</sub> and Hydrogen Storage, *ACS Sustain. Chem. Eng.*, 2015, **3**(7), 1658–1667, DOI: [10.1021/acssuschemeng.5b00351](https://doi.org/10.1021/acssuschemeng.5b00351).
- 174 X. Cheng, C. Tang, C. Yan, J. Du, A. Chen, X. Liu, *et al.*, Preparation of porous carbon spheres and their application as anode materials for lithium-ion batteries: A review, *Mater. Today Nano*, 2023, **22**, 100321, DOI: [10.1016/j.mtnano.2023.100321](https://doi.org/10.1016/j.mtnano.2023.100321).
- 175 Y. Fang, L. Liu, H. Xiang, Y. Wang and X. Sun, Biomass-based carbon microspheres for removing heavy metals from the environment: a review, *Mater. Today Sustain.*, 2022, **18**, 100136, DOI: [10.1016/j.mtsust.2022.100136](https://doi.org/10.1016/j.mtsust.2022.100136).
- 176 R. Li, L. Wang and A. Shahbazi, A Review of Hydrothermal Carbonization of Carbohydrates for Carbon Spheres Preparation, *Trends Renewable Energy*, 2015, **1**(1), 43–56, DOI: [10.17737/tre.2015.1.1.009](https://doi.org/10.17737/tre.2015.1.1.009).
- 177 N. Roy, Y. Anil Kumar, T. Ramachandran, A. M. Fouda, H. H. Hegazy, M. Moniruzzaman, *et al.*, Biomass-derived nanostructures and hydrothermal carbon spheres: A review of electrochemical applications in redox flow battery, *J. Ind. Eng. Chem.*, 2025, 228–254, DOI: [10.1016/j.jiec.2024.10.017](https://doi.org/10.1016/j.jiec.2024.10.017).
- 178 N. K. Tripathi, Porous carbon spheres: Recent developments and applications, *AIMS Mater. Sci.*, 2018, 1016–1052, DOI: [10.3934/MATERSCI.2018.5.1016](https://doi.org/10.3934/MATERSCI.2018.5.1016).
- 179 S. Yu, X. Dong, P. Zhao, Z. Luo, Z. Sun, X. Yang, *et al.*, Decoupled temperature and pressure hydrothermal synthesis of carbon sub-micron spheres from cellulose, *Nat. Commun.*, 2022, **13**, 3616, DOI: [10.1038/s41467-022-31352-x](https://doi.org/10.1038/s41467-022-31352-x), PubMed PMID: 35750677.
- 180 Z. Z. Chowdhury, B. Krishnan, S. Sagadevan, R. F. Rafique, N. A. B. Hamizi, Y. A. Wahab, *et al.*, Effect of temperature on the physical, electro-chemical and adsorption properties of carbon micro-spheres using hydrothermal carbonization process, *Nanomaterials*, 2018, **8**, 597, DOI: [10.3390/nano8080597](https://doi.org/10.3390/nano8080597).
- 181 J. Rizhikovs, J. Zandersons, B. Spince, G. Dobeles and E. Jakab, Preparation of granular activated carbon from



- hydrothermally treated and pelletized deciduous wood, *J. Anal. Appl. Pyrolysis*, 2012, **93**, 68–76, DOI: [10.1016/j.jaap.2011.09.009](https://doi.org/10.1016/j.jaap.2011.09.009).
- 182 C. Zhang, S. Lin, J. Peng, Y. Hong, Z. Wang and X. Jin, Preparation of highly porous carbon through activation of NH<sub>4</sub>Cl induced hydrothermal microsphere derivation of glucose, *RSC Adv.*, 2017, **7**(11), 6486–6491, DOI: [10.1039/c6ra26141h](https://doi.org/10.1039/c6ra26141h).
- 183 C. Ren, M. Li, W. Huang, Y. Zhang and J. Huang, Superhydrophobic coating with excellent robustness and UV resistance fabricated using hydrothermal treated lignin nanoparticles by one-step spray, *J. Mater. Sci.*, 2022, **57**(39), 18356–18369, DOI: [10.1007/s10853-022-07787-4](https://doi.org/10.1007/s10853-022-07787-4).
- 184 X. Zhang, H. Abushammala, D. Puglia, B. Lu, P. Xu, W. Yang, *et al.*, One-Step to Prepare Lignin Based Fluorescent Nanoparticles with Excellent Radical Scavenging Activity, *J. Renewable Mater.*, 2024, **12**(5), 895–908, DOI: [10.32604/jrm.2024.049810](https://doi.org/10.32604/jrm.2024.049810).
- 185 M. Morsali, A. Moreno, A. Loukovitou, I. Pylypchuk and M. H. Sipponen, Stabilized Lignin Nanoparticles for Versatile Hybrid and Functional Nanomaterials, *Biomacromolecules*, 2022, **23**(11), 4597–4606, DOI: [10.1021/acs.biomac.2c00840](https://doi.org/10.1021/acs.biomac.2c00840), PubMed PMID: 36237172.
- 186 S. Chen, G. Wang, W. Sui, A. M. Parvez, L. Dai and C. Si, Novel lignin-based phenolic nanosphere supported palladium nanoparticles with highly efficient catalytic performance and good reusability, *Ind. Crops Prod.*, 2020, **1**, 145, DOI: [10.1016/j.indcrop.2020.112164](https://doi.org/10.1016/j.indcrop.2020.112164).
- 187 T. Pang, G. Wang, J. Ge, N. Wei, W. Sui, A. M. Parvez, *et al.*, Novel Surfactant-Assisted Hydrothermal Fabrication of a Lignin Microsphere as a Green Reducer and Carrier for Pd Nanoparticles, *ACS Sustain. Chem. Eng.*, 2021, **9**(50), 17085–17095, DOI: [10.1021/acssuschemeng.1c06170](https://doi.org/10.1021/acssuschemeng.1c06170).
- 188 Y. Cui, X. Sheng, R. Anusuyadevi, M. Lawoko and A. J. Svagan, Self-assembled carbon spheres prepared from abundant lignin and urea for photocatalytic and self-propelling applications, *Carbon Trends*, 2021, **3**, 40, DOI: [10.1016/j.cartre.2021.10](https://doi.org/10.1016/j.cartre.2021.10).
- 189 Y. L. Cha, A. M. Alam, S. M. Park, Y. H. Moon, K. S. Kim, J. E. Lee, *et al.*, Hydrothermal-process-based direct extraction of polydisperse lignin microspheres from black liquor and their physicochemical characterization, *Bioresour. Technol.*, 2020, **297**, 122399, DOI: [10.1016/j.biortech.2019.122399](https://doi.org/10.1016/j.biortech.2019.122399), PubMed PMID: 31759855.
- 190 H. Mao, X. Chen, R. Huang, M. Chen, R. Yang, P. Lan, *et al.*, Fast preparation of carbon spheres from enzymatic hydrolysis lignin: Effects of hydrothermal carbonization conditions, *Sci. Rep.*, 2018, **8**, 9501, DOI: [10.1038/s41598-018-27777-4](https://doi.org/10.1038/s41598-018-27777-4), PubMed PMID: 29934533.
- 191 L. Fan, L. Fan, T. Yu, X. Tan and Z. Shi, Hydrothermal synthesis of lignin-based carbon microspheres as anode material for lithium-ion batteries, *Int. J. Electrochem. Sci.*, 2020, **15**(2), 1035–1043, DOI: [10.20964/2020.02.16](https://doi.org/10.20964/2020.02.16).
- 192 L. Fan, Z. Shi, Q. Ren, L. Yan, F. Zhang and L. Fan, Nitrogen-doped lignin based carbon microspheres as anode material for high performance sodium ion batteries, *Green Energy Environ.*, 2021, **6**(2), 220–228, DOI: [10.1016/j.gee.2020.06.005](https://doi.org/10.1016/j.gee.2020.06.005).
- 193 J. Gao, Z. Q. Wang, B. Li, W. Zhao, Z. R. Ba, Z. Y. Liu, *et al.*, Effect of hydrothermal pH values on the morphology of special microspheres of lignin-based porous carbon and the mechanism of carbon dioxide adsorption, *Bioresour. Technol.*, 2024, **393**, 130171, DOI: [10.1016/j.biortech.2023.130171](https://doi.org/10.1016/j.biortech.2023.130171), PubMed PMID: 38086460.
- 194 H. Wang, F. Xiong, Y. Tan, J. Yang, Y. Qing, F. Chu, *et al.*, Preparation and Formation Mechanism of Covalent-Noncovalent Forces Stabilizing Lignin Nanospheres and Their Application in Superhydrophobic and Carbon Materials, *ACS Sustain. Chem. Eng.*, 2021, **9**(10), 3811–3820, DOI: [10.1021/acssuschemeng.0c08780](https://doi.org/10.1021/acssuschemeng.0c08780).
- 195 H. Wang, F. Xiong, J. Yang, B. Ma, Y. Qing, F. Chu, *et al.*, Preparation of size-controlled all-lignin based carbon nanospheres and their electrochemical performance in supercapacitor, *Ind. Crops Prod.*, 2022, **1**, 179, DOI: [10.1016/j.indcrop.2022.114689](https://doi.org/10.1016/j.indcrop.2022.114689).
- 196 J. Yang, F. Xiong, H. Wang, B. Ma, F. Guo, Y. Qing, *et al.*, Facile and scalable construction of nitrogen-doped lignin-based carbon nanospheres for high-performance supercapacitors, *Fuel*, 2023, **343**, 128007, DOI: [10.1016/j.fuel.2023.128007](https://doi.org/10.1016/j.fuel.2023.128007).
- 197 H. Wang, M. He, Y. Qing, F. Chu, Y. Wu and F. Xiong, A molecular-chemistry-manipulation strategy toward functional lignin-based porous carbon nanospheres with tunable-pore structure, *Chem. Eng. J.*, 2024, **499**, 156615, DOI: [10.1016/j.ccej.2024.156615](https://doi.org/10.1016/j.ccej.2024.156615).
- 198 S. M. Krutov, D. V. Evtuguin, E. V. Ipatova, S. A. O. Santos and Y. N. Sazanov, Modification of acid hydrolysis lignin for value-added applications by micronization followed by hydrothermal alkaline treatment, *Holzforschung*, 2015, **69**(6), 761–768, DOI: [10.1515/hf-2014-0264](https://doi.org/10.1515/hf-2014-0264).
- 199 U. P. Agarwal, S. A. Ralph, R. S. Reiner, C. G. Hunt, C. Baez, R. Ibach, *et al.*, Production of high lignin-containing and lignin-free cellulose nanocrystals from wood, *Cellulose*, 2018, **25**(10), 5791–5805, DOI: [10.1007/s10570-018-1984-z](https://doi.org/10.1007/s10570-018-1984-z).
- 200 H. C. Ho, P. V. Bonnesen, N. A. Nguyen, D. A. Cullen, D. Uhrig, M. Goswami, *et al.*, Method to Synthesize Micronized Spherical Carbon Particles from Lignin, *Ind. Eng. Chem. Res.*, 2020, **59**(1), 9–17, DOI: [10.1021/acs.iecr.9b05143](https://doi.org/10.1021/acs.iecr.9b05143).
- 201 V. Pierpaoli, M. Grilc, G. Tofani, B. Likozar, E. Jasiukaitytė-Grojzdek, E. Segoloni, *et al.*, Lignin Derivatives in Chestnut Wood Hydrochar: Mild Solvolysis and Characterization, *ChemPlusChem*, 2025, **90**, DOI: [10.1002/cplu.202400697](https://doi.org/10.1002/cplu.202400697).
- 202 S. A. Nicolae, H. Au, P. Modugno, H. Luo, A. E. Szego, M. Qiao, *et al.*, Recent advances in hydrothermal carbonisation: From tailored carbon materials and biochemicals to applications and bioenergy, *Green Chem.*, 2020, **22**(15), 4747–4800, DOI: [10.1039/d0gc00998a](https://doi.org/10.1039/d0gc00998a).
- 203 M. Usman, H. Chen, K. Chen, S. Ren, J. H. Clark, J. Fan, *et al.*, Characterization and utilization of aqueous pro-



- ducts from hydrothermal conversion of biomass for bio-oil and hydro-char production: A review, *Green Chem.*, 2019, **21**(7), 1553–1572, DOI: [10.1039/c8gc03957g](https://doi.org/10.1039/c8gc03957g).
- 204 Y. Wang, C. Yuan, K. Zhang, J. Tong, N. Ma, M. M. Ali, *et al.*, Rapid humification of biomass via hydrothermal conversion: a comprehensive review, *Green Chem.*, 2024, 1588–1603, DOI: [10.1039/d4gc05362a](https://doi.org/10.1039/d4gc05362a).
- 205 C. Yang, S. Wang, J. Yang, D. Xu, Y. Li, J. Li, *et al.*, Hydrothermal liquefaction and gasification of biomass and model compounds: A review, *Green Chem.*, 2020, **22**(23), 8210–8232, DOI: [10.1039/d0gc02802a](https://doi.org/10.1039/d0gc02802a).
- 206 I. A. Basar, H. Liu, H. Carrere, E. Trably and C. Eskicioglu, A review on key design and operational parameters to optimize and develop hydrothermal liquefaction of biomass for biorefinery applications, *Green Chem.*, 2021, 1404–1446, DOI: [10.1039/d0gc04092d](https://doi.org/10.1039/d0gc04092d).
- 207 I. A. Basar, H. Liu and C. Eskicioglu, Incorporating hydrothermal liquefaction into wastewater treatment – Part III: Aqueous phase characterization and evaluation of on-site treatment, *Chem. Eng. J.*, 2023, **1**, 467, DOI: [10.1016/j.cej.2023.143422](https://doi.org/10.1016/j.cej.2023.143422).
- 208 . Organisation for Economic Co-operation and Development (OECD) assessments. <https://hpvchemicals.oecd.org/ui/Default.aspx> Accessed on 20.03.2026.
- 209 C. Mao, J. Byun, H. W. MacLeod, C. T. Maravelias and G. A. Ozin, Green urea production for sustainable agriculture, *Joule*, 2024, 1224–1238, DOI: [10.1016/j.joule.2024.02.021](https://doi.org/10.1016/j.joule.2024.02.021).
- 210 M. Tobiszewski, M. Marć, A. Gałuszka and J. Namieśnik, Green chemistry metrics with special reference to green analytical chemistry, *Molecules*, 2015, 10928–10946, DOI: [10.3390/molecules200610928](https://doi.org/10.3390/molecules200610928), PubMed PMID: 26076112.
- 211 M. Zhou, K. Taiwo, H. Wang, J. N. Ntihuga, L. T. Angenent and J. G. Usack, Anaerobic digestion of process water from hydrothermal treatment processes: a review of inhibitors and detoxification approaches, *Bioresour. Bioprocess.*, 2024, **11**, 47, DOI: [10.1186/s40643-024-00756-6](https://doi.org/10.1186/s40643-024-00756-6).
- 212 T. Ender, V. S. Ekanthalu, H. Jalalipour, J. Sprafke and M. Nelles, Process Waters from Hydrothermal Carbonization of Waste Biomasses like Sewage Sludge: Challenges, Legal Aspects, and Opportunities in EU and Germany, *Water*, 2024, **16**, 1003, DOI: [10.3390/w16071003](https://doi.org/10.3390/w16071003).
- 213 D. V. Cabrera and R. A. Labatut, Outlook and challenges for recovering energy and water from complex organic waste using hydrothermal liquefaction, *Sustainable Energy Fuels*, 2021, 2201–2227, DOI: [10.1039/d0se01857k](https://doi.org/10.1039/d0se01857k).
- 214 N. N. Boamah and S. A. Salaudeen, Process water from the hydrothermal carbonization of biomass: A review on the characterization, applications, and potential for future work, *J. Water Process Eng.*, 2025, **77**, 108531, DOI: [10.1016/j.jwpe.2025.108531](https://doi.org/10.1016/j.jwpe.2025.108531).
- 215 R. Posmanik, R. A. Labatut, A. H. Kim, J. G. Usack, J. W. Tester and L. T. Angenent, Coupling hydrothermal liquefaction and anaerobic digestion for energy valorization from model biomass feedstocks, *Bioresour. Technol.*, 2017, **233**, 134–143, DOI: [10.1016/j.biortech.2017.02.095](https://doi.org/10.1016/j.biortech.2017.02.095), PubMed PMID: 28267660.
- 216 R. Li, D. Liu, Y. Zhang, N. Duan, J. Zhou, Z. Liu, *et al.*, Improved methane production and energy recovery of post-hydrothermal liquefaction waste water via integration of zeolite adsorption and anaerobic digestion, *Sci. Total Environ.*, 2019, **651**, 61–69, DOI: [10.1016/j.scitotenv.2018.09.175](https://doi.org/10.1016/j.scitotenv.2018.09.175), PubMed PMID: 30227293.
- 217 F. Wang, W. Yi, D. Zhang, Y. Liu, X. Shen and Y. Li, Anaerobic co-digestion of corn stover and wastewater from hydrothermal carbonation, *Bioresour. Technol.*, 2020, **315**, 123788, DOI: [10.1016/j.biortech.2020.123788](https://doi.org/10.1016/j.biortech.2020.123788), PubMed PMID: 32652438.
- 218 J. A. Villamil, A. F. Mohedano, J. J. Rodríguez, R. Borja and M. A. De la Rubia, Anaerobic Co-digestion of the Organic Fraction of Municipal Solid Waste and the Liquid Fraction From the Hydrothermal Carbonization of Industrial Sewage Sludge Under Thermophilic Conditions, *Front. Sustain. Food Syst.*, 2018, **2**, 17, DOI: [10.3389/fsufs.2018.00017](https://doi.org/10.3389/fsufs.2018.00017).
- 219 M. A. De la Rubia, J. A. Villamil, J. J. Rodríguez, R. Borja and A. F. Mohedano, Mesophilic anaerobic co-digestion of the organic fraction of municipal solid waste with the liquid fraction from hydrothermal carbonization of sewage sludge, *Waste Manage.*, 2018, **76**, 315–322, DOI: [10.1016/j.wasman.2018.02.046](https://doi.org/10.1016/j.wasman.2018.02.046), PubMed PMID: 29500082.
- 220 S. K. Bhargava, J. Tardio, J. Prasad, K. Föger, D. B. Akolekar and S. C. Grocott, Wet oxidation and catalytic wet oxidation, *Ind. Eng. Chem. Res.*, 2006, 1221–1258, DOI: [10.1021/ie051059n](https://doi.org/10.1021/ie051059n).
- 221 Y. Zhang and Y. Wang, Application and improvement of wet oxidation technology. In: IOP Conference Series: Earth and Environmental Science. IOP Publishing Ltd, 2020. DOI: [10.1088/1755-1315/514/5/052042](https://doi.org/10.1088/1755-1315/514/5/052042).
- 222 B. Weiner, M. Breulmann, H. Wedwitschka, C. Fühner and F. D. Kopinke, Wet Oxidation of Process Waters from the Hydrothermal Carbonization of Sewage Sludge, *Chem. Ing. Tech.*, 2018, **90**(6), 872–880, DOI: [10.1002/cite.201700050](https://doi.org/10.1002/cite.201700050).
- 223 L. Wang, Y. Chang and Q. Liu, Fate and distribution of nutrients and heavy metals during hydrothermal carbonization of sewage sludge with implication to land application, *J. Cleaner Prod.*, 2019, **225**, 972–983, DOI: [10.1016/j.jclepro.2019.03.347](https://doi.org/10.1016/j.jclepro.2019.03.347).
- 224 X. Zhuang, Y. Huang, Y. Song, H. Zhan, X. Yin and C. Wu, The transformation pathways of nitrogen in sewage sludge during hydrothermal treatment, *Bioresour. Technol.*, 2017, **245**, 463–470, DOI: [10.1016/j.biortech.2017.08.195](https://doi.org/10.1016/j.biortech.2017.08.195), PubMed PMID: 28898845.
- 225 U. Ekpo, A. B. Ross, M. A. Camargo-Valero and L. A. Fletcher, Influence of pH on hydrothermal treatment of swine manure: Impact on extraction of nitrogen and phosphorus in process water, *Bioresour. Technol.*, 2016, **214**, 637–644, DOI: [10.1016/j.biortech.2016.05.012](https://doi.org/10.1016/j.biortech.2016.05.012), PubMed PMID: 27187568.
- 226 J. Chen, L. Ding, R. Liu, S. Xu, L. Li, L. Gao, *et al.*, Hydrothermal Carbonization of Microalgae-Fungal



- Pellets: Removal of Nutrients from the Aqueous Phase Fungi and Microalgae Cultivation, *ACS Sustain. Chem. Eng.*, 2020, **8**(45), 16823–16832, DOI: [10.1021/acssuschemeng.0c05441](https://doi.org/10.1021/acssuschemeng.0c05441).
- 227 S. Celletti, M. Lanz, A. Bergamo, V. Benedetti, D. Basso, M. Baratieri, *et al.*, Evaluating the Aqueous Phase From Hydrothermal Carbonization of Cow Manure Digestate as Possible Fertilizer Solution for Plant Growth, *Front. Plant Sci.*, 2021, **12**, 687434, DOI: [10.3389/fpls.2021.687434](https://doi.org/10.3389/fpls.2021.687434).
- 228 M. Tsarpali, N. Arora, J. N. Kuhn and G. P. Philippidis, Beneficial use of the aqueous phase generated during hydrothermal carbonization of algae as nutrient source for algae cultivation, *Algal Res.*, 2021, **60**, 102485, DOI: [10.1016/j.algal.2021.102485](https://doi.org/10.1016/j.algal.2021.102485).
- 229 Y. B. Brandão, J. G. C. de Oliveira and M. Benachour, Phenolic Wastewaters: Definition, Sources and Treatment Processes, in *Phenolic Compounds - Natural Sources, Importance and Applications*, InTech, 2017. DOI: [10.5772/66366](https://doi.org/10.5772/66366).
- 230 F. I. da Silva Aires, D. N. Dari, I. S. Freitas, J. L. da Silva, J. R. de Matos Filho, K. M. dos Santos, *et al.*, Advanced and prospects in phenol wastewater treatment technologies: unveiling opportunities and trends, *Discover Water*, 2024, **4**, 20, DOI: [10.1007/s43832-024-00076-y](https://doi.org/10.1007/s43832-024-00076-y).
- 231 F. Mumtaz, B. Li, M. R. Al Shehhia, X. Feng and K. Wang, Treatment of phenolic-wastewater by hybrid technologies: A review, *J. Water Process Eng.*, 2024, **57**, 104695, DOI: [10.1016/j.jwpe.2023.104695](https://doi.org/10.1016/j.jwpe.2023.104695).

